20. Nationale Photovoltaik-Tagung 2022, Bern
20e Congrès photovoltaïque national 2022

Liste der Aussteller / Liste d'exposant

Aussteller / Exposant	Nummer / Numéro
Younergy SA	1
Sputnik Engineering International AG	2
Ernst Schweizer AG	3
Weidmüller Schweiz AG	4
Megasol Energie AG	5
TRITEC AG	6
Huawei Technologies Switzerland AG	7
SolarEdge Technologies GmbH	8
Fronius Schweiz AG	9
Schletter Solar GmbH	10
SMA Solar Technologies AG	11
CKW	12
Eternit (Schweiz) AG	13
Solarmarkt GmbH	14
Novagrid AG	15
3S Solar Plus AG	16
IBC Solar AG	17
Alternative Bank Schweiz	18
Egon AG	19
Kromatix SA	20
Contec AG	21
Vögelin GmbH	22
Urbio	23
Smartsuna SA	24
Solar Swiss Connect	25
Glaromat AG	26
Hager AG	27
Solar Manager AG	28
Energie Wasser Bern	29
Krannich Solar AG	30
NeoVac ATA AG	31
SFG Schweizerische Fachvereinigung Gebäudebegrünung	32
Activ Glass (Issol Schweiz AG)	33

Posterbeiträge Photovoltaik-Tagung 2022, Bern
Poster contribution congrès photovoltaïque national 2022

No.	Cat.	Titel	Institution	Contact	E-Mail	Authors
1	A	**Thin film solar cell research at Empa**	**EMPA, Laboratory for Thin Films and Photovoltaics Überlandstrasse 129 CH - 8600 Dübendorf**	Severin Siegrist	severin.siegrist@empa.ch	S. Siegrist, S.-C. Yang, H. Lai, Y. Zwirner, S. Nishiwaki, F. Fu, R. Carron, A. N. Tiwari
2	A	**Inkjet printing of perovskite solar cells on flexible substrates using industrial printheads**	**Hochschule für Technik und Architektur Freiburg (HEFR) iPrint Route de l'Ancienne Papeterie 180 1723 Marly**	Lucie Castens Vitanov	lucie.castensvitanov@hefr.ch	L. Castens Vitanov, G. Gugler, P. Kessler, C. Michaud, Xiao-xin Gao, S. Kinge
3	A	**Understanding and Mitigating the Degradation of Perovskite Solar Cells Based on a Nickel Oxide Hole Transport Material during Damp Heat Testing**	**CSEM SA Rue Jaquet-Droz 1 CH - 2002 Neuchâtel**	Quentin Jeangros	quentin.jeangros@csem.ch	M. Dussouillez, S. J. Moon, C. Wolff, Y. Liu, J. H. Yum, B. Kamino, A. Walter, F. Sahli, L. Lauber, G. Christmann, K. Sivula, Q. Jeangros, C. Ballif, S. Nicolay, A. Paracchino
4	A	**Tandem solar cells activities at CSEM and EPFL in Neuchâtel**	**CSEM SA Rue Jaquet-Droz 1 CH - 2002 Neuchâtel**	Quentin Jeangros	quentin.jeangros@csem.ch	A. Walter, X. Y. Chin, B. Kamino, A. Ingenito, A. Descoeudres, A. Paracchino, B. Paviet-Salomon, D. Türkay, F. Sahli, K. Artuk, M. Dussouillez, S. J. Moon, C. Wolff, Q. Jeangros, C. Ballif
5	A	**Sputtered poly-Si and its implementation in passivating contacts at the rear of industrial n-PERT solar cells**	**CSEM SA Rue Jaquet-Droz 1 CH - 2002 Neuchâtel**	Christophe Allebé	christophe.allebe@csem.ch	C. Allebé, A. Descoeudres, J.J Diaz leon, A. Ingenito, B. Paviet-Salomon, C. Ballif
6	B	**The Sirius project: From single cell laminate to full size demonstration IBC modules**	**Meyer Burger Research AG Rouges-Terres 61 2068 Hauterive**	Derk Bätzner	Derk.Baetzner@meyerburger.com	D. L. Bätzner, D. Lachenal, L. Barraud, T. Kössler, W. Frammelsberger, B. Legradic, R. Grischke, G. Marti, J. Champliaud, L. Baume, M. Despeisse, B. Paviet-Salomon, R. Kramer, L.Vouthier, N. Holm
7	B	**A Radically Simpler Way to Manufacture Thin-Film Solar Panels, On the Scale-Up to Meet Future Photovoltaic Goals**	**Solaronix SA Rue de l'Ouriette 129 CH - 1170 Obonne**	David Martineau	david.martineau@solaronix.com	D. Martineau, S. Narbey, A. Verma, T. Meyer, R.Schneider, J. Heier, F. Nüesch
8	C	**PERFORMANCE ASSESSMENT OF BIPV PRODUCTS: COMBINED TEST PROCEDURES FOR ELECTRICAL AND MECHANICAL SAFETY**	**SUPSI-DACD-ISAAC Via Flora Ruchat-Roncati 15 CH-6850 Mendrisio**	Pierluigi Bonomo	pierluigi.bonomo@supsi.ch	P. Bonomo, F. Parolini, M. Caccivio, G. Bellenda, F. Frontini
9	C	**BIPV demo-sites with novel Glass-free colored Lightweight modules**	**Ecole Polytechnique Fédérale de Lausanne (EPFL) IMT PV-Lab Rue de la Maladière 71b CH 2002 Neuchâtel**	Fabiana Lisco	fabiana.lisco@epfl.ch	F. Lisco, A. Virtuani, C. Ballif
10	C	**Swiss fire safety framework on BIPV – new fire test procedures**	**SUPSI-DACD-ISAAC Via Flora Ruchat-Roncati 15 CH-6850 Mendrisio**	Fabio Parolini	fabio.parolini@supsi.ch	F. Parolini, P. Bonomo, F. Frontini, M. Caccivio
11	C	**Building-integrated photovoltaics (BIPV): more than anecessity for our building culture**	**SUPSI-DACD-ISAAC Via Flora Ruchat-Roncati 15 CH-6850 Mendrisio**	Cristina S. Polo López	cristina.polo@supsi.ch	C. S. Polo López, F. Frontini, R. Rudel
12	D	**Performance comparison of a P370 power optimizer system and a string inverter system.**	**ZHAW School of Engineering, IEFE Technikumstrasse 9 CH - 8401 Winterthur**	Arturo Bänziger	abanziger@gmail.com	C. Allenspach, A. Bänziger, A. Schneider, F. Baumgartner, F. Carigiet
13	F	**What drives performance in data-driven and weather-based techniques for short-term PV forecasting?**	**CSEM SA Rue Jaquet-Droz 1 CH - 2002 Neuchâtel**	Pierre-Jean Alet	pierre-jean.alet@csem.ch	R. Carrillo, P.-J. Alet, S. Müller, J. Remund

No.	Cat.	Titel	Institution	Contact	E-Mail	Authors
14	F	**Hydrogen as seasonal storage for a swiss neighbourhood**	**HES-SO Valais-Wallis Route de Rawil 47 CH - 1950 Sion**	Christoph Ellert	Christoph.Ellert@hevs.ch	M. Schopfer, C. Ellert
15	G	**Long-term performance of BIPV in Switzerland**	**Ecole Polytechnique Fédérale de Lausanne (EPFL) IMT PV-Lab Rue de la Maladière 71b CH 2002 Neuchâtel**	Hugo Quest	hugo.quest@epfl.ch	H. Quest, A. Fairbrother, E. Özkalay, P. Wälchli, G. Friesen, C. Ballif, A. Virtuani
16	G	**Quantifying Performance Loss Rates of PV Modules using Ground-Based vs Satellite-Based Meteorological Data**	**SUPSI-DACD-ISAAC Via Francesco Catenazzi 23 CH-6850 Mendrisio**	Ebrar Özkalay	Ebrar.Ozkalay@supsi.ch	E. Özkalay, A. Virtuani, A. Fairbrother, A. Skoczek, G. Friesen, M. Caccivio, C. Ballif
17	G	**40 years of the TISO PV plant: update on the oldest PV system connected in Europe**	**SUPSI-DACD-ISAAC Via Francesco Catenazzi 23 CH-6850 Mendrisio**	Mauro Caccivio	mauro.caccivio@supsi.ch	M. Caccivio, D. Chianese, G. Friesen, G. Bellenda
18	G	**Installation photovoltaïque sur l'orphelinat au Togo**	**HES-SO Valais-Wallis Rue de l'industrie 23 CH - 1950 Sion**	Christoph Ellert	Christoph.Ellert@hevs.ch	A. Buchard, J. Udry, C. Ellert
19	G	**Incidence Angle Modifier von blendarmen PV-Modulen**	**Berner Fachhochschule (BFH) Technik und Informatik, Photovoltaiklabor Jlcoweg 1, CH-3400 Burgdorf**	Christof Bucher	christof.bucher@bfh.ch	M. Burri, P- Wüthrich, C. Bucher
20	G	**IV Curve Tracer**	**Berner Fachhochschule (BFH) Technik und Informatik, Photovoltaiklabor Jlcoweg 1, CH-3400 Burgdorf**	Christof Bucher	christof.bucher@bfh.ch	M. Müller, C. Bucher, L. Borgna
21	G	**Vergleich optischer Methoden zur PV-Moduluntersuchung**	**Berner Fachhochschule (BFH) Technik und Informatik, Photovoltaiklabor Jlcoweg 1, CH-3400 Burgdorf**	Christof Bucher	christof.bucher@bfh.ch	C. Bucher, S. Danaci, M. Burri
22	G	**Hagelschäden bei PV-Modulen**	**SPF Institut für Solartechnik, OST Ostschweizer - Fachhochschule Oberseestrasse 10 CH - 8640 Rapperswil**	Evelyn Bamberger	evelyn.bamberger@spf.ch	E. Bamberger et al
23	G	**Improvement of hail test setup for larger hailstones**	**SUPSI-DACD-ISAAC Via Francesco Catenazzi 23 CH-6850 Mendrisio**	Mauro Caccivio	mauro.caccivio@supsi.ch	M. Caccivio, G. Bellenda, F. Valoti, M. Ronchi
24	H	**Laborautomatisierung mit dem Muscle-Konzept**	**Berner Fachhochschule (BFH) Technik und Informatik, Photovoltaiklabor Jlcoweg 1, CH-3400 Burgdorf**	Christof Bucher	christof.bucher@bfh.ch	D. Joss, M. Müller, P. Wüthrich, M.Zaugg, M. Burri, C. Bucher
25	L	**Solarpotenzial auf Schweizer Dächern**	**ZHAW Wädenswil Campus Grüntal CH-8840 Wädenswil**	Jürg Rohrer	rohu@zhaw.ch	D. Anderegg, S. Strebel, J. Rohrer
26	K	**Micro Stockage Intelligent Distributed(SFOE MSID)**	**HES-SO Valais-Wallis Route de Rawil 47 CH - 1950 Sion**	David Wannier	david.wannier@hevs.ch	D. Wannier, J. Vianin, H. Pereira, J-M. Alder, J. Silva, L. Perrier, P.-A. Clivaz
27	A	**SHAMAN: Shadow mask localization of thin films for back-contacted crystalline silicon solar cells & energy harvesters**	**CSEM SA Rue Jaquet-Droz 1 CH - 2002 Neuchâtel**	Gizem Nogay	gizem.nogay@csem.ch	G. Nogay, J. Zhao, J. Geissbuhler, N. Badel, L.-L. Senaud, P. Wyss, C. Allebe, G. Christmann, M.Despeisse, B. Paviet-Salomon, C. Ballif

Thin film solar cell research at Empa

Severin Siegrist, Shih-Chi Yang, H. Lai, Y. Zwirner, S. Nishiwaki, F. Fu, R. Carron and A. N. Tiwari

Laboratory for Thin Films and Photovoltaics, Empa – Swiss Federal Laboratories for Materials Science and Technology, Ueberlandstrasse 129, 8600 Duebendorf, Switzerland

Empa
Materials Science and Technology

Bifacial CIGS solar cells

Bifacial device structure

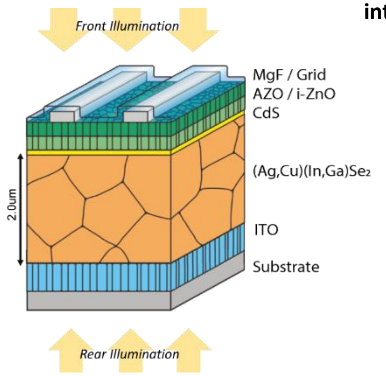

Suppression of detrimental GaO_x interlayer by low-temperature process

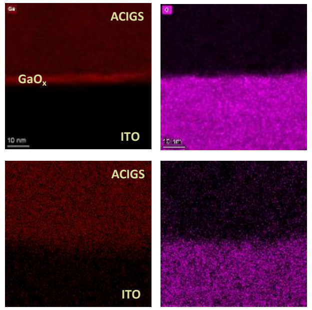

Externally Certified by Fraunhofer ISE

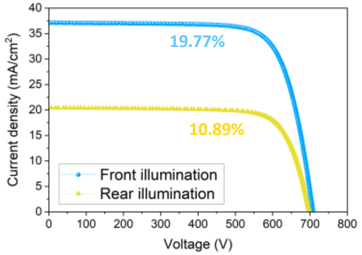

Comparison with state-of-the-art

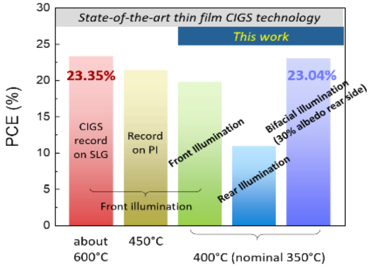

Summary

- New low-temperature process overcomes the long-existing hurdles in bifacial CIGS solar cells
- Comparable bifacial device performance with state-of-the-art monofacial devices
- Great potential for building-integrated photovoltaics (BIPV)

Outlook

- Realization on light-weight and flexible substrates, e.g. Polyimide

Bifacial Perovskite/CIGS tandem solar cells

Device structure

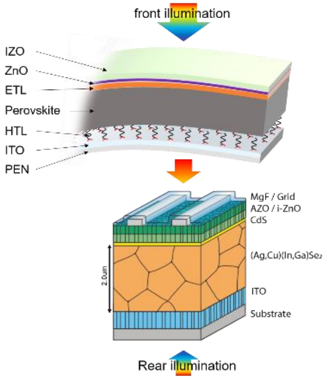

Bifacial Perovskite/CIGS tandem solar cells

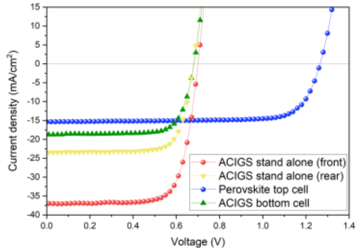

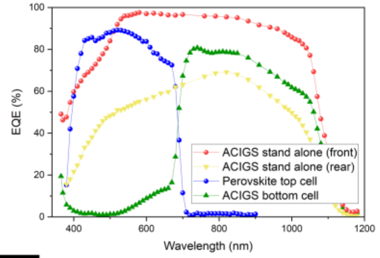

Solar Cells	V_{OC} (V)	J_{SC} (mA/cm²)	FF (%)	PCE (%)	Estimated PCE gain
Perovskite top cell	1.268	15.33	77.9	15.1	
CIGS (stand alone)	0.700	37.00	74.4	19.3	
CIGS bottom cell	0.681	18.70	75.1	9.6	
CIGS rear illumination	0.679	23.40	76.1	12.1	
Perovskite/CIGS 4-terminal bifacial tandems (under 30% albedo)				28.3	9

Summary

- First demonstration of high performance 4T bifacial Perovskite/CIGS tandem solar cells

Outlook

- 2T bifacial Perovskite/CIGS tandem solar cells

Flexible perovskite/CIGS and all-perovskite tandem solar cells

Motivation:
Development of high efficiency flexible tandem solar cells for light weight applications (e.g. wearable electronics, etc.).

Results:

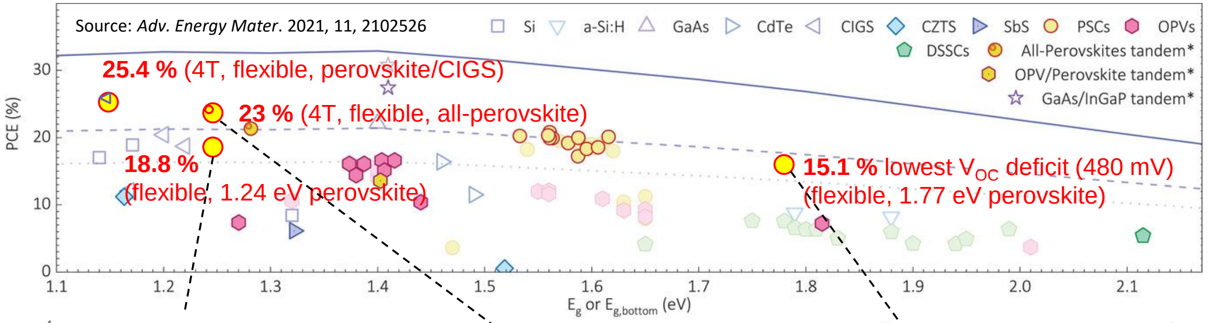

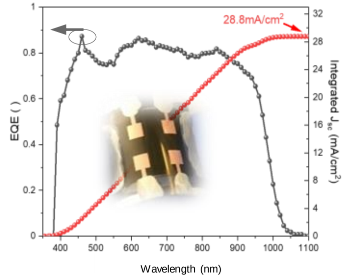

18.8 % efficient narrow bandgap (1.24 eV) perovskite solar cell on flexible substrates

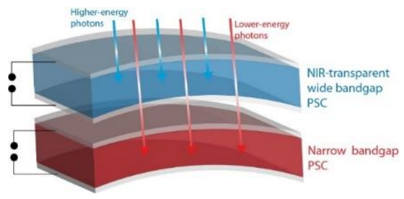

25.4 % efficient flexible perovskite/ CIGS 4T tandem solar cell and flexible all-perovskite 4T tandem solar cell with 23 % efficiency

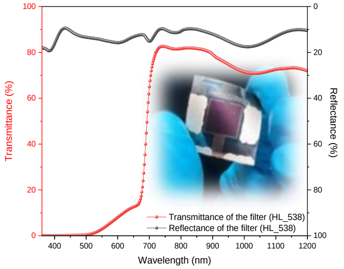

Flexible, wide bandgap (1.77 eV) perovskite solar cell with record low open-circuit voltage deficit (only 480 mV)

Outlook

- Boost efficiency of flexible, thin film 4-terminal tandem solar cells to over 25 %.
- Scale-up flexible tandem solar cells/modules.
- Demonstrate stable and high efficiency thin film tandem solar cells and modules by cost-effective, solution-based methods (slot-die coating).

Acknowledgements

Partial funding through the following projects is gratefully acknowledged: SFOE-BFE (SI/501805-01, SI/502310-01); SNF-Bridge (20B2-1_176552/1); the European Union's Horizon 2020 research and innovation programme under grant agreement No 850937

Schweizerische Eidgenossenschaft Confédération suisse Confederazione Svizzera Confederaziun svizra
State Secretariat for Education, Research and Innovation SERI

Contacts

For CIGS: Shih-Chi Yang, email: shih-chi.yang@empa.ch, phone: +41 58 765 4299
For perovskite: Severin Siegrist, email: severin.siegrist@empa.ch, phone: +41 58 765 60 83

Inkjet printing of perovskite solar cells on flexible substrates using industrial printheads

Lucie Castens Vitanov[1], Gilbert Gugler[1], César Michaud[1], Vincent Schneuwly[1], Philip Kessler[1], Xiao-xin Gao[2], Maria Cristina Momblona Rincón[2], Keith Brooks[2], Mohammad Khaja Nazeeruddin[2], Sachin Kinge[3]

1. iPrint, HEIA-FR, HES-SO University of Applied Sciences and Arts Western Switzerland, Fribourg CH-1700, Switzerland
2. GMF, EPFL-Valais, Sion CH-1951, Switzerland
3. Toyota Motors Europe, Brussels, Belgium

Three printed layers solar cell process

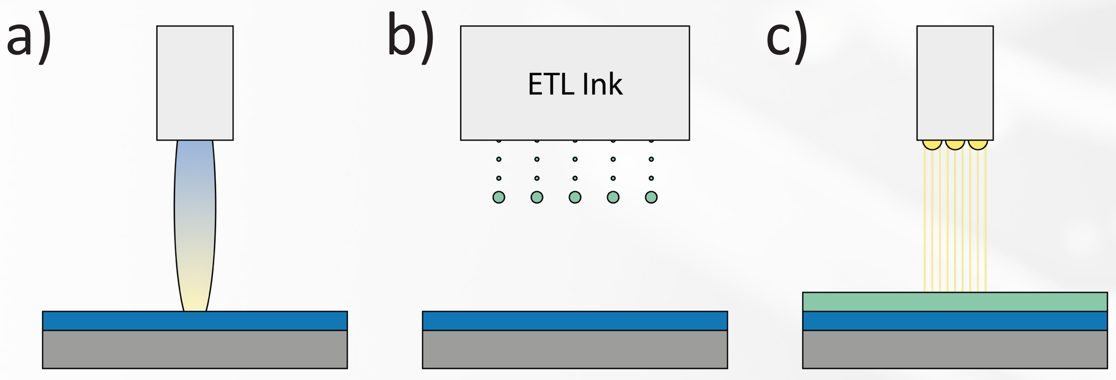

a) A cleaned commercial ITOPEN substrate was treated with a plasma torch.
b) The electron transport layer (ETL) SnO2 was printed .
c) It was dried by a near-infrared lamp.

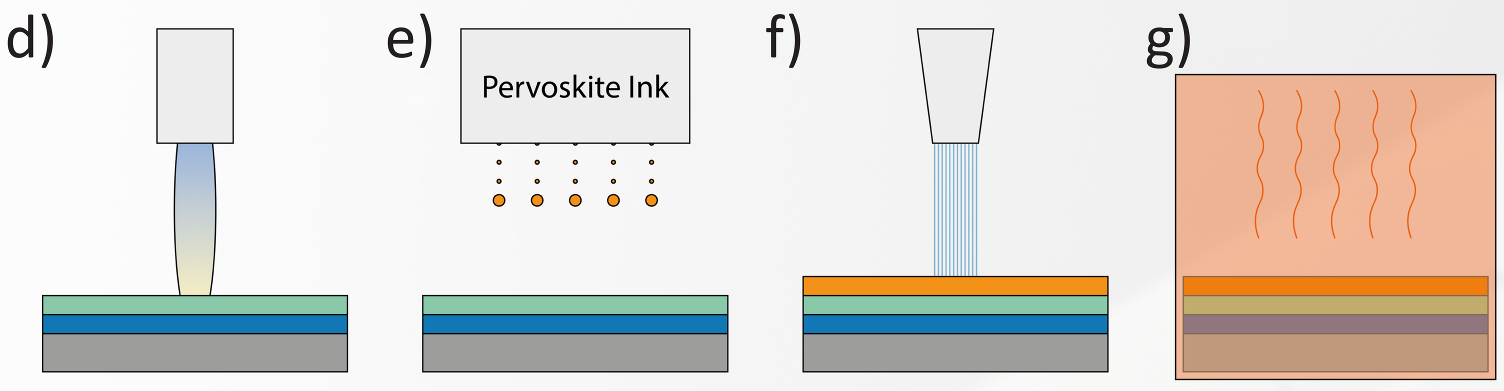

d) The ETL coated sample was treated with a plasma torch.
e) The perovskite layer was printed.
f) The perovskite layer was dried by an airknife.
g) The perovskite layer was annealed in a vacuum-oven.

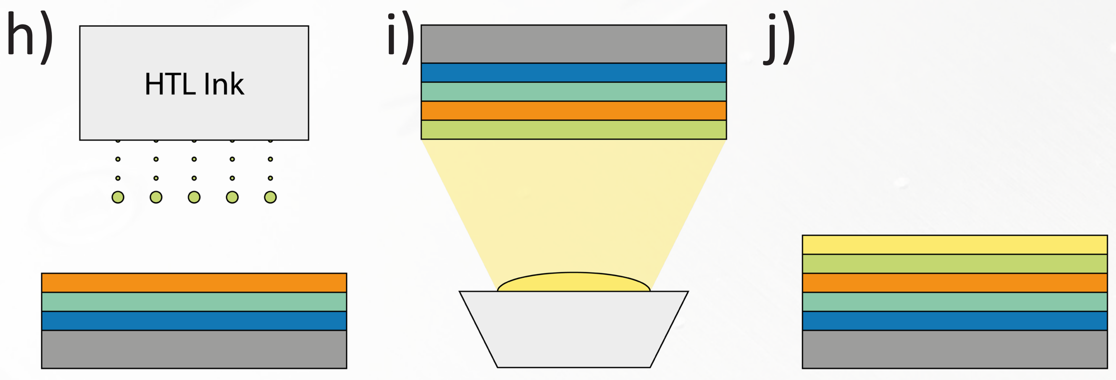

h) The hole transport layer (HTL) Spiro-OMeTAD was printed.
i) The gold contact layer was evaporated on the stack.
j) The finished solar cell

Layers of the solar cell

Back Contact: Gold
Hole Transport Layer (HTL): SPIRO (Inkjet printed)
Perovskite Layer (Inkjet printed)
Electron Transport Layer (ETL): SNO2 (Inkjet printed)
Front Contact: Transparent Conductive Oxide (TCO) ITO
Transparent Substrate: PEN

Results

The three printed layers solar cell yielded a photovoltaic energy conversion efficiency (PCE) of 0.6%. The crystallinity of the perovskite layer was too low and ETL layer and HTL layer not optimized. The functionality is checked layer by layer. After improving the ETL layer a solar cell with printed ETL and spin-coated perovskite and HTL-layer had a PCE of 16.76%.

Printing

The three layers were printed using industrial printheads. Drop watching allowed the tuning of the waveforms to jet the three different inks. The inks are jetted in greyscale mode with several drops merging into one big drop.

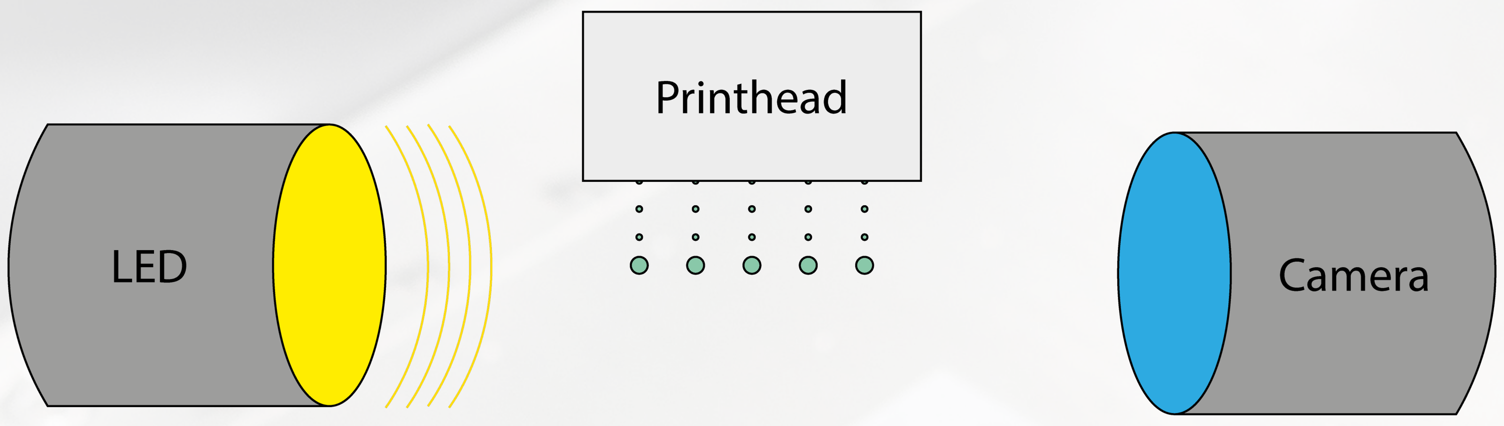

Figure 1: Schema of drop watching setup

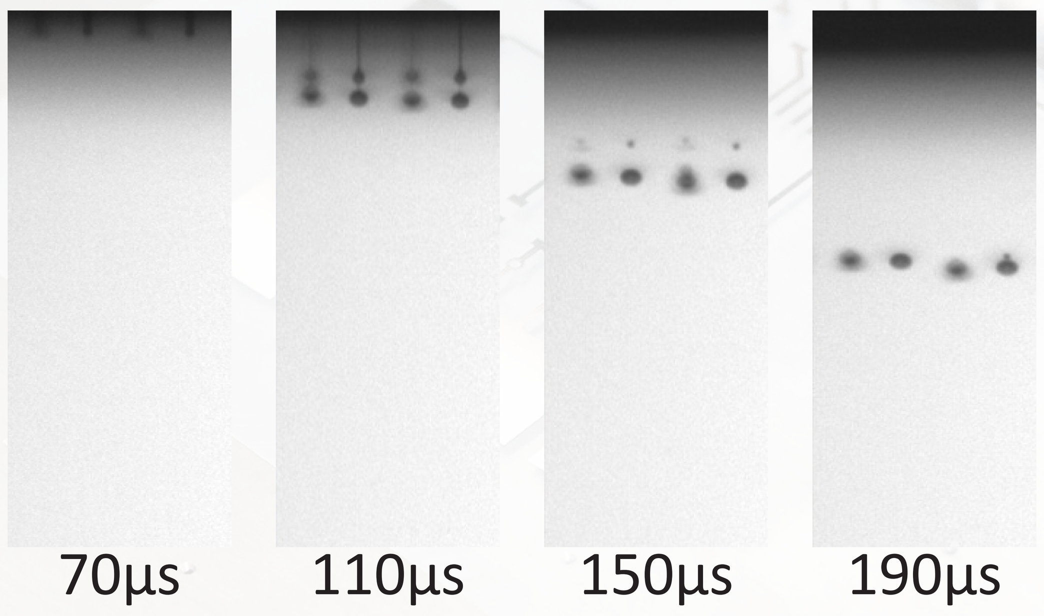

Figure 2: ETL ink drops at different delays after the first pulse

Figure 4: Realised cell array

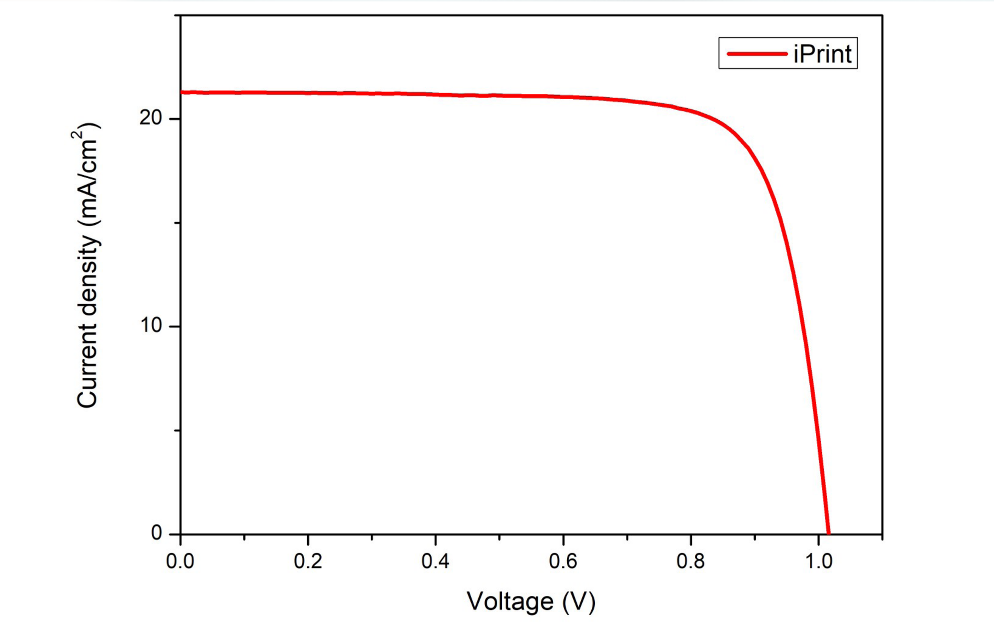

	100.1% Sun
$Power_{in}$	100.054 mW/cm^2
Norm. Std. Dev.	0.04
Module U_{oc}	1.016 V
Cell U_{oc}	1.016 V
I_{sc}	-1.917 mA
J_{sc}	-21.30 mA/cm^2
U_{pmax}	847.81 mV
I_{pmax}	-19.8 mA/cm^2
$Power_{out}$	16.77 mW/cm^2
Total $Power_{out}$	1.51 mW
Fill Factor	0.775
Efficiency μ	16.76%

Figure 3: IV curve for cell with printed ETL and spin coated perovskite and HTL layer

We thank Toyota Motors Europe for funding.

TOYOTA MOTOR EUROPE NV/SA

EDAM Day

marion.dussouillez@csem.ch

Understanding and Mitigating the Degradation of Perovskite Solar Cells Based on a Nickel Oxide Hole Transport Material during Damp Heat Testing

Marion Dussouillez, [a, b] Soo-Jin Moon, [a] Christian M. Wolff, [b] Yongpeng Liu, [c] Jun-Ho Yum, [c] Brett A. Kamino, [a] Arnaud Walter, [a] Florent Sahli, [a] Ludovic Lauber, [a] Gabriel Christmann, [a] Kevin Sivula, [c] Quentin Jeangros, [a, b] Christophe Ballif, [a, b] Sylvain Nicolay, [a] Adriana Paracchino[a]

[a]CSEM SA, Switzerland; [b]PV-Lab EPFL Neuchâtel; [c]LIMNO EPFL Lausanne.

Abstract: The development of stable, large-scale, processable materials is a prerequisite to industrialize perovskite solar cells (PSCs). Beyond the perovskite absorber itself, this prerequisite should also guide the development of the device-contacting layers. In this regard, the use of NiO_x as a hole transport material (HTM) offers several advantages as this inorganic p-type semiconductor can be deposited with high throughput on large flat or textured surfaces via sputtering, a well-established industrial method. However, NiO_x may trigger the degradation of PSCs when exposed to high temperature, light illumination, or humidity. A strong fill factor (FF) loss appears already after 100 hours of damp heat stressing, in conjunction with the appearance of a characteristic S-shaped J-V curve. This poster focuses on the understanding of this degradation.

High Eff vs. Upscaling: the choice of the HTM

- Best efficiencies on 1.04 cm²: MeO-2PACz.
- Better reproducibility over larger areas (15 cm²): NiO_x (continuous coverage).

→ Bilayer **NiO_x/MeO-2PACz**: high efficiency and good reproducibility on large area devices.

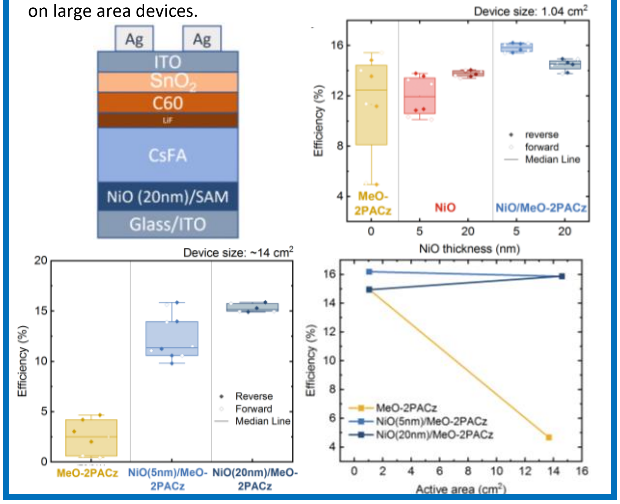

NiO_x leads to the formation of a barrier at elevated T°

NiO_x-based PSCs show strong degradation under damp heat (DH) test (85°C / 85% relative humidity) regardless of the presence of the MeO-2PACz:

- Strong S-shape already visible after 100h of DH → FF and J_{SC} drop.
- Degradation linear with the NiO_x thickness
- Best compromise: NiO_x (5 nm) + MeO-2PACz

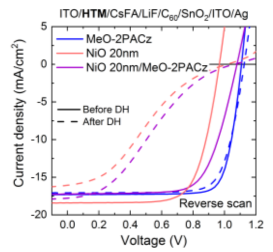

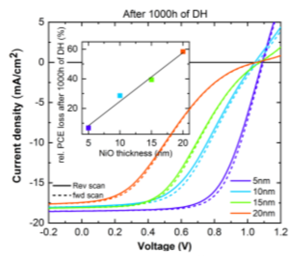

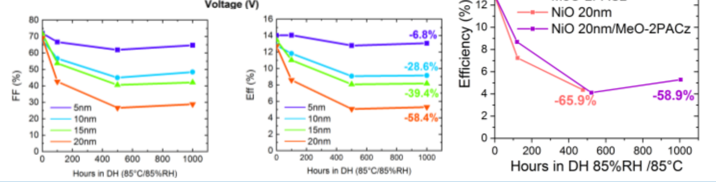

Understanding the degradation diagram

S-shape: barrier extraction?

- PLQY(V): the steeper the slope, the more efficient the carrier extraction.
  → Steeper slope for fresh NiO_x.
  → About aged NiO_x: lower PLQY (≈ 2x) across the whole voltage range for thicker NiO_x.

  Formation of a barrier for hole extraction upon DH testing

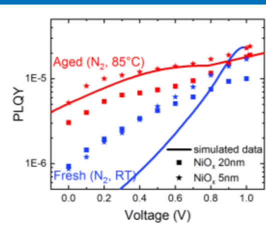

- IV(T) and simulation on SCAPS software:
  → S-shape removes when temperature increases: barrier overcomes
  → to obtained at RT this characteristic S-shape on the simulated aged device and a good FF at 90°C: need to increase the NiO_x band-gap and decrease its doping level simultaneously.

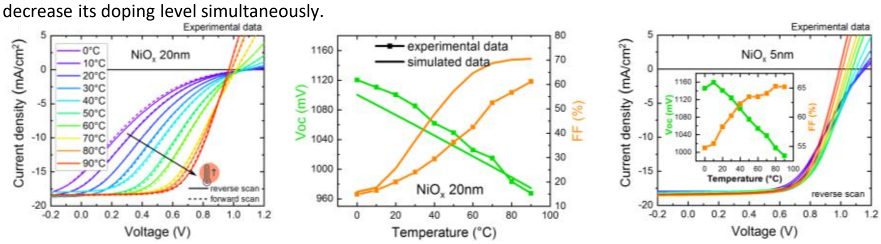

Band diagram

	NiO_x fresh	NiO_x aged
Band gap (eV)	3.66	3.85
E(eV vs vacuum)	-4.56	-4.65
Doping concentration (1/cm³)	$1.01 \times 10^{+20}$	$3.01 \times 10^{+17}$

Values extracted from Tauc plot, EIS measurements and literature.

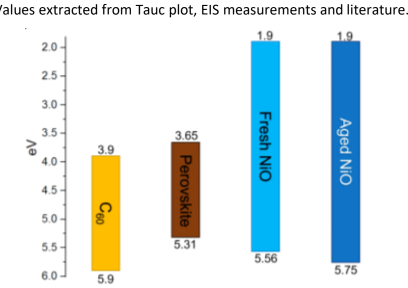

Conclusion

- NiO_x (20 nm) + MeO-2PACz bilayer: high efficiency, good reproducibility over large area (15 cm²).
- However, the thicker the NiO_x, the bigger the cell performances drop during the DH testing: band alignment mismatch between NiO_x and perovskite valence band + drop in NiO_x conductivity.
  → Formation of a barrier that scales with the thickness of the NiO_x layer.

Best compromise: **NiO_x (5 nm) + MeO-2PACz** bilayer:

- **similar efficiencies** on 1 cm² cells and on 14.6 cm² minimodules (16.2% and 14.4%, respectively),
- **superior stability**: the bilayer devices retain **>94% efficiency after 1000 h at 85°C, 85% R.H.**

Tandem solar cells activities at CSEM and EPFL in Neuchâtel

A Walter,[a] XY Chin,[a,b] BA Kamino,[a] A Ingenito,[a] A Descoeudres,[a] A Paracchino,[a] B Paviet-Salomon,[a] D Türkay,[b] F Sahli,[a] K Artuk,[b] M Dussouillez,[a,b] SJ Moon,[a] CM Wolff,[b] Q. Jeangros,[a,*] C. Ballif.[a,b]

[a] Sustainable Energy Center
Swiss Center for Electronics and Microtechnology
Switzerland

[b] Photovoltaics and Thin Films Electronics Laboratory
Ecole Polytechnique Fédérale de Lausanne
Switzerland

* quentin.jeangros@csem.ch

Silicon solar cell technologies approach their efficiency limit

Solar cells using a single light absorber are limited in efficiency to about 30% or less

With a record at 26.7%, best-in-class silicon solar cells are close to their practical efficiency limit (about 27%)

Problematic on the longer term due to the cost distribution of a PV system dominated by balance of system components

Best way to lower the cost of PV electricity is to increase the efficiency of the solar cells/modules (provided this efficiency gain comes at reasonable costs)

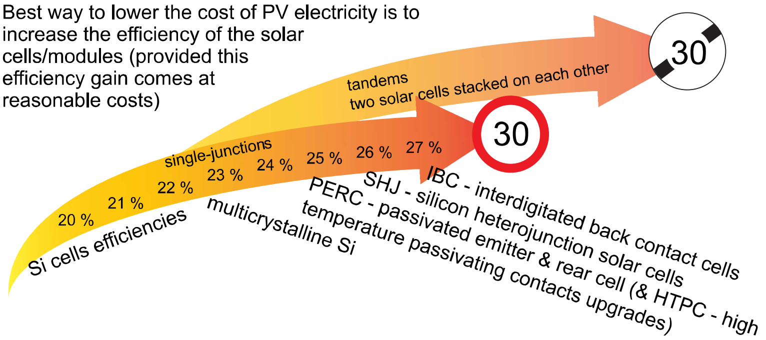

Tandem solar cells promise higher efficiencies

Reduction of losses by adding a second cell on a conventional silicon cell

Silicon, due to its intrinsic optical properties, is an ideal bottom cell

Record efficiency of 32.8% for a III-V-on-silicon tandem solar cell

Metal halide perovskite materials as cheaper alternatives to III-V materials

- Soft deposition conditions (<150°C), tunable bandgap, sharp absorption edge
- High single-junction perovskite performance >25%

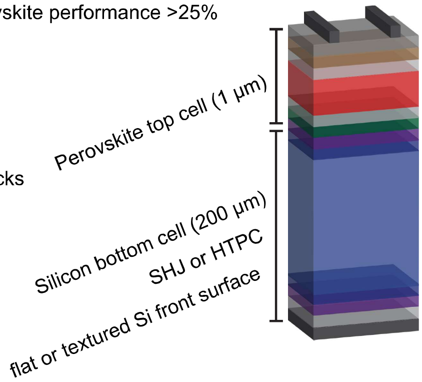

Objectives of the research on tandems at CSEM & EPFL PVLAB

Increase the efficiency of perovskite-on-silicon tandem solar cells by developing materials, processes & device stacks

Scale-up the device dimensions from the 1 cm² of today to full-area >M6 wafers (silicon industry standard)

Develop **cell interconnection & encapsulation processes** leading to minimal cell-to-module losses

Extend the operational stability of perovskite solar cells, ideally to match the standards of silicon-based PV

Literature review of the efficiency of perovskite single junctions & perovskite-on-silicon tandem solar cells as function of device dimension

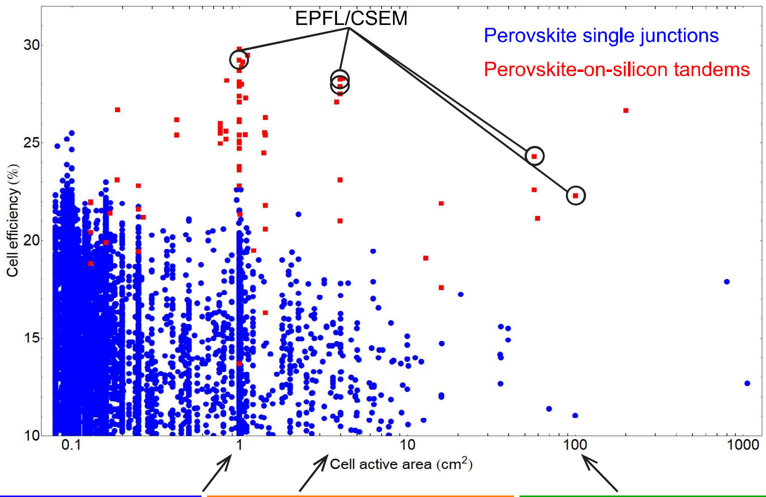

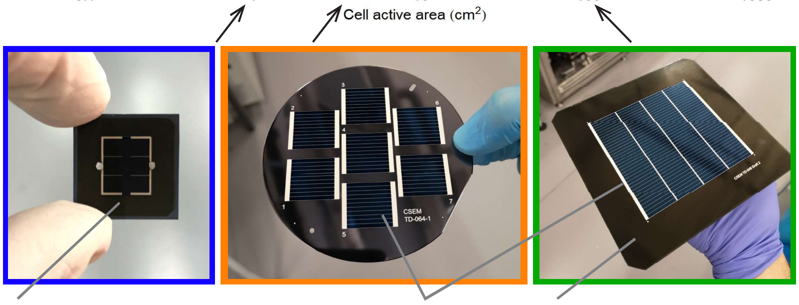

Development of materials & processes on small dimensions

Industrial metallisation method - screen-printing of Ag paste at low temperature

Chemical etching of silicon wafer for compatibility with the deposition of the perovskite by meniscus coating

Current-voltage properties of tandem cells made at EPFL/CSEM as a function of solar cell dimension

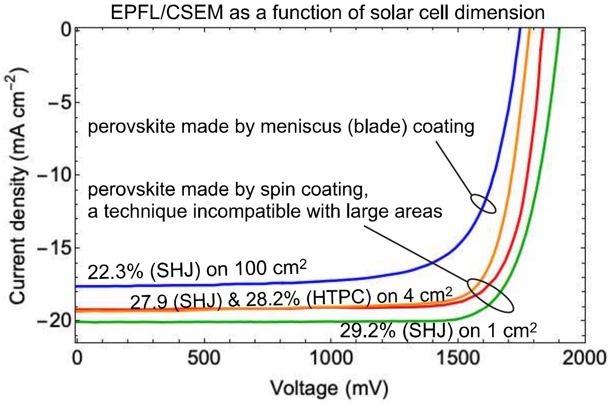

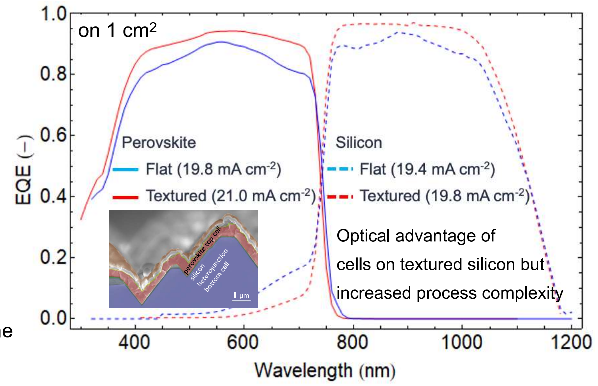

Summary of our results on perovskite-on-silicon tandem solar cells

Demonstration of **state-of-the-art perovskite-on-silicon tandem efficiencies from 1 cm² (29.2%), 4 cm² (28.2%) to 100 cm² (22.3%)**

Perovskite materials & deposition processes compatible with silicon cells that are either **textured (the industry standard) or chemically polished (to simplify the perovskite deposition process) on their front side**

High-efficiencies demonstrated on different types of bottom cells made in-house, **silicon heterojunction & cells based on high temperature passivating contacts** (PERC upgrades)

Demonstration of **processing techniques compatible with mass-manufacturing constraints** (meniscus coating to deposit the perovskite absorber, screen-printing for the front-side metallisation of the tandem)

Tandem solar cells made at EPFL/CSEM pass some of the IEC stability tests (damp heat, thermal cycling), the light soaking stability at elevated temperature needs to be improved (tests & improvements in progress)

Acknowledgments
SNSF (PAPET, EPISODE)
BRIDGE (POWER)
SFOE (INTENT, PRESTO)
European Commission (CHEOPS, PeroCUBE, PertPV, TEXTA)
PVLAB & CSEM teams

SOLARONIX

www.solaronix.com
T +41 21 821 22 80
F +41 21 821 22 89
info@solaronix.com

Solaronix SA
Rue de l'Ouriette 129
CH-1170 Aubonne
Switzerland

A RADICALLY SIMPLER WAY TO MANUFACTURE THIN-FILM SOLAR PANELS ON THE SCALE-UP TO MEET FUTURE PHOTOVOLTAIC GOALS

In partnership with:

Empa
Materials Science and Technology

David Martineau[•], Stéphanie Narbey[•], Anand Verma[•], Toby Meyer[•], René Schneider[*], Jakob Heier[*], and Frank Nüesch[*]
[•] Solaronix SA, Rue de l'Ouriette 129, CH-1170 Aubonne, Switzerland [*] EMPA, Überlandstrasse 129, 8600 Dübendorf, Switzerland

With the support of:

Schweizerische Eidgenossenschaft
Confédération suisse
Confederazione Svizzera
Confederaziun svizra

Swiss Federal Office of Energy SFOE

WHY OUR PEROVSKITE THIN-FILM PANELS?

Photovoltaics are undeniably playing an increasing role in the transition to renewable energy sources. Consequently, solar installations are poised to grow at a staggering rate.

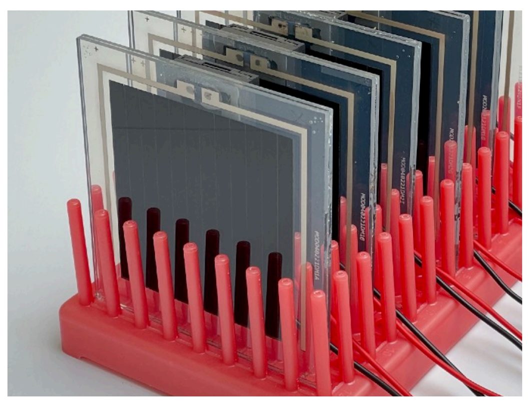

Solar panel manufacturing is particularly under pressure to scale up production in order to match even the most conservative photovoltaic deployment scenarios. Mainstream solar panels have seen impressive improvements in efficiency, though with increased manufacturing complexity.

Affordable solar energy for all

While cost per panel has gradually decreased, the initial investments to build production facilities remains all-time high.

Herein, we demonstrate a radically simpler way to produce stable perovskite thin-film solar panels with extremely low material usage, and industry-proven high throughput techniques.

As a result, we project that such panels will require much lower capital expenditure and achieve unrivaled production cost.

This also represents an opportunity to localize photovoltaic panel production, and hereby further reduce environmental impact.

A TECHNOLOGY THAT SCALES UP

STABLE

The solar architecture presented here rely on a ceramic-like scaffold that's hosting a perovskite absorber. This especially skips the use of the fragile organic compounds commonly employed in other perovskite solar cells, making our technology inherently stable.

Best, we have proven stability of over 11'000 hours under continuous simulated solar sunlight[1]. That is already the equivalent of over 11 years in real daylight cycles!

SCALABLE

Perovskite solar cells are certainly all the rage in scientific research, but very few could actually scale up to any meaningful device area.

Winning technologies can scale up big

Our modules are capable of retaining the same efficiency as obtained with small R&D cells. This is notably thanks to our module design that is already on par with state-of-the-art thin-film panel geometrical fill factor (>93%).

NIMBLE

Ingredients are used in very small amounts: the active component is as thin as a fifth of a human hair.

More importantly, they are only made of low-cost, abundant materials that do not threat of any supply shortage. Our devices don't employ precious metal back-contact but simply rely on a carbon layer instead.

Our wet coating fabrication methods are relying on own-developed functional inks that we formulated with green solvents in the perspective of mass manufacturing.

UNRIVALED EASE OF FABRICATION

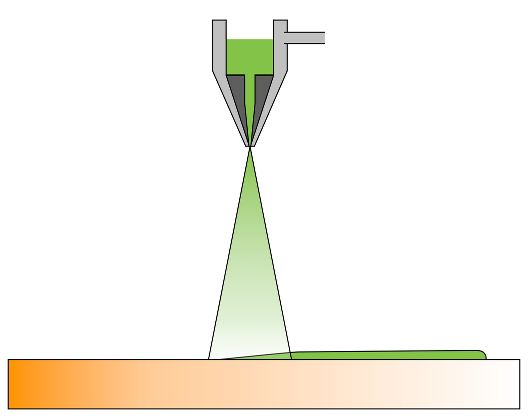

❶ *Spray coating of conductive and underlayer on float glass.*

Likewise any thin-film solar panel, the fabrication starts with a float glass that is coated with a transparent and conductive layer. In the present case, the substrate also takes an underlayer similarly to existing self-cleaning glasses.

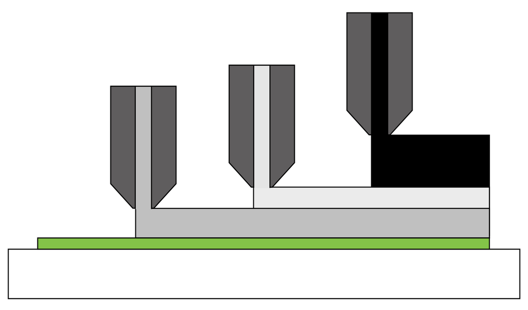

❷ *Slot-die coating of anode, spacer, and cathode layers.*

Next, the layered metal-oxide and carbon structure is deposited by means of slot-die coating[3,4], undeniably the fastest deposition method found in the industry. This is also how electric car batteries are being produced.

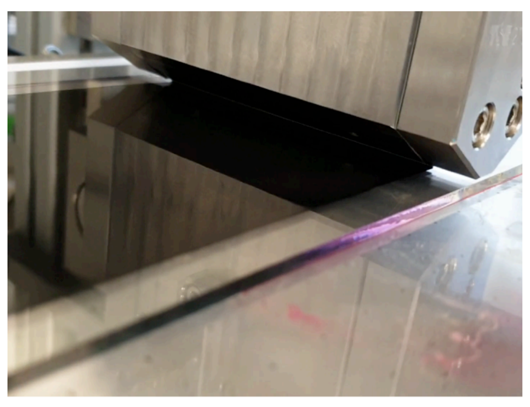

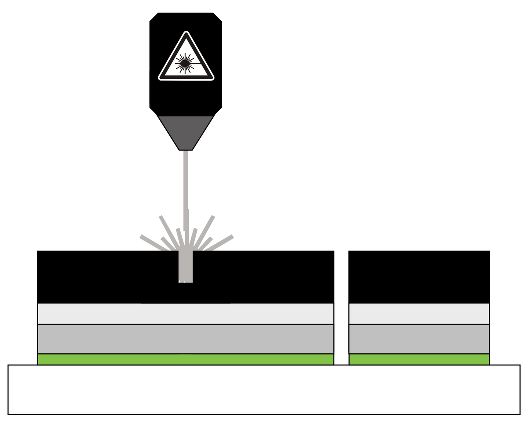

❸ *Selective laser ablation of interconnections.*

Solar cells are individualized and connected in series by selective laser ablation of the different layers. This layout commonly found in thin-film solar panels greatly reduces resistive losses and maximizes power output.

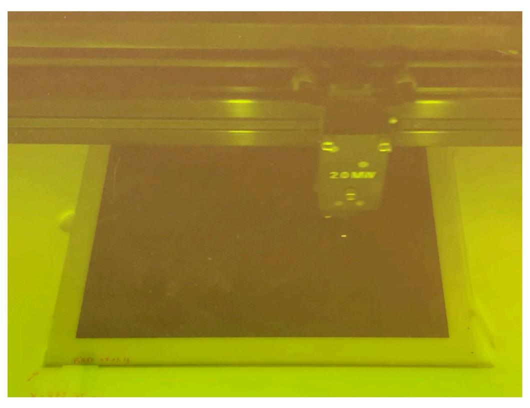

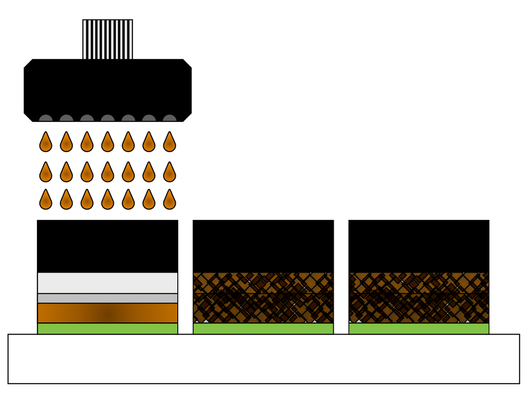

❹ *Deposition and annealing of the perovskite absorber.*

The perovskite absorber is introduced last, via inkjet deposition of a precursor solution that crystallizes upon drying. We found this digital coating method extremely clean and precise, while offering excellent device performance.

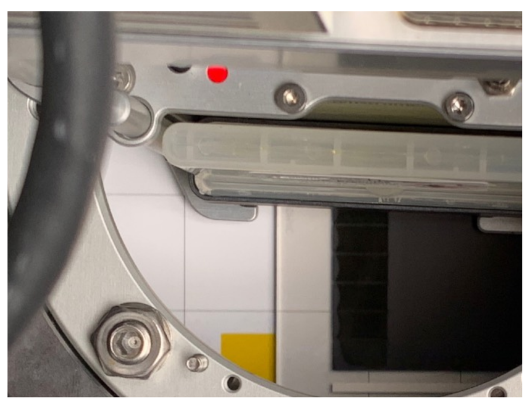

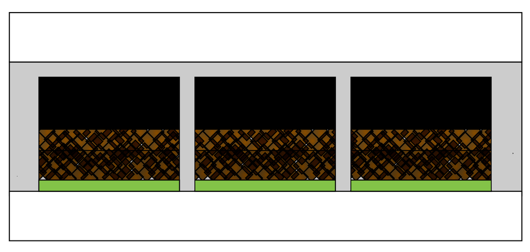

❺ *Lamination and connection with existing methods.*

Finally, the solar module is laminated with a back glass to protect it from the environment, and receives junction box and wiring just like any other solar panel technology.

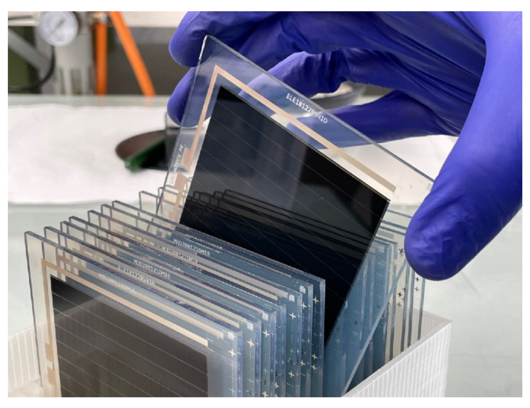

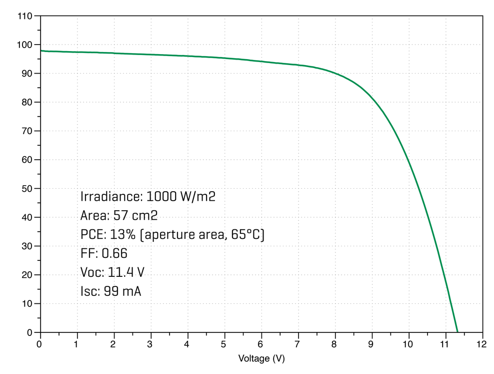

Typical current-voltage plot of a module prototype.

This entire fabrication relies on extremely simple manufacturing processes already being employed in other high volume industries.

A paradigm shift in PV manufacturing

All is realized in ambiant air, and does not require ingot growth nor vacuum deposition. As a result, such photovoltaic panels feature a reduced embodied energy, and a lower carbon footprint than incumbent technologies.

A VERSATILE TECHNOLOGY

In addition to the above fabrication path, we actually developed a host of alternative methods to choose from, depending on targeted application.

Many more options

All of the ingredients could very well be casted by slot-die coating, screen-printing, or even inkjet[2].

While the first offers the highest throughput, the other two printing techniques bring interesting patterning methods, even able to replace laser interconnection patterning.

BILL OF MATERIALS

The active materials employed in our solar technology are so inexpensive that most of the bill of materials is constituted by ancillary items such as glass and encapsulant.

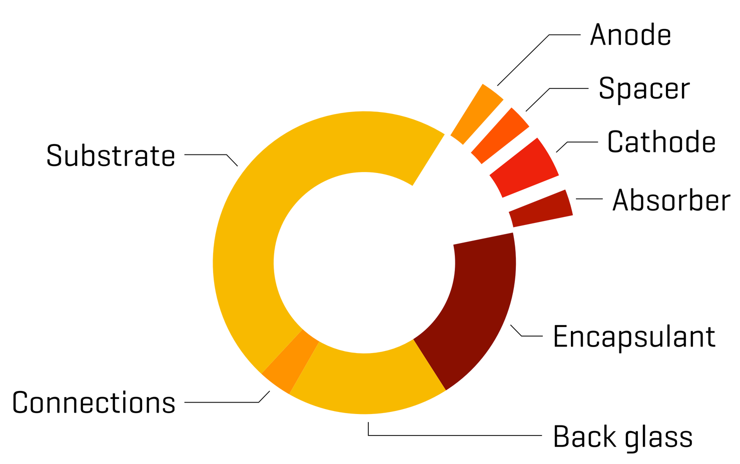

Total materials: 0.07 CHF/Wp

SETUP COSTS

The use of simple fabrication techniques really shines when it comes to capital expenditure. Initial investments are much reduced.

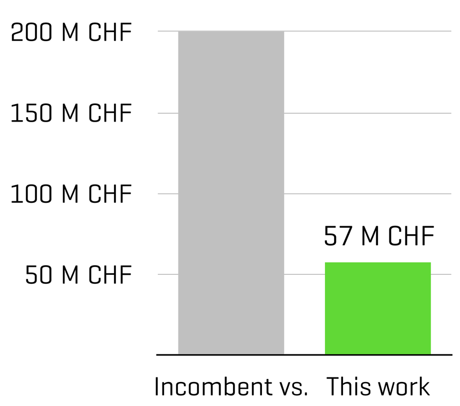

CAPEX for a 2 GWp/year facility

Slashed setup costs & halved production costs

PRODUCTION COSTS

By combining inexpensive materials and extraordinary simple fabrication techniques, we forecast production costs to almost half of incumbent technologies.

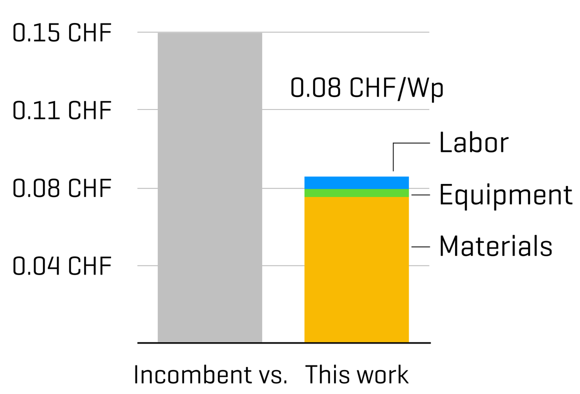

Production cost/Wp

Acknowledgment:

Specials thanks to all of the contributors to this endeavor at EMPA, and the Swiss Federal Office of Energy for their PeroPrint and UPero projects fundings.

References:

[1] One-Year stable perovskite solar cells by 2D/3D interface engineering, Nature Communications 2017, 8, 15684 [doi:10.1038/ncomms15684]
[2] Inkjet printed mesoscopic perovskite solar cells with custom design capability, Mater. Adv. 2020, 1, 153-160 [doi:10.1039/d0ma00077a]
[3] INovel Electronic Device and Method for Slot-Die Depositing Lavers of the Same, Patent WO2019219952A1
[4] INovel electronic device and method for producing layers of the same, Patent WO2019219951A1

Scuola universitaria professionale
della Svizzera italiana
SUPSI

PERFORMANCE ASSESSMENT OF BIPV PRODUCTS:

COMBINED TEST PROCEDURES FOR ELECTICAL AND MECHANICAL SAFETY

P. Bonomo[a]*, F. Parolini[a], F. Frontini[a], M. Caccivio[a], G. Bellenda[a]

[a] SUPSI-ISAAC, Via Flora Ruchat 15, CH-6850 Mendrisio, Switzerland

* pierluigi.bonomo@supsi.ch

ABSTRACT

Building Integrated Photovoltaics (BIPV) sector is progressively achieving an advanced level of technical maturity and market transfer. In the last kilometer for considerable market implementation, major challenges are mostly related to cost-effectiveness and products quality. BIPV multifunctional products are still framed in uncertain certification processes in the EU, in the grey area between electrotechnical and construction sectors, impacting commercialization and market confidence. The standards in force for product certification, such as EN50583, in most national and local contexts are not yet harmonized and imply wide margins of interpretation for product and project requirements. The product's qualification is therefore mainly based on electrical standards for PV (IEC 61215, IEC 61730) and, on the other hand, on procedures for "non-active" traditional construction products in accordance with the prevision of the EU Regulation 305/2011 or by National and Local regulations specific to each country. The H2020 EU project "BIPVBOOST" (www.bipvboost.eu) is focused on obtaining a reduction in costs along the entire production chain by pursuing product and process innovation. New test procedures, which will aim at combining both PV and construction requirements in a harmonized assessment, are being developed and expected to provide a valuable starting point for BIPV manufacturers to ease the assessment of the technical requirements for BIPV products/systems development, as well as for reducing costs of the current testing approach.

STATE OF ART OF CERTIFICATION FRAMEWORK

PV NORMATIVE

IEC 61730-1:2016 *"This international standard defines the basic requirements for various applications of PV modules, but it cannot be considered to en- compass all national or regional codes.*
Specific requirements, e.g. for building, marine and vehicle applications, are not covered"

BUILDING NORMATIVE

EN 50583: 2016 *"Photovoltaic modules are considered to be building-integrated if the PV modules form a construction product providing a function as defined in the European Construction Product Regulation CPR 305/2011 "*

BIPV: DOUBLE CERTIFICATION?

- The CE mark already applied to PV modules is in accordance with the 2014/35/UE (LVD) -EN 61730: the performances are not relat- ed to building application.
- The CE mark for BIPV, according to the CPR 305/2011, has to be released also in accordance with building product harmonized standards or harmonized technical specification (EAD)

TOWARDS A CONSTRUCTION-BASED APPROACH FOR BIPV PRODUCTS

- **Performance-based approach: the concept beyond a pass/fail test-based approach**

The *prescriptive codes* require that each element has a minimum acceptable standard. (PASS/FAIL). It may be hard to define the exact performance levels in BIPV, since the scenarios in the built environment cannot be standardized. The *performance-based* approach does not prescribe the value of the characteristics, nor the criteria for deciding on the suitability of a particular product, but provides the means to assess them for the Limit States. Engineering approach is usually adopted (e.g. in Eurocodes for structural design)

- **Limit states: towards a construction engineering-based approach**

A limit state is a condition of a system (a structure in case of structural engineering where the method was introduced) beyond which it no longer fulfills the relevant pre-defined design criteria. The proposed methodology introduces combined electrical and construction LS considering the product's multifunctionality.

- **Combined stress approach: to consider (non-standard) scenario relevant for BIPV**

The procedures to qualify a BIPV product family will have to deal with composite units for building skin claddings including a functional construction element of the building skin with an external PV active layer for energy production.

EXAMPLES OF NEW TEST PROCEDURES FOR BIPV ELECTRICAL AND MECHANICAL SAFETY

- **BIPV maximum temperatures in non-conventional scenarios of serviceability LS**

Problem:
The integration of passive and active parts and BIPV shading scenarios in operation can introduce additional overheating which can affect max serviceability temperature
Proposal:
Combination of the temp. test (MST21) with non- conventional shading scenarios (IEC TS 63140 "Partial shade endurance testing)
Result:
accurate determination of the maximum temp. in non-conventional operative scenarios

- **BIPV impact resistance for Safeguard and Ultimate LS**

Problem:
the standard test methods (PV and building) don't consider temperatures effects. Moreover, the consequence of impact on electrical parts is not considered
Proposal:
Combination of the impact test (e.g. hard body according to EADs) with temperature by considering both glass and electrical limit states (LS)
Result:
Combination of CPR (impact resistance) and LVD (breakage) tin a combined test

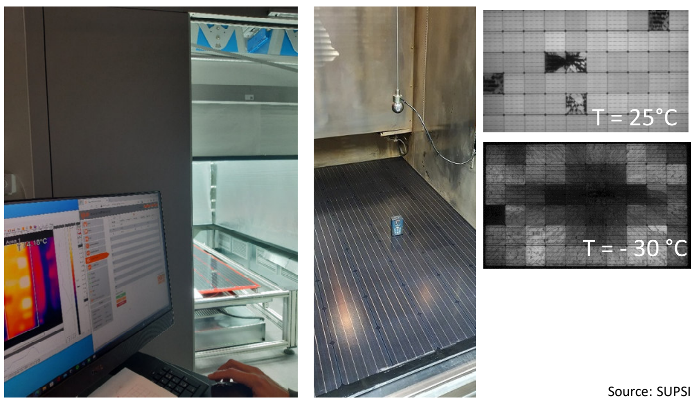

Source: SUPSI

CONCLUSIONS

The construction of multifunctional BIPV products involves more and more the use of several materials in the same component. These elements, electrically active and non-active, assembled together, mutually induce and influence changes both in the energy performance and in the construction requirements. These performance relations have been only partially investigated at the state of art of BIPV quality assessment: it is required to go further than the application of the test methodologies provided separately by the PV or the building regulations. To make tangible innovation, unified and effective procedures ensuring reliable, safe and efficient products for the market in a cost-effective way will have to be developed and transferred in normative, to create a supporting impact on the real market.

Consortium

This project has received funding from the European Union's Horizon 2020 research and innovation programme under grant agreement Nº 817991

Find us on: #BIPVBOOST
www.bipvboost.com

BIPV demo-sites with novel Glass-free colored Lightweight modules

F. Lisco[1], A. Virtuani[1], C. Ballif[1,2]

[1] École Polytechnique Fédérale de Lausanne (EPFL), Institute of Microengineering (IMT), Photovoltaics and Thin Film Electronics Laboratory (PV-Lab), Rue de la Maladière 71b, 2000 Neuchâtel, Switzerland; [2] CSEM, PV-center, Jaquet-Droz 1, 2000 Neuchâtel, Switzerland

Lightweight PV modules with a **weight of 5-6Kg/m** (compared to 15-20Kg for conventional BIPV products) are **manufactured by EPFL**.

*By substituting typical front glass, with a thin ETFE polymer sheet, the "combi-encapsulant", as a front sheet, and replacing the standard back sheet with a composite, Al-honeycomb core, sandwich structure

CSEM and **EPFL** are currently **combining their technologies** to develop ***Ligthweight/coloured BIPV products.***

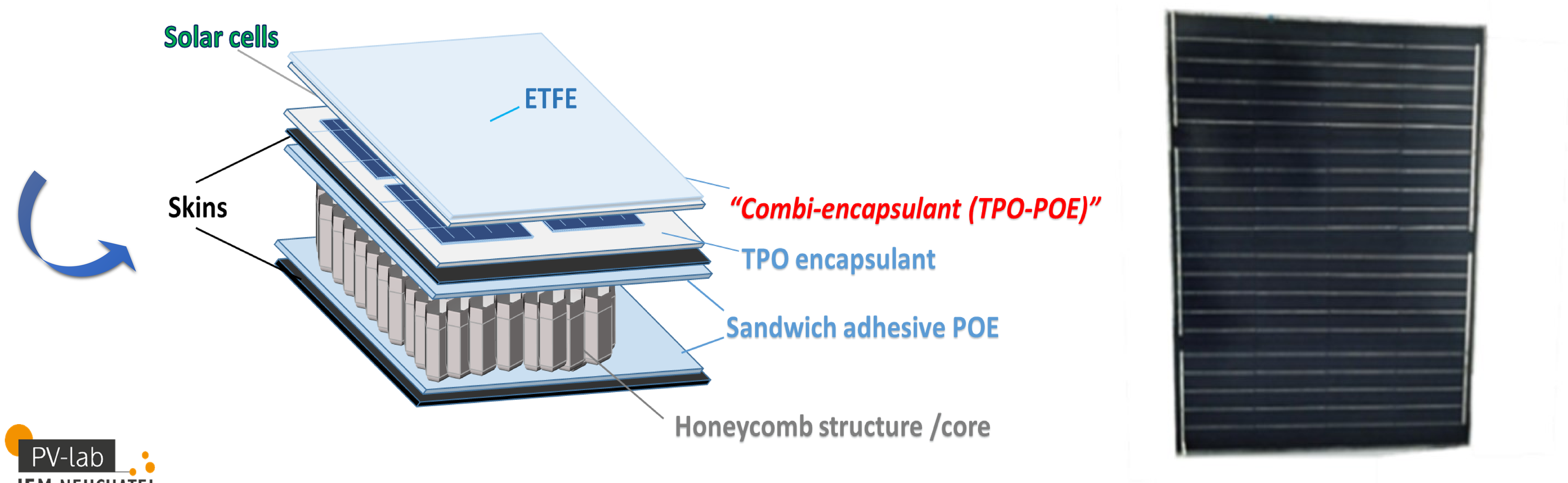

Figure 1: Schematic diagram of the LW structure proposed for this work; 16-cells LW PV modules manufactured @EPFL

Lightweight glass-free crystalline silicon (c-Si) **PV modules** with the standard and colored configuration,, will be installed on two BIPV demo sites, in UK and Romania, as part of the goals of a H2020 European project, **RE-COGNITION** [*https://re-cognition-project.eu/*].

Preliminary view of demo PV systems

Case Study 1
Corby (UK)

Case Study 2
Technical University
of Cluj-Napoca (Romania)

Figure 2: prototype of the2 demo sites for the installation of ventilated façades with LW glass-free c-Si PV modules

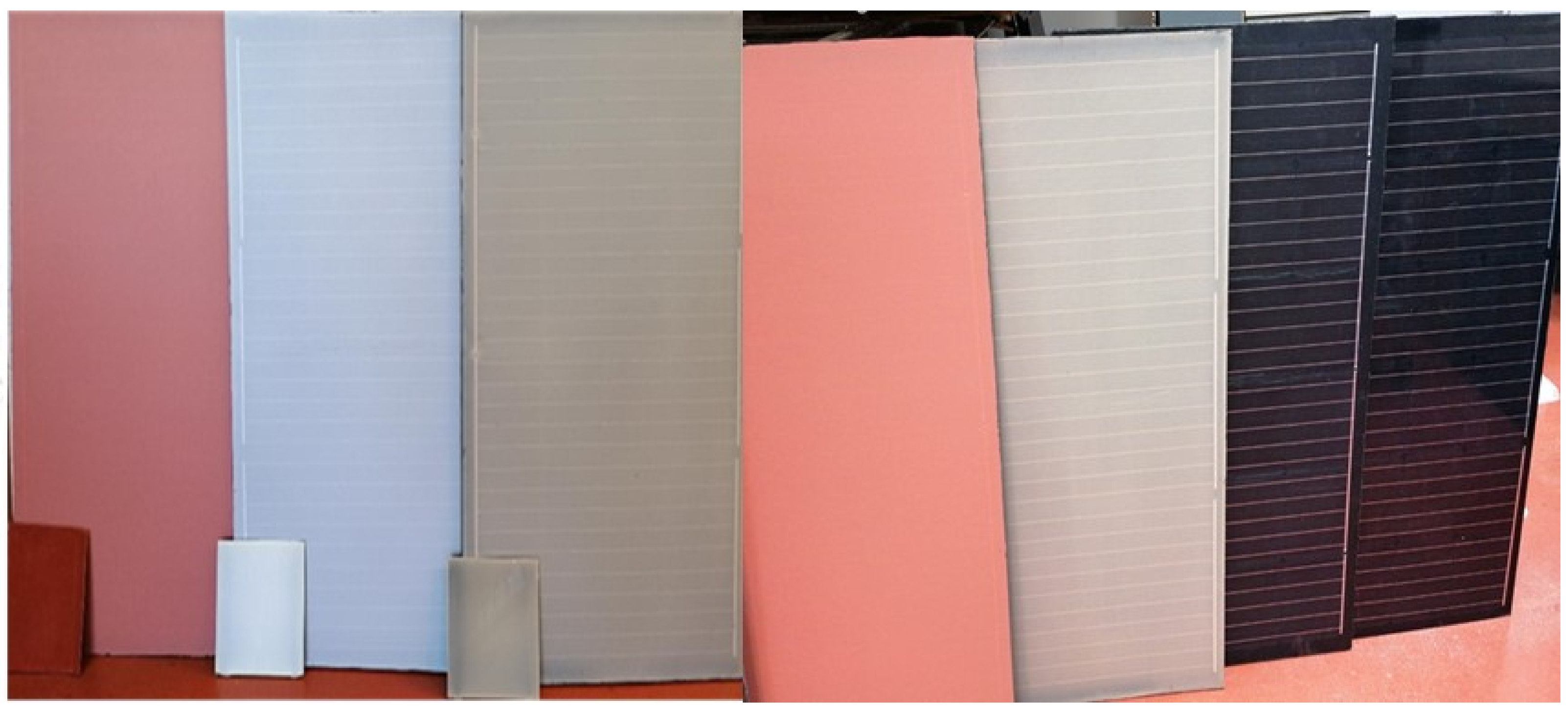

Figure 3: photo of colored (0.1x1) m2 LW PV modules and the respective mini-modules at the bottom

Reliability and **long-term performance** ↔ careful **optimization** of the **module structure** and **processing methods** as careful **materials selection!** static **mechanical load (SML)**, and **fire test**; showing no degradations, nor visual defects (delamination, corrosion, or bending of the module).

Excellent mechanical performance

This is one of the most challenging test to pass, since the rigidity of the glass is missing and the integrity of the solar cells is exposed to high risk.

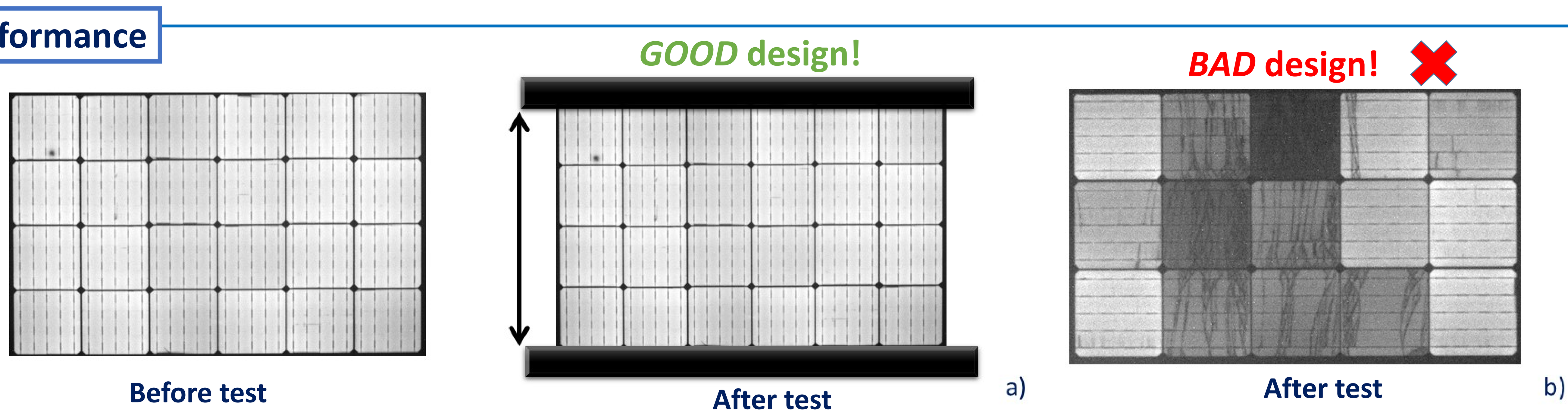

Figure 5: EL images of a 24-cells LW PV module, before and after being exposed to the mechanical load test (a); example of bad design and failure after the mechanical test(b)

Excellent resistance to HAIL impact

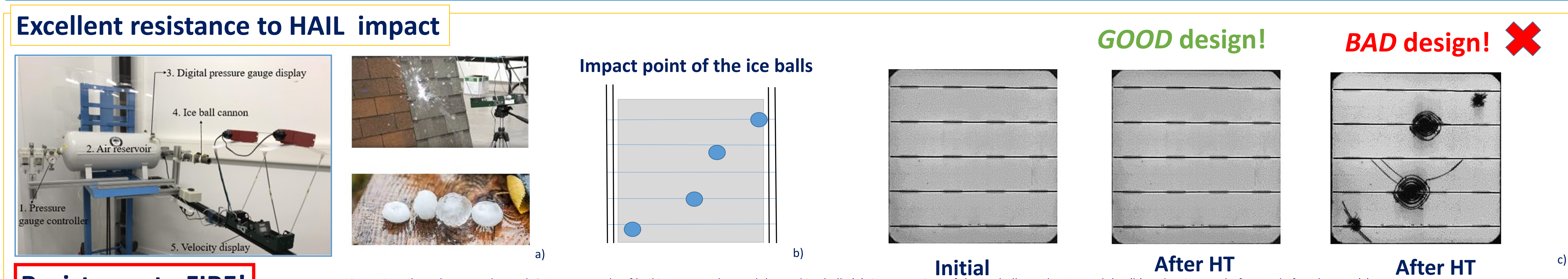

Figure 6: Hail test homemade used @EPFL, example of hail impact on the modules and ice balls (a), impact points of the ice balls on the PV modules (b) and EL images before and after the test (c)

Resistance to FIRE!

Preliminary test performed at a "fire station" gave promising results: with both colored and standard configurations the fire self-extinguished, leaving the structure with obvious, inevitable defects, primarily by visual inspection.

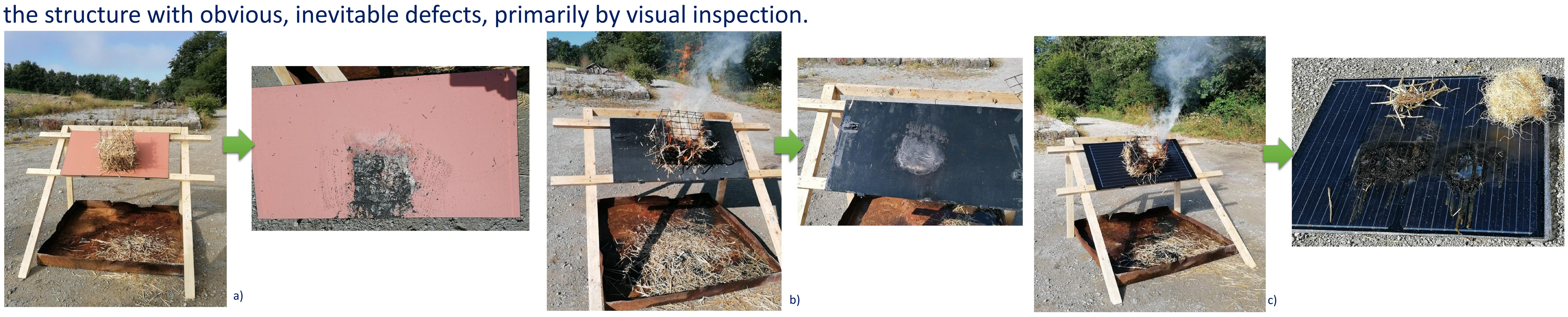

Figure 7: preliminary results of the fire test, performed on colored LW PV modules (a); at the back of the LW PV module(b), and on the standard black LW PV modules ©

In summary:

*Robust and resilient glass-free lightweight c-Si PV modules, with a weight of ~5Kg/m2, were designed with optimal BOM
*successfully passing the criteria of the IEC 61215 and 61730, maintaining high optical properties and ideal thermo-mechanical performances.
*Within the frame of a an H2020 European project, RE-COGNITION, two BIPV ventilated façades will be realised, in UK and Romania, as part of the final goals.

Acknowledgments
This research project is part of the H2020 European Project RE-COGNITION GAID: 815301

University of Applied Sciences and Arts of Southern Switzerland
SUPSI

SWISSOLAR

energieschweiz

VSE AES

Schweizerische Eidgenossenschaft
Confédération suisse
Confederazione Svizzera
Confederaziun svizra

Swiss Federal Office of Energy SFOE

20. Nationale Photovoltaik-Tagung

Swiss fire safety framework on BIPV – new fire test procedures

Fabio Parolini*[1], Pierluigi Bonomo[1], Francesco Frontini[1], Mauro Caccivio[1], Giovanni Bellenda[1]

[1] ISAAC, University of Applied Sciences and Arts of Southern Switzerland (SUPSI), Mendrisio, Switzerland.

*Corresponding author: fabio.parolini@supsi.ch

SWISS FRAMEWORK

The Swiss confederation is an extra European country but it has undersigned mutual recognition agreements (MRAs) with the European Community.

The EU regulation 305/2011 (CPR) has been adopted by Swiss legislation

BUILDING MATERIALS COULD BE CLASSIFIED

- according **to the EN standard** (SN EN 13501-1:2009; SN EN 13501-5:2009; SN EN 13501-6:2014)
- or according **to VKF/AEAI** carried out on the basis of the provisions determining for the recognition of the VKF/AEAI (Fire protection standard, fire fighting directive, fire fighting support publication, solar systems firefighting memorandum)

V K F A E A I

BUILDING REQUIREMENTS

- Construction Products Regulation (CPR)
- EN 50583 "Photovoltaics in buildings - Part 1/2: BIPV modules/systems"

ELECTRICAL REQUIREMENTS

- Low Voltage Directive (LVD) (2014/35/EU)
- Electromagnetic Compatibility Directive (EMCD) DIRECTIVE 2014/30/EU

MISSING GAPS ON BIPV FIRE SAFETY STANDARDS

- Electrical and building separation
- Harmonised standards leakage
- Test procedures only for non-active products only

NEW REFERENCE AND TEST PROCEDURES ARE DEVELOPING

CEI TR 82-89:2021 – PV ON ROOF

Today fire tests are based on separate tests results which are carried out separately on photovoltaic modules and on roof element and not on real assemblies made of PV module and roof portion.

In Italy, the technical report **CEI TR 82-89:2021** has been published. The document's aim is the development of specific tools for the fire rating of PV modules placed, with different technical solutions, on the building roof performing tests on the **complete system** (PV module system plus a representative portion of the roof covering) to get the fire behavior of the complete assembly.

Source: Istituto Giordano S.p.A.

CEN EN 13501-1
CEN EN 13823
CENELEC TR 50670

HRR (Heat Release Rate) [kW] *(figure 01)*
THR (Total Heat Release) [MJ] *(figure 02)*
FIGRA (FIre Growth RAte) [W/s] *(figure 03)*
SPR (Smoke Production Rate) [m^2/s],
TSP (Total Smoke Production) [m^2],
SMOGRA (SMOke Growth RAte) [m^2/s^2],
LSF (Lateral Spread of Flame) fire towards the side "far" from the sample burner) [mm];

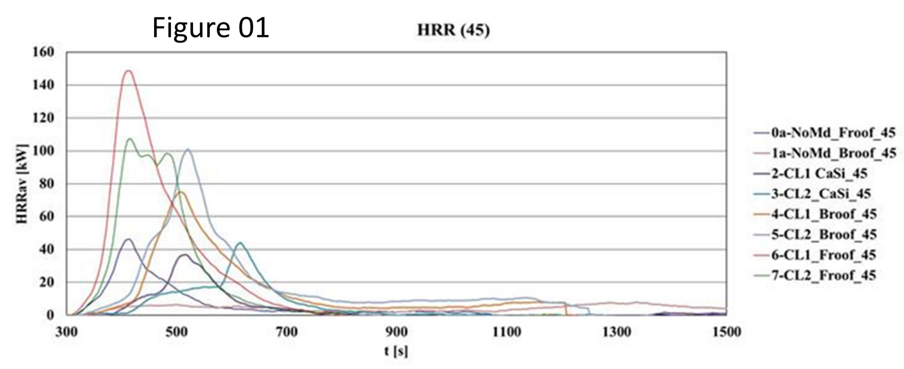

Figure 01

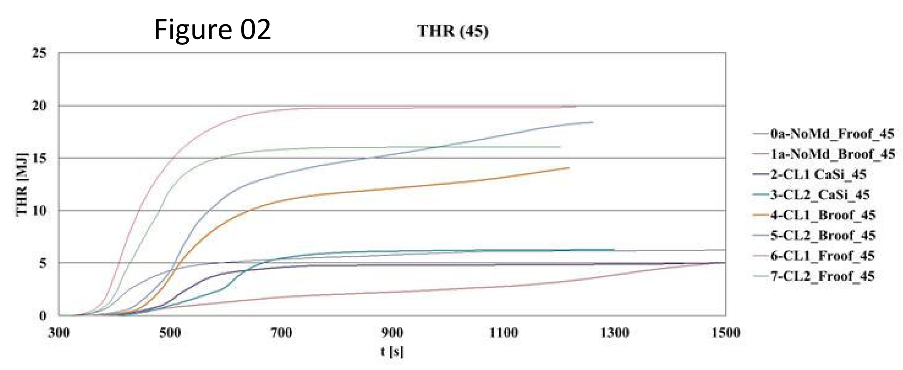

Figure 02

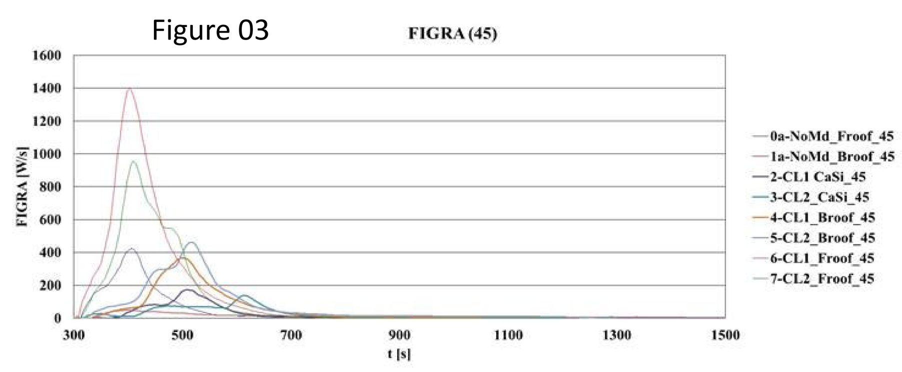

Figure 03

Source: Istituto Giordano S.p.A.

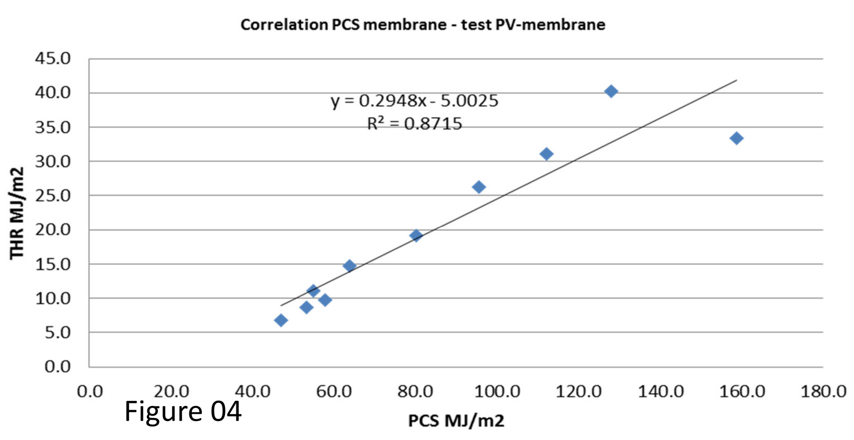

Figure 04

Source: Istituto Giordano S.p.A.

RESULTS

Different tests have been performed according to the new procedure by the partners

- National classification is inconsistent with the classification resulting by tests
- Dependence of the fire behavior and fire rating from the substrate
- HHV (high heating value) correlation with fire rating *(figure 04)*

NEW TESTING PROCEDURES UNDER DEVELOPING

- Combination of building and electrical requirements
- Interference of the active part (PV)
- fire behavior changing with aging

Instrument	Reference
SBI Platform	EN 13823 test
Small Flame attack	EN ISO 11925-2 / EN 61730-2
Calorimetric bomb	ISO 1716
Cylindrical furnace	ISO 1182
Flammability Classification	IEC 60695-2-11 / = UL 94

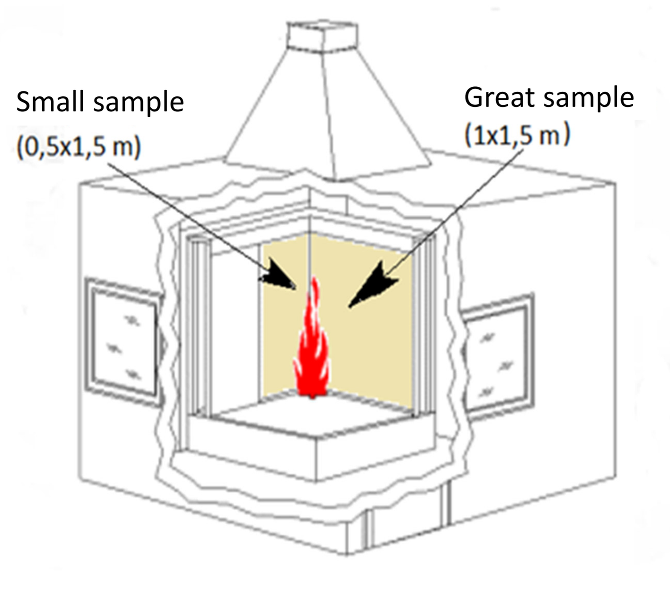

ELECTRICAL INSULATION DURING THE TEST APPLYING AN ELECTRICAL LOAD

E.G. - Test Voltage applied between the PV circuit (+/- shorted) and a ground reference – Insulation mode

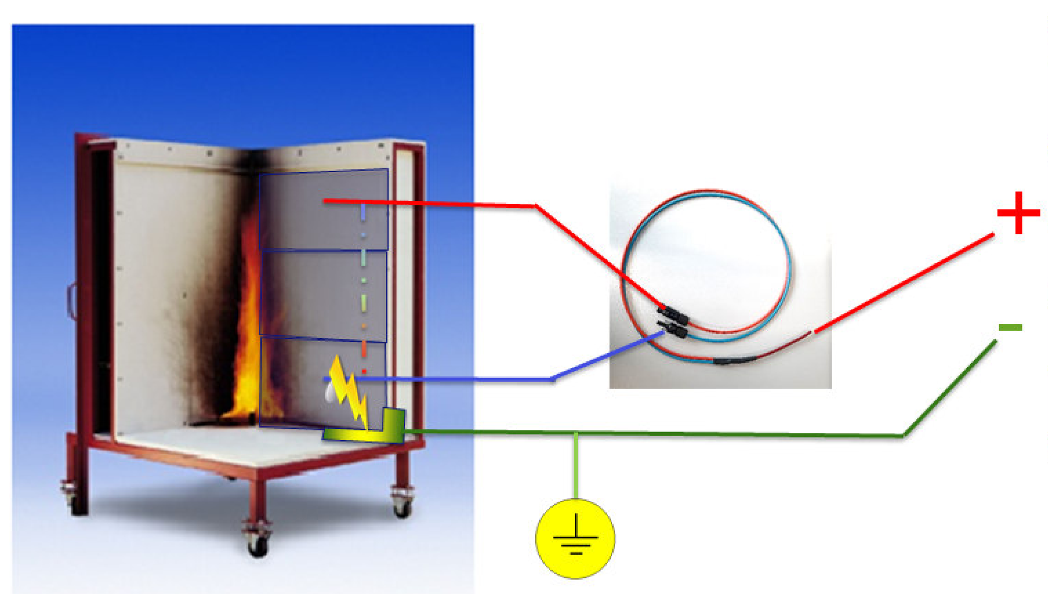

HV Power supply (or Insulation tester)
TEST VOLTAGE= Max System Voltage of the PV module (i.e. 1000 V or 1500V) to be applied continuously during the test.

- Case a): if the array is exposed to the light, the PV circuit will carry a current (up to Isc if G=1000W/m²)
- Case b): if the array is in the dark or quasi dark conditions, the flowing current will be nearly =0

Acknowledgment: Part of this contribution is developed in collaboration with Istituto Giordano, Ricerca Sistema Energetico (RSE) and Corpo Nazionale Vigili del fuoco VVF and in the framework of BIPVBOOST Project

ISTITUTO GIORDANO · RSE · CSTB · BIPV boost

This project has received funding from the *European Union's Horizon 2020 research and innovation programme under grant agreement N° 817991*

Building-integrated photovoltaics (BIPV): more than a necessity for our building culture

SUPSI

University of applied sciences and arts of southern Switzerland
Department for environment construction and design
Institute for applied sustainability to the built environment

The Energy Strategy 2050 represent a major challenge for building culture (Baukultur). Energy renovation of the building stock, solar energy and especially photovoltaics are of central importance. Solar systems are still afflicted with many negative prejudices to be integrated into historical and existing buildings and disfigure our landscapes. Today's innovative building-integrated photovoltaic (BIPV) solutions open up completely new architectural and aesthetic design, which should significant increase their acceptance. Well-conceived solar installations are more than a technical necessity paying a role to rediscover and valorize traditional alpine architecture, expression of a building culture that focuses on people and their needs and form an important basis for sustainability. Three main research experiences show ways to preserve and develop historic buildings in a culturally sensitive way, applying energy efficiency principles and optimizing existing best practices. To this end, tools and strategies can be applied also to historical buildings contributing the energy efficiency, sufficiency, decarbonisation, and climate change adaptation challenges.

RENOVATION PROCESS

HERITAGE SIGNIFICANCE

ATLAS project aims at (re-) discovering and valorizing traditional alpine architecture (beyond the level of protection). HiBERatlas database, presents best-practice examples of how historic buildings can be renovated to achieve high levels of energy efficiency while respecting and protecting its heritage significance.

www.alpine-space.org/projects/atlas/en/home

Highlights Swiss best-practice examples:

ENERGY	LISTED	AGE	BiPV-Solar	COST
Energy performance 26 to 66 kWh/m²y **Energy performance** NZEB – Minergie	**Listed?** Maximum / Medium / Not listed **Conservation area?** Yes / No	**Age** 1400-1850-1950 **Renovation period** 2014 - 2018	**Power supply** 24kWp – 136 kWp **Self-sufficient rate** 17% – 345%	**Investment energy renovation** 775 – 4'740 CHF/m² **PV/BIPV Plant cost** 785 – 1'960 CHF/m²

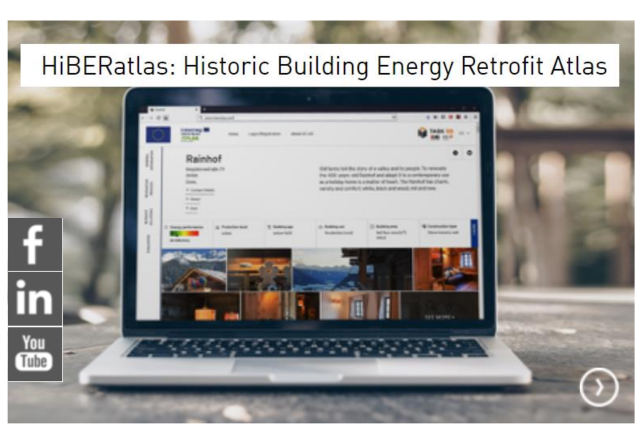

HiBERatlas - Historic Building Energy Retrofit Atlas

RETROFIT SOLUTIONS

ENVELOPE, WINDOWS, HVAC, SOLAR

Ideas and inspiration on how solar and BiPV work in synergy with other renovation measures to make our buildings more energy efficient. HiBERtool documents solutions for windows, walls, ventilation, heating and solar. A decision tree filters to the documentation and technical information that are interesting for your project.

www.hiberatlas.com / www.hibertool.com

After

Best-practice case example:
Glaserhaus - Affoltern im Emmental (BE-CH)

Envelope: Roof and façade returned to their original shape to ensure the load-bearing capacity with new insulation between the wooden rafters to achieve the Minergie-P standard
Windows: Replica windows with the same characteristics and dimensions as the previous ones were made, but which could accommodate a triple glazing.
HVAC: RES implementation - geothermal boreholes and DHW system is integrated in the heating system
Solar: integrated BIPV

Before

RENEWABLE ENERGY

BiPV MEETS HISTORY

Photovoltaic technology has made gigantic steps, and today it offers aesthetically pleasing and harmonically integrated solutions in the landscape. The "BIPV meets history" project allows new business opportunities to all players in the supply chain: planners, designers, architects, builders through networking and training.

www.bipvmeetshistory.eu

ENERGY EFFICIENCY
Up to 100% energy savings

CUSTOMIZATION
100% customisable building skin

COST BENEFIT
Payback time of approximately 10 years

Innovative solar BIPV products developed by Swiss PV manufactures: (a) [2021, Sunage SA]; (b) [2021, Solar Retrofit Sgal]

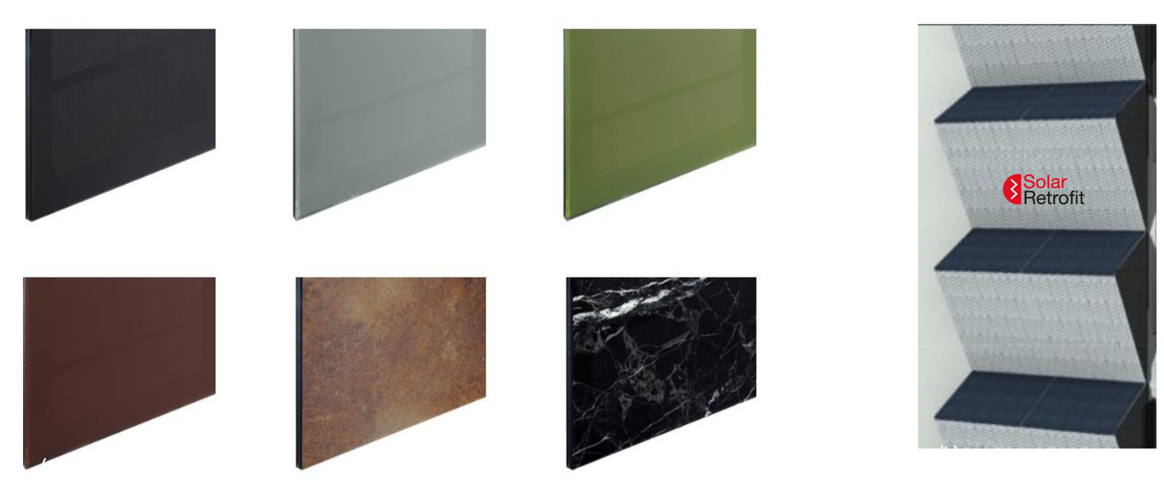

Operation co-financed by the European Union, the European Regional Development Fund, the Italian State, the Swiss Confederation and the Cantons within the framework of the Interreg V-A Italy-Switzerland Cooperation Programme. (Project code 603882)

Interreg Fondo Europeo di Sviluppo Regionale ITALIA SVIZZERA - ITALIE SUISSE - ITALIEN SCHWEIZ — UNIONE EUROPEA — Repubblica e Cantone Ticino
BIPV MEETS HISTORY
PV meets history

Interreg Alpine Space ATLAS — TASK 59 SHC

HISTORIC BUILDING ENERGY RETROFIT ATLAS

A best-practice database of exemplary energy efficient interventions in historic buildings

Photo credits from right to left, from top to bottom: (a) Rural building Galley (FR, CH), photo © solaragentur.ch; (b) Rural building Glaserhaus (BE, CH), photo © C. Martig; (c); Industrial building Solar Silo (BS, CH), photo © M. Zeller; (d) Schlossgut Meggenhorn, Meggen (LU, CH), photo © C. Martig; (e) Apartment building Magnusstrasse – Zürich (ZH, CH), photo © M. Mobiglia SUPSI; (f) Hôtel des Associations (NE, CH) photo© C. Martig; (g) Single Family House –Gstaad, Bern (BE-CH), photo: ©Solar agentur schweiz Swiss Solar prize 2019; (h) MFH Kettner, 5620 Bremgarten (AG. CH), BFE-; (i) Doragno Castle, Doragno (TI, CH) Source: DeltaZero Architects, photo © L. Carugo; (j) PEB-Ebmatingen Church (ZH, CH), photo: © Swiss Solar prize 2019; (k) Kindergarten and apartments, Chur (GR, CH), photo © R. Feiner Malans; (l) SFH Hütterli Rothlisberger (BE, CH), photo © C. Martig.

University of Applied Sciences and Arts of Southern Switzerland
SUPSI

Contacts:

Institute for applied sustainability to the built environment

Innovative Building Envelope Team
Swiss BiPV Competence Center
Dr Arch. Cristina S. Polo López
T +41 (0)58 666 63 14
cristina.polo@supsi.ch
www.supsi.ch/isaac

Head of Building System Sector
Dr Frontini Francesco
T +41 (0)58 666 63 20
francesco.frontini@supsi.ch
www.supsi.ch/isaac

SOLARCHITECTURE
sun as a building material
https://solarchitecture.ch/

Performance comparison of a P370 power optimizer system and a string inverter system

Cyril Allenspach, Arturo Bänziger, Andrin Schneider, Franz Baumgartner, Fabian Carigiet

ZHAW IEFE Winterthur, www.zhaw.ch/=bauf

Zürcher Hochschule für Angewandte Wissenschaften

Research objectives

- Yearly performance comparison of a residential decentralized SolarEdge P370 buck-boost power optimizer system and a centralized string inverter (SINV) system under unshaded and partially shaded (chimney and tree) conditions.
- Analysis of voltage conversion performance for a SolarEdge P370 power optimizer.

Methodology

- Indoor laboratory measurements were used to create a system model. The system model was fed into a ZHAW ray tracing simulation tool, allowing yearly performance comparisons of various system configurations at minute time steps (Table 1). Both systems were fitted with the optimum number of modules for the optimizer system.
- Simulation results are presented in the form of a MLPE gain. MLPE gain represents the value of the shading adaption efficiency of the optimizer system when compared to the SINV. The shading adaption efficiency (SAEta) describes the performance of SINV and MLPE systems based on the same reference – the theoretical performance of a lossless system with module-level tracking for a specific shading case [1][2][3] (Figure 1):

$$\eta_{shad,a}\ (SAEta) = \frac{P_{ac}}{\sum_{i=1}^{k} P_{mod,i}}$$

Table 1: Datasheet values of simulated system configurations

	PV Modules	# PV Modules	String inverter system	MLPE system Inverter	MLPE system Power Optimizer
1 Phase	Pn = 400 W 60 Cells 3 bypass diodes	12	Huawei SUN2000-3.68KTL-L1 Uin,rated = 360V EURO-Eff = 97.3%	Solaredge SE3500H Uin,rated = 380V DC/AC EURO-Eff: 98.8%	Solaredge P370 DC/DC Efficiencies: Wght.-Eff = 98.8% Max.-Eff = 99.5%
3 Phase		14 & 21	Fronius Symo 10kW Uin,rated = 600V EURO-Eff = 97.4%	Solaredge SE10k Uin,rated = 750V DC/AC EURO-Eff: 97.6%	

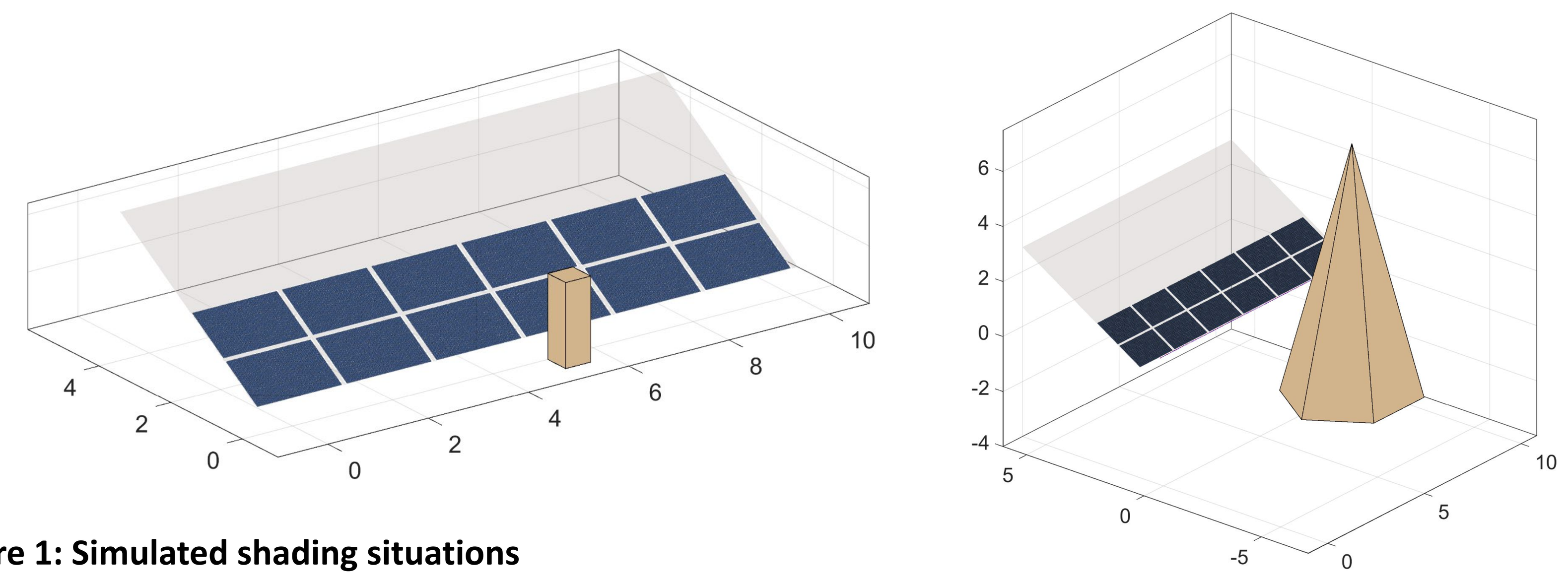

Figure 1: Simulated shading situations

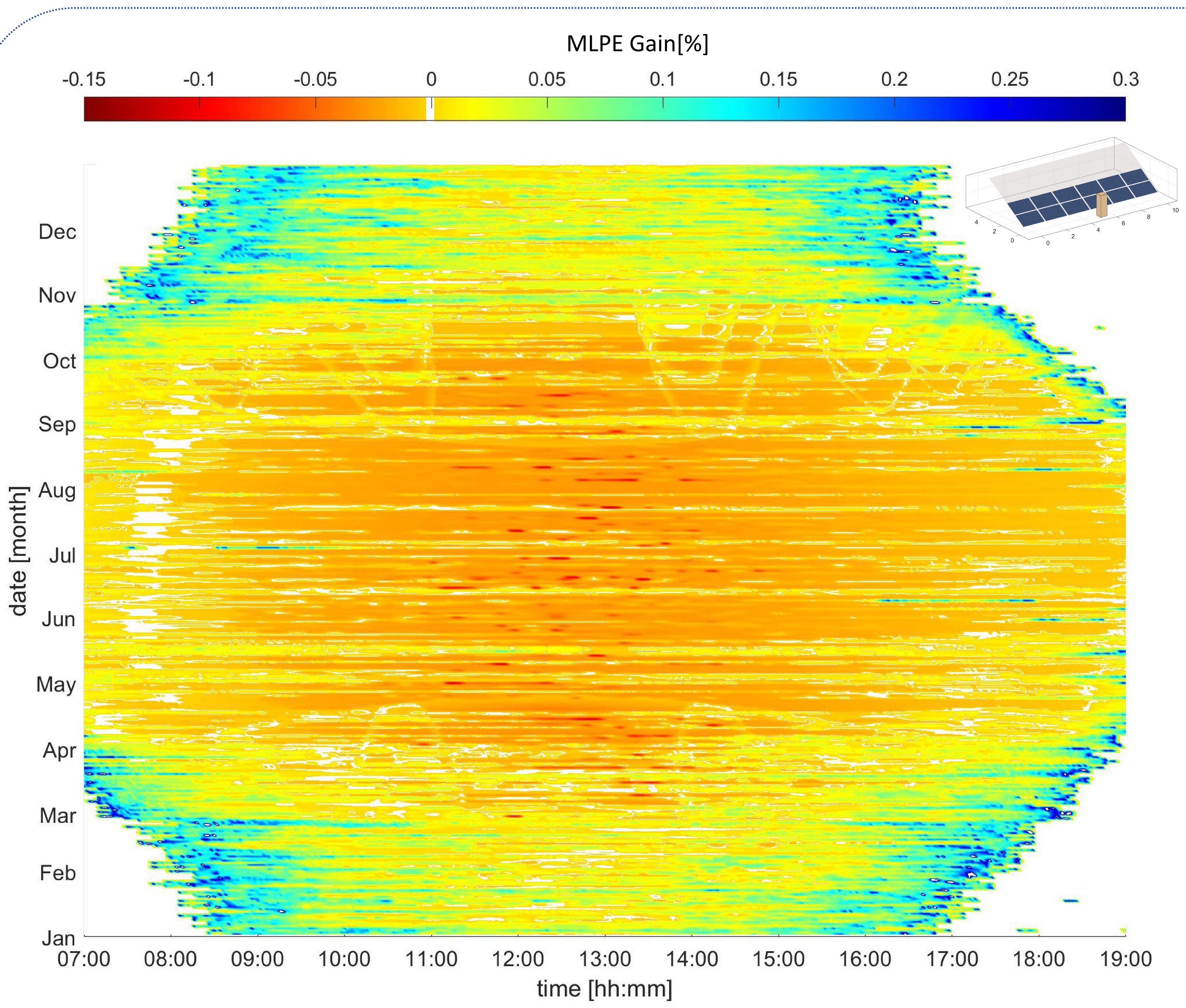

Figure 2: Yearly MLPE gain [%] (combined DC/DC & DC/AC efficiency) for a 3 phase system partially shaded by a chimney, dt=2min, simulation output of the ZHAW MLPE Shade software.

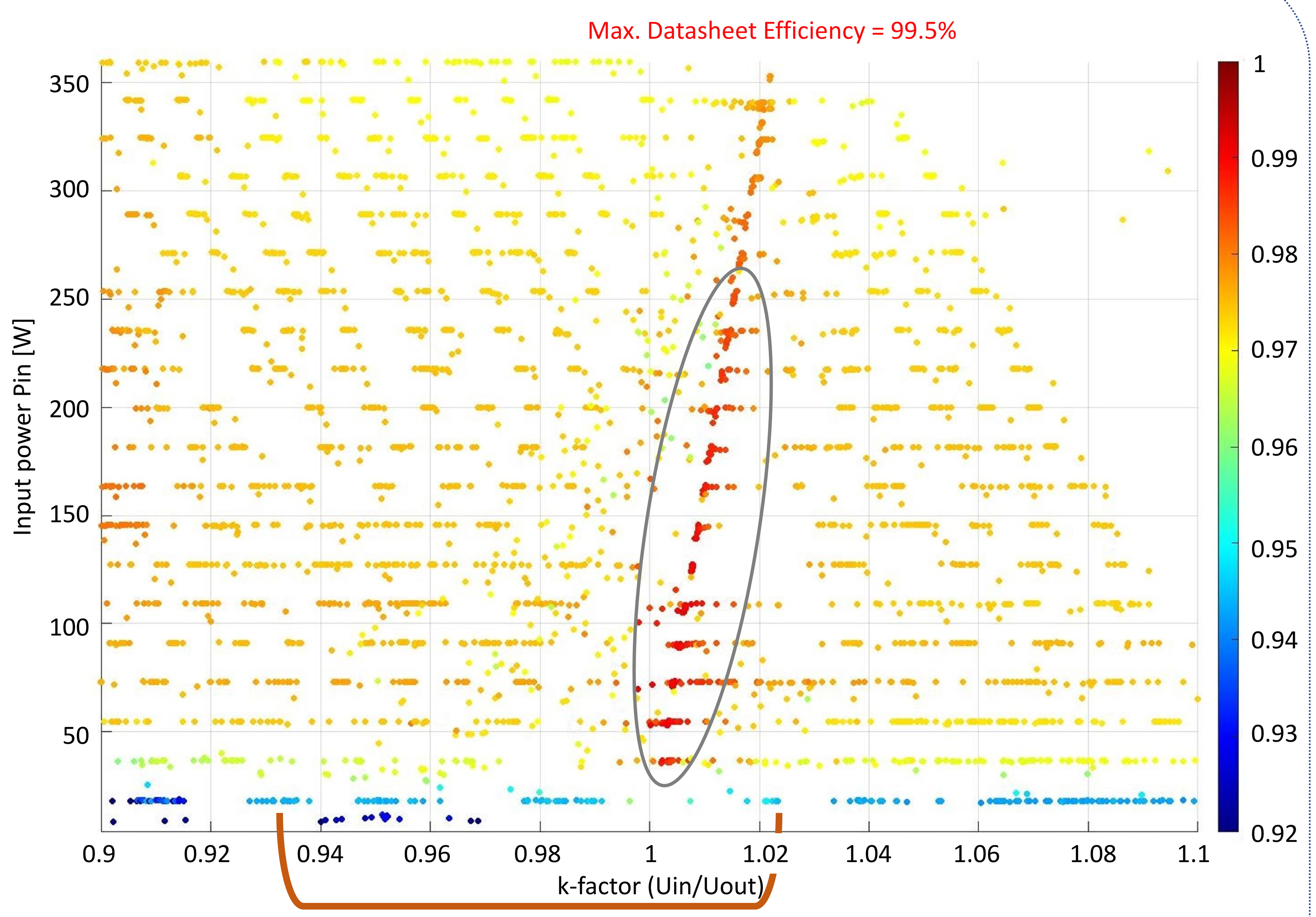

Figure 3: Static efficiencies of a SolarEdge power optimizer P370 as a function of voltage conversion ratios (measured in the laboratory)

Table 3: Yearly shading adaption efficiency (SAEta) for a 1-phase (dt = 1 min) and a 3-phase (dt = 2 min) system

Shading situation	System	1-phase system	3-phase system	
		SAEta (12 modules)	SAEta (21 modules)	SAEta (14 modules)
Unshaded	SINV	97.7%	96.9%	96.7%
	Optimizer	96.5%	95.4%	93.0%
Chimney	SINV	96.7%	96.3%	95.7%
	Optimizer	96.5%	$\boxed{95.4\%}$	94.5%
Tree	SINV	95.1%	94.9%	94.0%
	Optimizer	96.4%	95.3%	94.4%

Results

- Shading adaption efficiency comparison revealed that for the single-phase system, the optimizer system performs worse in cases without shading obstacles, achieving a SAEta 1.2% lower than the SINV. When partial shading was present, the optimizer system's efficiency was 0.2% lower (chimney) and 1.3% higher (tree) compared to the SINV.
- Results for the unshaded SAEta 1-phase simulation of the SINV (97.7%) are very close to the SINV's stated Euro efficiency (97.3%). In the MLPE System's case, the unshaded 1-phase simulation SAEta of 96.5% is considerably below the expected weighted efficiency of the system of 97.6% (98.8% Inverter x 98.8% Optimizer = 97.6% Total System).
- The three-phase system performed similarly to the 1-phase system, achieving a lower SAEta for the MLPE system of 1.5% (unshaded) and 0.9% (chimney) and a 0.4% SAEta gain when partially shaded by the tree (measurement uncertainty ±0.3%, k=1).
- In addition to testing both systems with an optimal number of modules, SAEta for a suboptimal number of modules (14) was also calculated. The MLPE system performed worse than the SINV in the unshaded and chimney cases (3.7% and 1.2% lower SAEta respectively) and slightly better when partially shaded by the tree (0.4% SAEta increase).
- Figure 3 reveals how all measured SolarEdge P370 optimizer efficiencies at 99% or above (maximum datasheet efficiency = 99.5%) occurred at voltage conversion factors when the power optimizer was not in pulse-width modulation (PWM) mode, but rather just conducting.

[1] C. Allenspach, F. Baumgartner, V. Gonzalez de Echavarri Castro, S. Richter, C. Meier, and C. Carigiet, "MODULE-LEVEL POWER ELECTRONICS UNDER INDOOR PERFORMANCE TESTS," 37th European Photovoltaic Solar Energy Conference and Exhibition (EUPVSEC).

[2] F. Baumgartner, R. Vogt, C. A. Allenspach, and F. Carigiet, "Performance analysis of shaded PV module power electronic systems," presented at the 38th European Photovoltaic Solar Energy Conference and Exhibition (EUPVSEC), Sep. 2021. doi: 10.21256/zhaw-23261.

[3] M. Littwin, F. Baumgartner, Mi. Green, and W. van Sark, "Performance of New Photovoltaic System Designs," *Int. Energy Agency - Photovolt. Power Syst. Programme*, p. 89, Apr. 2021.

[4] F. Baumgartner, "Effizienzvergleich PV-String-Inverter versus dezentrale PV-Modulelektronik ", *presentation at 18th Swiss National PV Conference*, Lausanne, Mar. 2020, (presentation available online: https://youtu.be/yKz-zbxijFU) see also bulletin.ch p. 62, 5 / 2021.

Contact:
Cyril Allenspach: alls@zhaw.ch
Franz Baumgartner: bauf@zhaw.ch

Project funded by Bundesamt für Energie BFE, contract #: SI/502247-01. Previous results [4] were published as a part of IEA PVPS Task 13 and future findings will be part of the Task 13 Project 2022 – 2025. Within the IEC TC82 WG6 committees a standard about MLPE is proposed.

info@csem.ch www.csem.ch

What drives performance in data-driven and weather-based techniques for short-term PV Forecasting?

Rafael E. Carrillo[1], Pierre-Jean Alet[1], Stefan C. Müller[2] and Jan Remund[2]

[1]CSEM SA, Switzerland, [2]Meteotest AG, Switzerland

Motivation:

- CloudMove solution from Meteotest offers a nowcasting service for irradiance and PV production with SoA accuracy up to six hours ahead (15 min. resolution)
- CloudMove is based on satellite images and numerical weather models to propagate the cloud movements in the future
- Additionally, CloudMove uses online ground data to correct the forecasts
- Recently, CSEM developed a data-driven forecast model for multi-site PV production forecasting based on Graph neural networks (GNNs)
- These methods can accelerate the computation of forecasts by a factor 100 (after initial training)

Objective: compare CSEM's data-driven solution with CloudMove for different scenarios to provide insight into their performance drivers

Graph-based multi-site PV forecasting

Intuition

- CSEM's data-driven solution relies entirely on production data
- PV stations can be used as a network of virtual weather stations
- By exploiting the spatio-temporal relations of the power production data, cloud movements can be forecasted

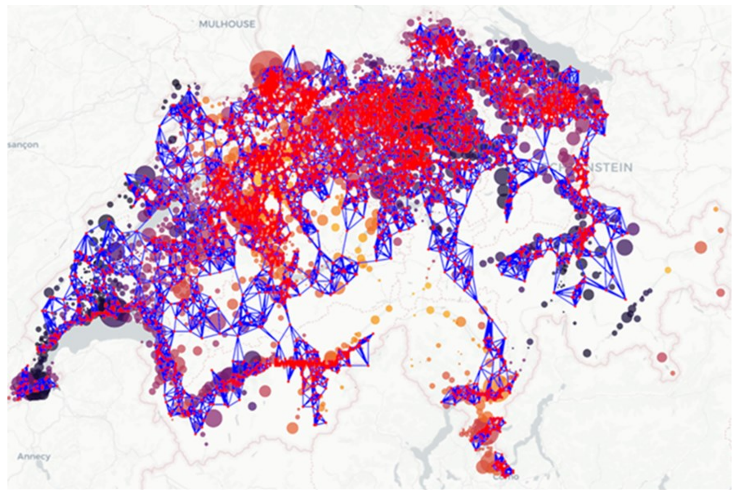

Architecture

- The GNN model is an encoder-decoder architecture with graph-convolutional Long-Short-Term-Memory (GCLSTM) cells[1]
- Inputs: production data from past 3 hours and clear-sky irradiance for the forecasting horizon
- Output: power production for all sites in the forecasting horizon (6 hours ahead, 15 min, resolution)

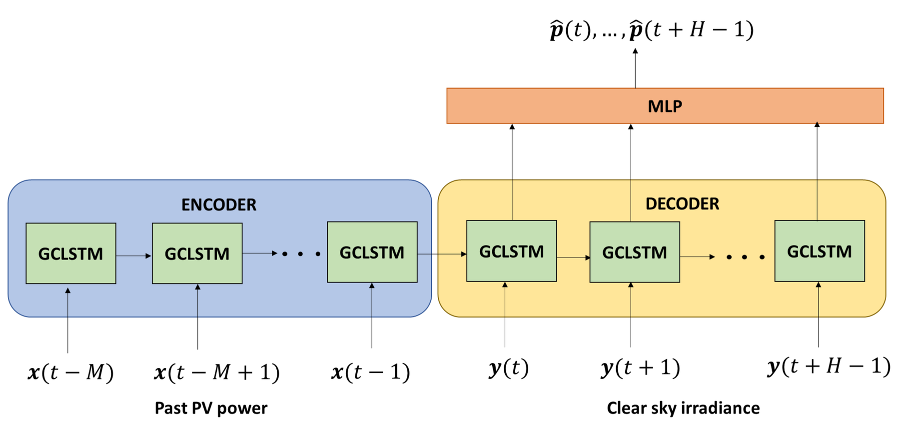

[1]J. Simeunović, B. Schubnel, P. -J. Alet and R. E. Carrillo, "Spatio-Temporal Graph Neural Networks for Multi-Site PV Power Forecasting," in IEEE Transactions on Sustainable Energy, vol. 13, no. 2, pp. 1210-1220, April 2022.

Evaluation set-up

Dataset:

- Power production data from 304 PV stations over Switzerland
- Data from all stations (blue) used as input to GNN (training and evaluation)
- GNN trained using data from whole 2016
- Evaluation in 18 stations (red) for 21 representative days in 2017

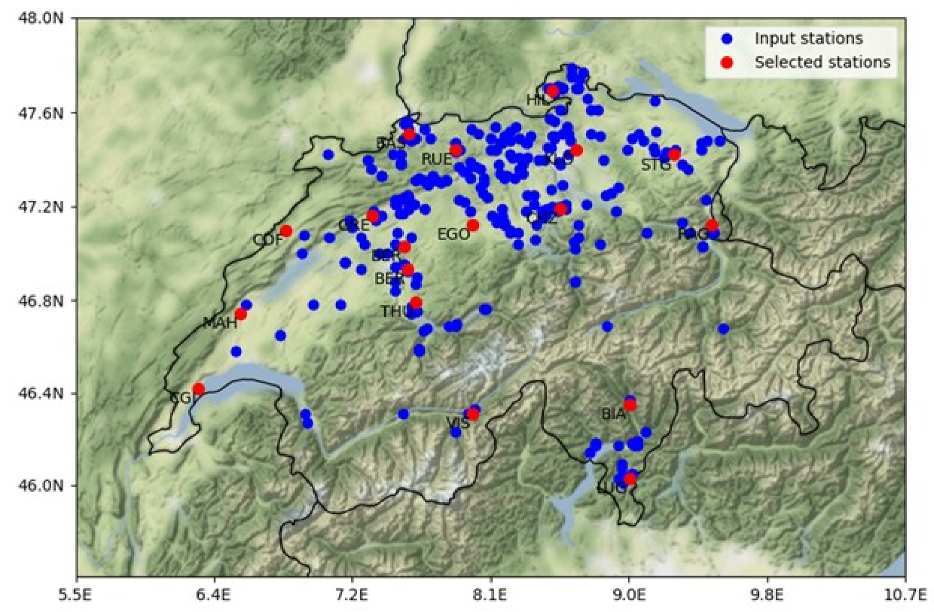

Selection criteria: sites

- Regional coverage
- Climate
- Proximity of SwissMetNet stations
- Density of PV stations around selected sites

Selection criteria: days

- At least 5 representative days per season
- Mixture of different day categories (according to cloud level)

Evaluation metric: Peak-Normalized Root Mean Squared Error (NRMSE)

Results and Discussion

Overall results

- NRMSE vs forecasting horizon:
  - Errors very similar up to two hours ahead (8 steps)
  - More pronounced slope for CloudMove after 2.5 hours ahead (10 steps)
  - Larger spread for CSEM's GNN
- NRMSE vs prediction time of the day (hourly):
  - Largest errors in early morning (5:00 – 7:00) due to scarcity of information due to zero production over night
  - Large spread in errors between 7:00 and 12:00 because forecasting horizon includes peak of solar noon
- NRMSE vs target time of the day (hourly): largest errors near solar noon
- The spatial error distribution is almost uniform for CloudMove, except for the Alpine regions where no weather station was available nearby
- CSEM's solution yields a spreader spatial error with highest errors near borders and lakes

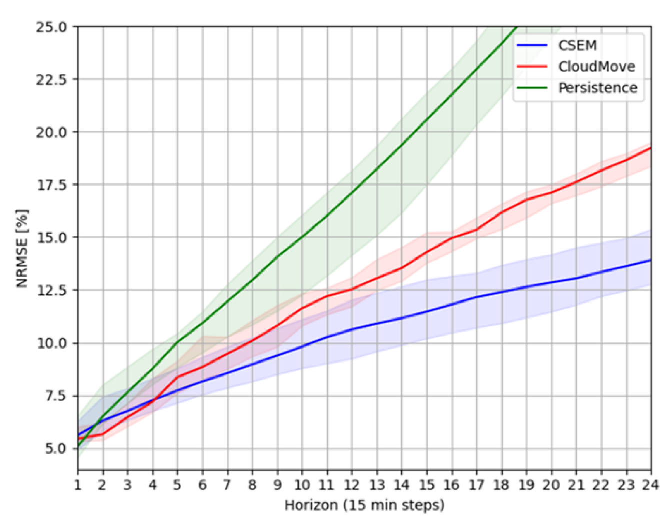

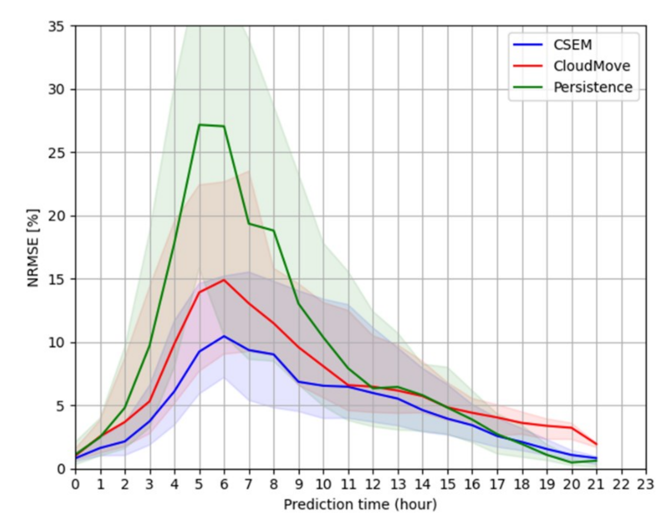

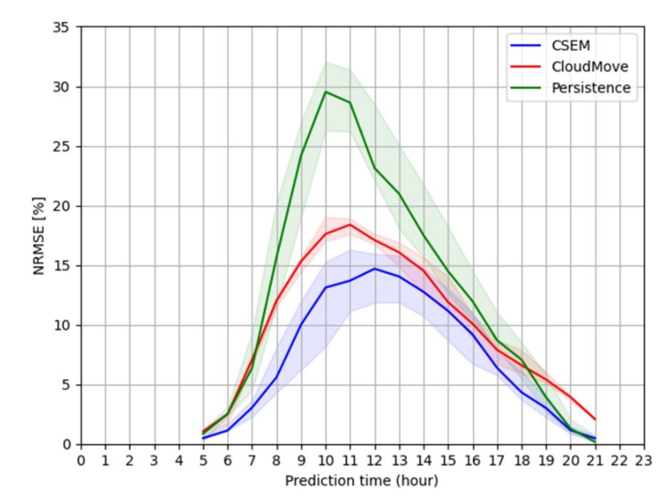

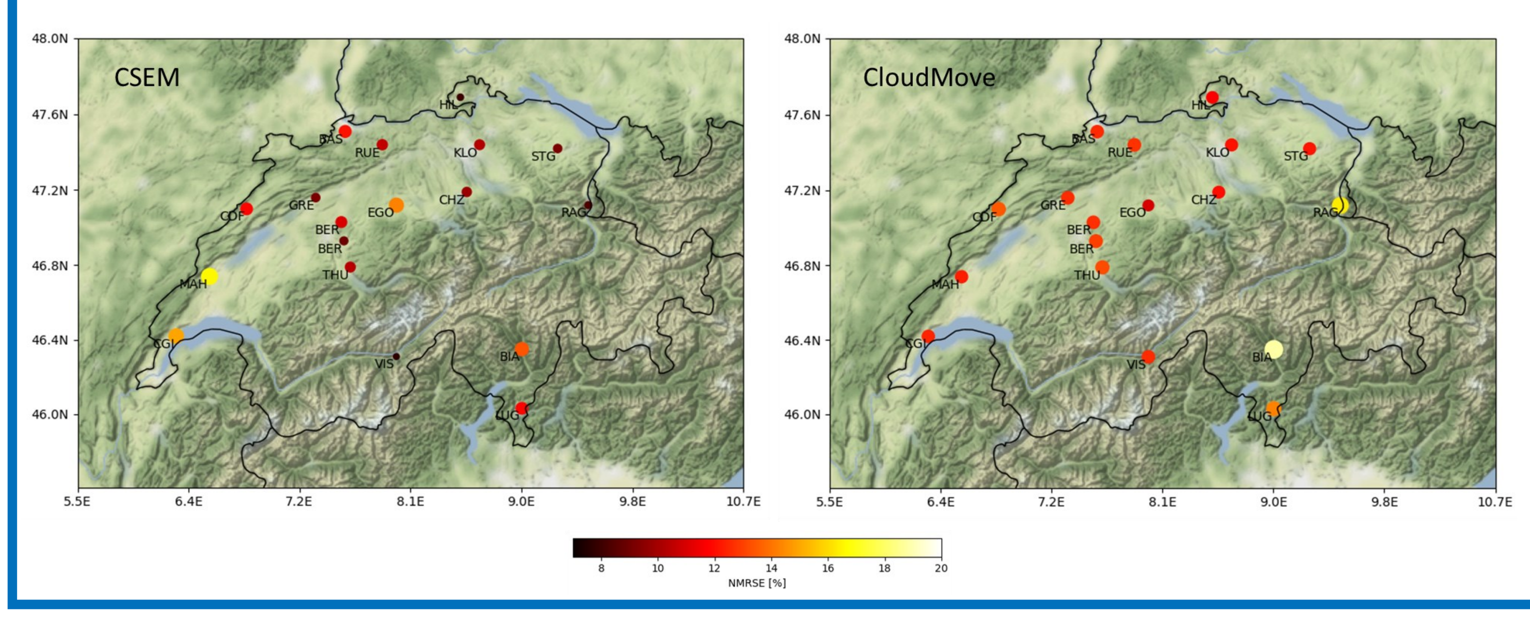

Seasonal dependency

- NRMSE vs forecasting horizon:
  - Larger errors for CloudMove in winter and summer
  - Significantly larger slope in the error evolution in spring for CloudMove
  - Larger errors for CSEM's GNN in fall
  - Larger spread for CSEM's GNN except in summer
- NRMSE vs prediction time of the day (hourly):
  - Larger errors for CloudMove for winter and summer and significantly larger errors in spring
  - Larger spread of errors in winter for CloudMove
  - CSEM's GNN has a large error spread summer around the solar noon due to large peak production

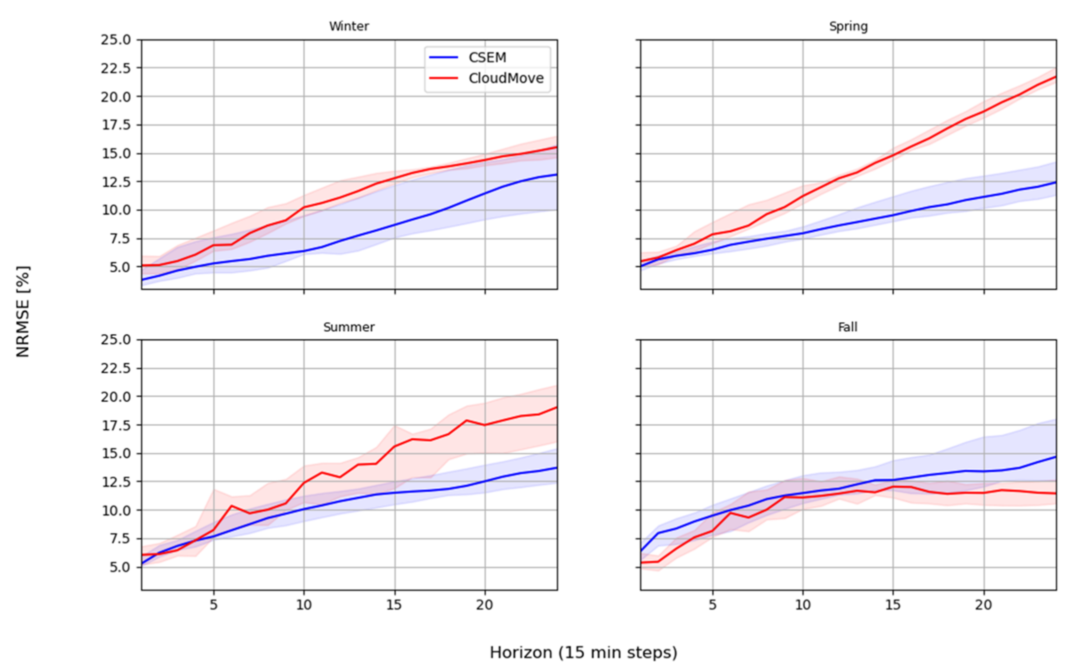

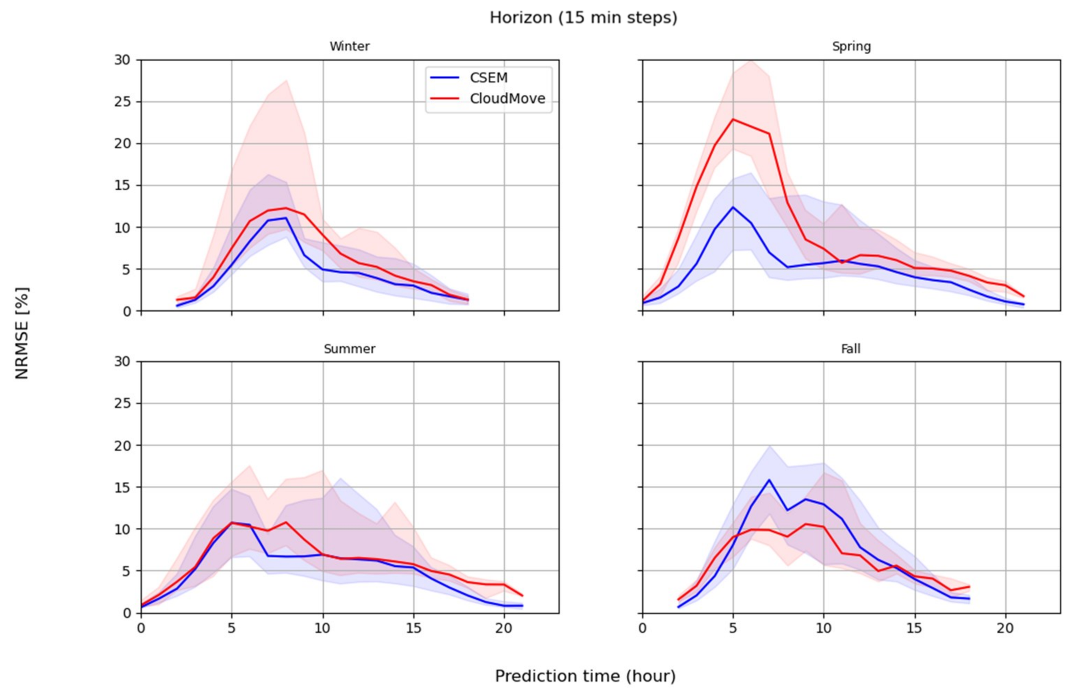

Discussion

- CloudMove and CSEM data-driven method yield a similar error between 0-2 hours ahead predictions but CSEM' method yields smaller errors from 2-6 hours ahead
- CloudMove has a smaller spread of errors across sites and days benefiting from the larger coverage of satellite images except in sites where there aren't nearby weather stations available
- CSEM data-driven method yields a larger spread of errors across sites and days. The error can be very low for sites with a high density of PV stations but high for sites with low density and at the border of the graph
- CloudMove achieves a lower error in fall but CSEM's solution yields lower errors (and spread) during summer when the production is the highest

Hydrogen as seasonal storage for a swiss neighbourhood

Mathieu Schopfer, David Martinet, Christoph Ellert*

PV-tagung
Bern 29.03.2022

Contact : christoph.ellert@hevs.ch

* HES-SO Valais-Wallis : Institute of Systems Engineering, Rue de l'Industrie 23, 1950 Sion

MOTIVATION : PHOTOVOLTAIC FOR NEIGHBOURHOOD 100 INHABITANTS

While in the PV-Community the agreement is overwhelming that the installation rate of 700 MWp per year, which the new Swiss energy law intents to reach are insufficient by more than of a factor of two, it is still a matter of debate how to transfer the overshooting summer PV-generation into the less favourable winter season in central Europe. Therefore we propose here a scalable solution for a neighbourhood in a typical swiss city. Two trials for an appropriate dimensioning of the central components are suggested. In an iterative process we reach to the favourite recommendations for seasonal Hydrogen storage system transferring the summer overproduction into the «dark» winter months.

Key data :

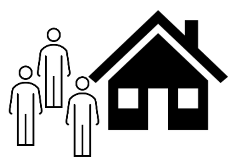

3 inhabitants in house
3450 kWh/year

Neighbourhood
100 inhabitants
115 000 kWh/year

Source :
OFEN suisseenergie.ch
fact sheet August 2021,
private communication Oiken

First sizing : annual observation consumption and PV

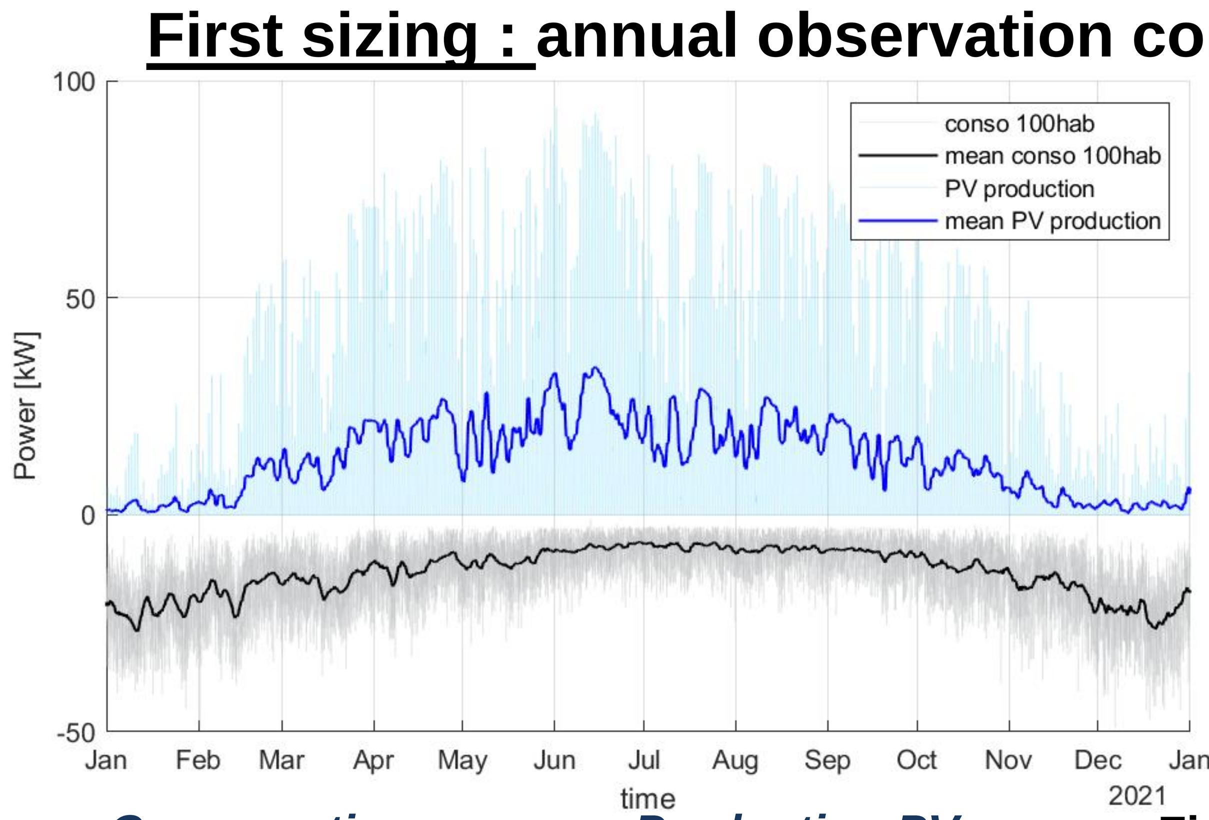

Consumption energy = Production PV energy **Fig. 1**

Problematic:

Annual imbalance between photovoltaic production (fig.1) and consumption.

One year :
PV : +115 000kWh
Cons. : -115 000kWh

Second sizing :

Winter observation consumption and PV

Sizing the photovoltaic power required for the needs of a day in winter (05.01.2021 cons. -23kW)

Problematic:

Huge overproduction in summer. Huge over-dimensioning PV (3000kW).

One year :
Surplus : 3 651 000kWh

HYDROGEN STORAGE

Annual distribution of hydrogen storage

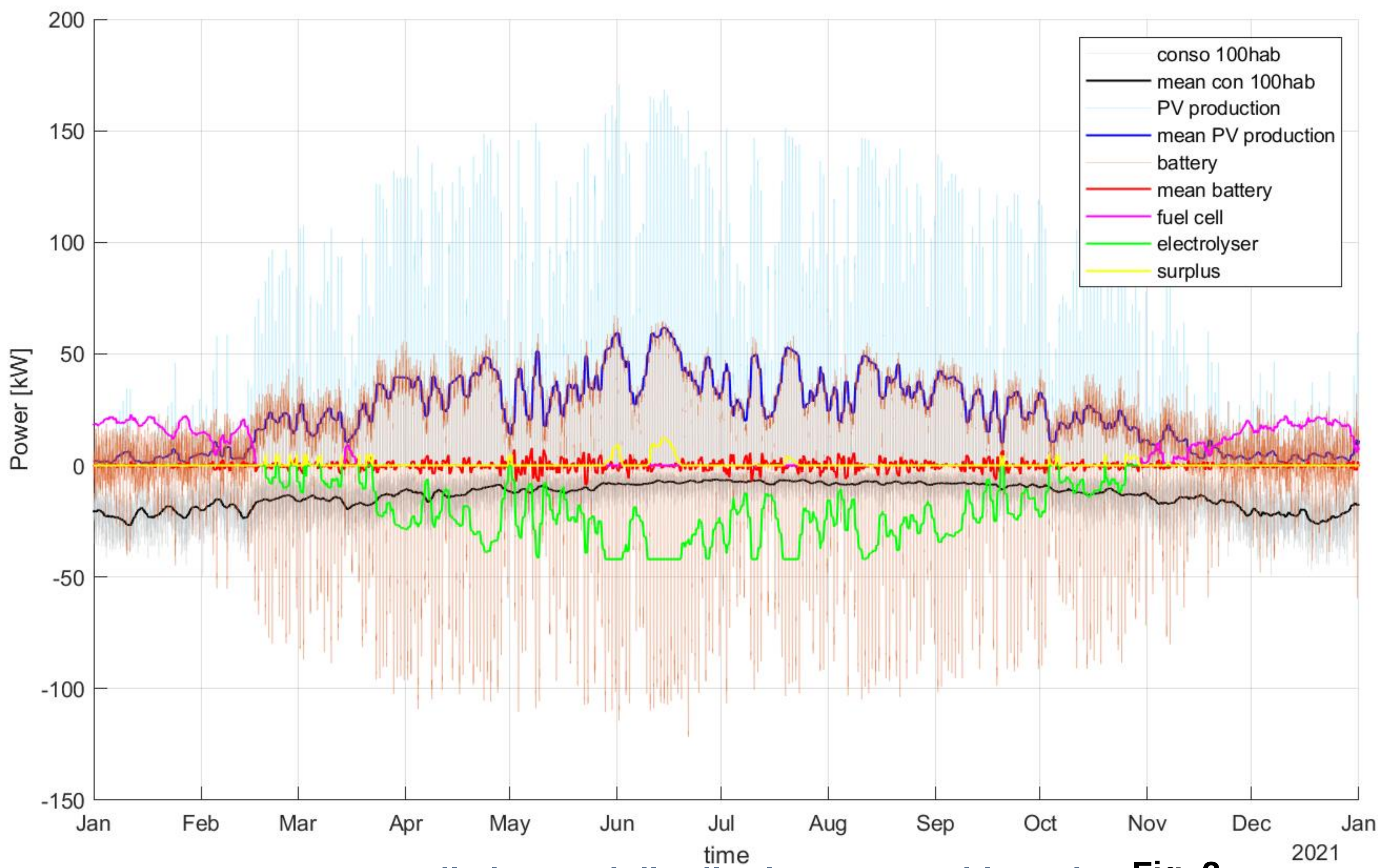

Detailed annual distribution power with peak **Fig. 2**

For ease of reading, there are moving means with a 2-day window (fig.2). High power is exchanged with PV and batteries. To reduce costs, the electrolyser is limited to -45 kW. A minimum power of -5 kW is required to switch it on and thus avoid deterioration at low power.

Main components

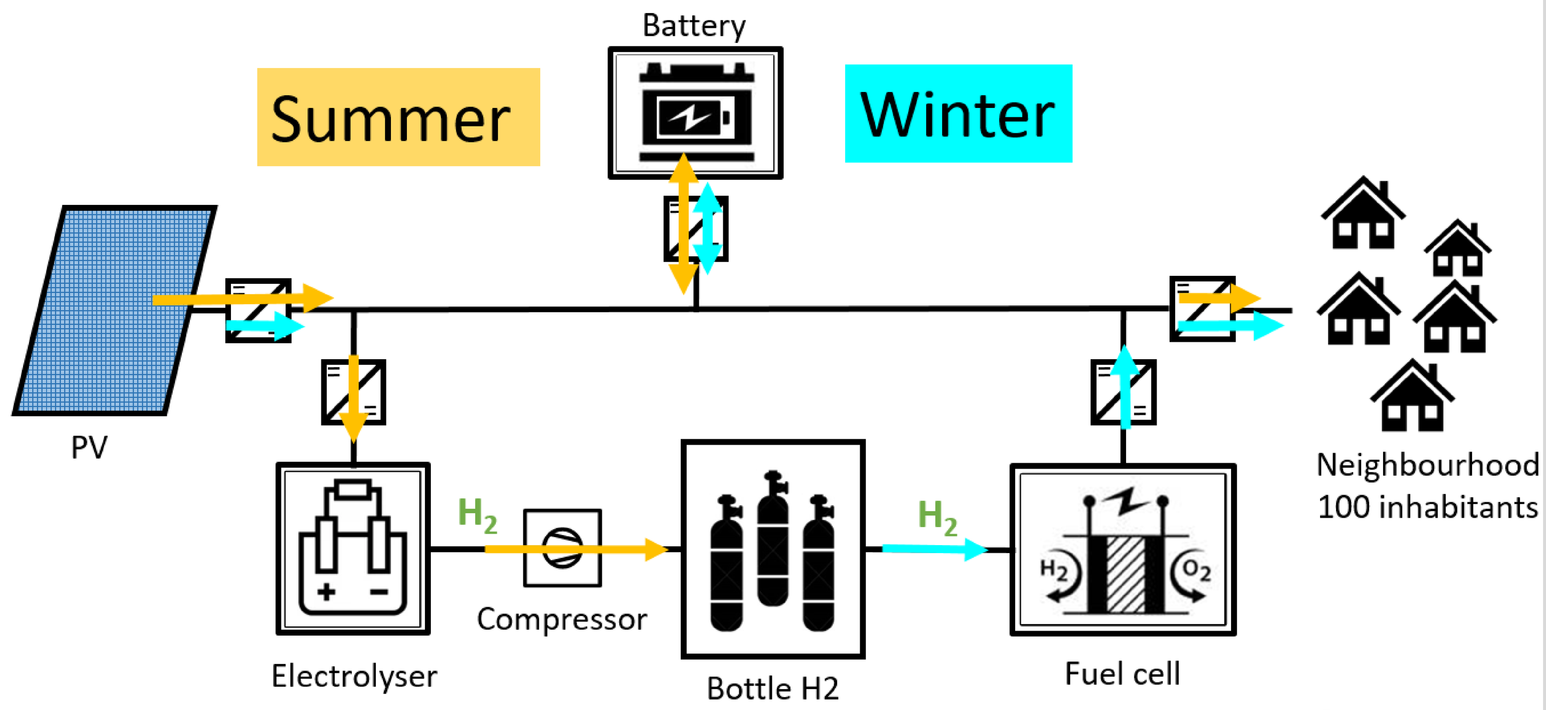

Components for seasonal hydrogen storage **Fig. 3**

Hydrogen devices are added to the existing ones (fig.3). Then 2 flow paths are possible to store or use H2.

The power of the electrolyser follows the moving average of the PV production (fig.4). Fuel cells fill the gap in the winter months. A small surplus of 4230 kWh is not valorized

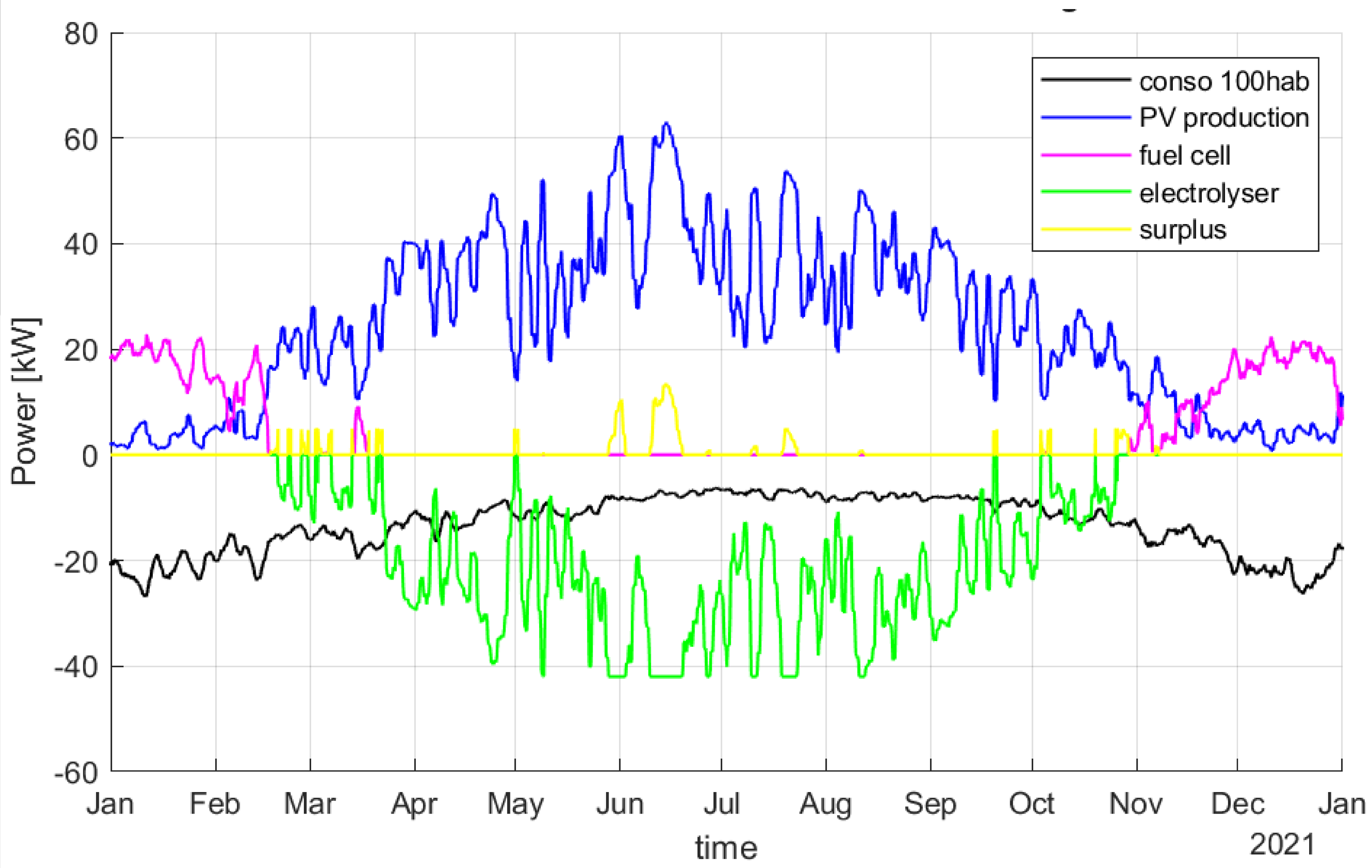

Mean power with the influence of electrolysis and fuel cells **Fig. 4**

RESULTS

PV	145kW	+216 000 kWh	365 day
Electrolyser	-45kW	-132 000 kWh	230 day
Fuel cell	23kW	+38 300 kWh	116 day
Battery	110kW	800 kWh	11m^3
Hydrogen	2324kg	76 680 kWh	200 bar
Storage H2	131 m^3	Area 164 m^2	218 frame

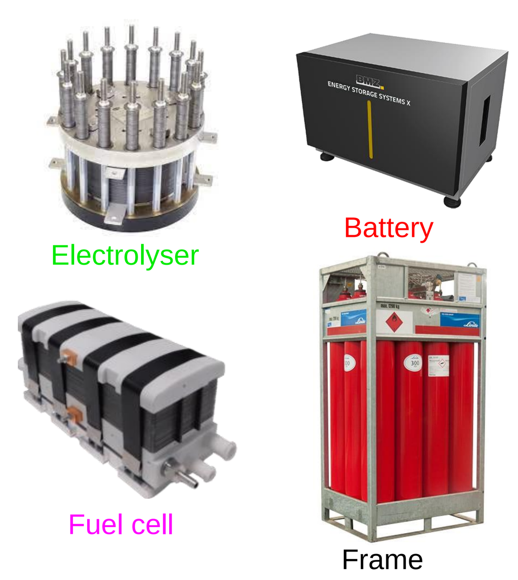

CONCLUSION

Important sizing factor :

The photovoltaic production needs to be **1.85x** higher (216 MWh) than the energy consumed during the year (115 MWh).

1. Hydrogen as transfer medium from summer to winter seems technically feasible, with reasonable size of the storage volume, based on industrial standard 200 bar H2-bottles.

2. The cost considerations for such as seasonal storage solution need to consider the heavy impact that a significant overproduction of PV-power in summer will have on the kWh-market prize.

Long-term performance of BIPV in Switzerland

Hugo Quest[1,2], Andrew Fairbrother[1], Ebrar Özkalay[1,3], Philipp Wälchli[2], Gabi Friesen[3], Christophe Ballif[1,3], Alessandro Virtuani[1]

1 – EPFL, Institute of Microengineering (IMT), Photovoltaics and Thin-Film Electronics Laboratory (PV-LAB), 2002 Neuchâtel (Switzerland)
2 – 3S Solar Plus AG, 3645 Thun (Switzerland)
3 – University of Applied Sciences and Arts of Southern Switzerland (SUPSI-PVLab), 6850 Mendrisio (Switzerland)
4 – CSEM Sustainable Energy Centre, 2002 Neuchâtel (Switzerland)

1 Context and goal

- Building integrated photovoltaics (BIPV) are key to achieving Switzerland's 2050 Energy Strategy targets for renewable energy.
- BIPV systems often operate at high temperatures and can face recurrent shading, and these stresses could lead to accelerated performance loss.
- Up to now there are few reports on the long-term performance of these systems, even though they constitute the vast majority of Swiss PV plants.

This work presents a **long-term performance analysis** of 50+ systems (200+ strings) in central Switzerland, along with a parallel **fault detection and diagnosis (FDDA)** to link performance losses to system faults.

2 Modelling approach

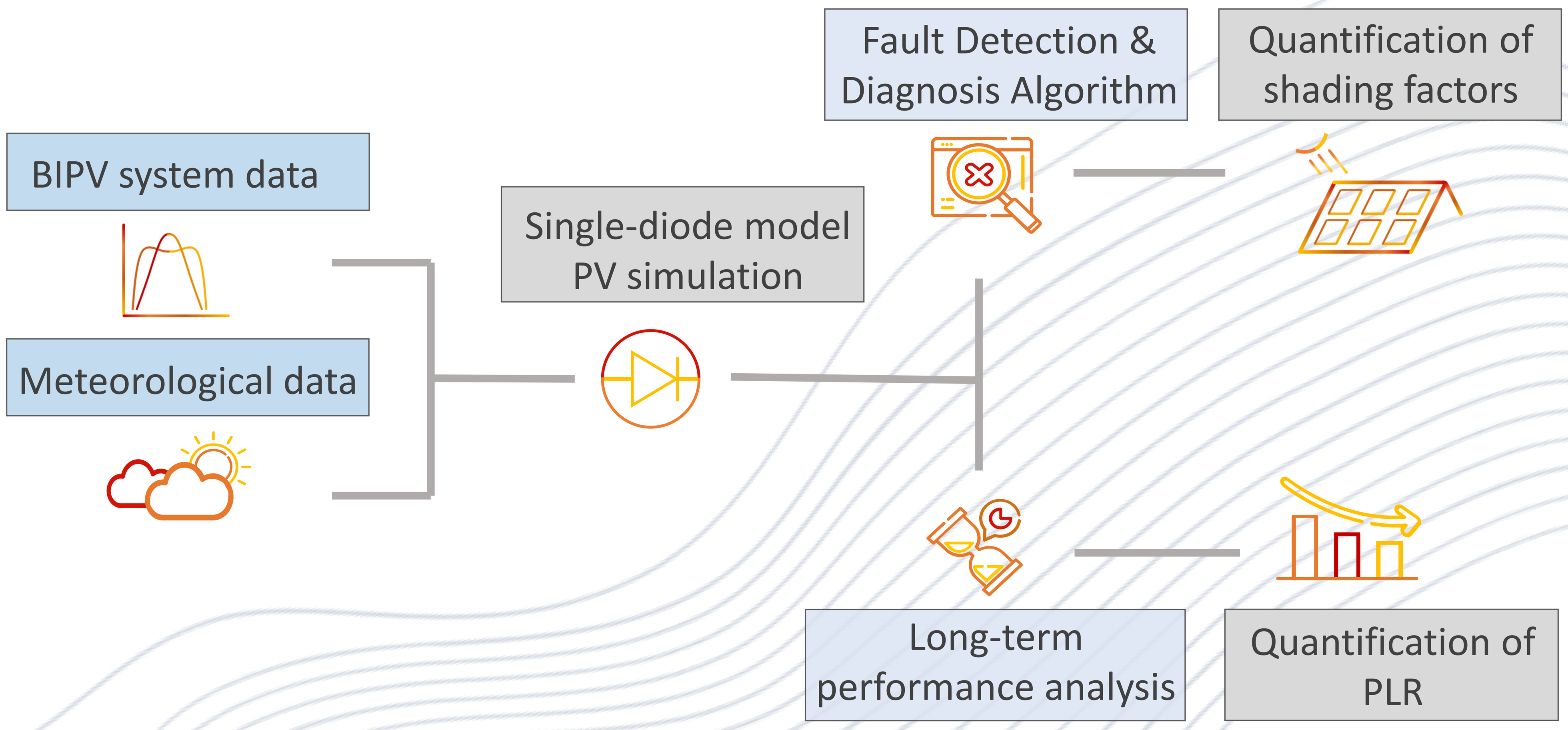

3 Results – fleet analysis

- On average, low performance loss rates (PLR) were observed with a fleet median and mean of **0.1 %/year** and **0.04%/year** respectively, i.e. essentially no degradation though there is a large spread of rates. *N.B.: negative value denotes performance loss, positive value signifies performance gain*
- No trend by installation year was identified (see **Fig. 1**), and no systems exhibited obviously non-linear performance loss behavior.
- **Fig. 2** shows the fleet characteristics – most systems were South-facing with 30° tilts, the average string capacity was 5.9 kWp, and the PLR ranged from -3.2 %/year to 1.8%/year.

Next step: analyse the **confounding factors** that lead to outliers in PLR (shading, climate, installation...)

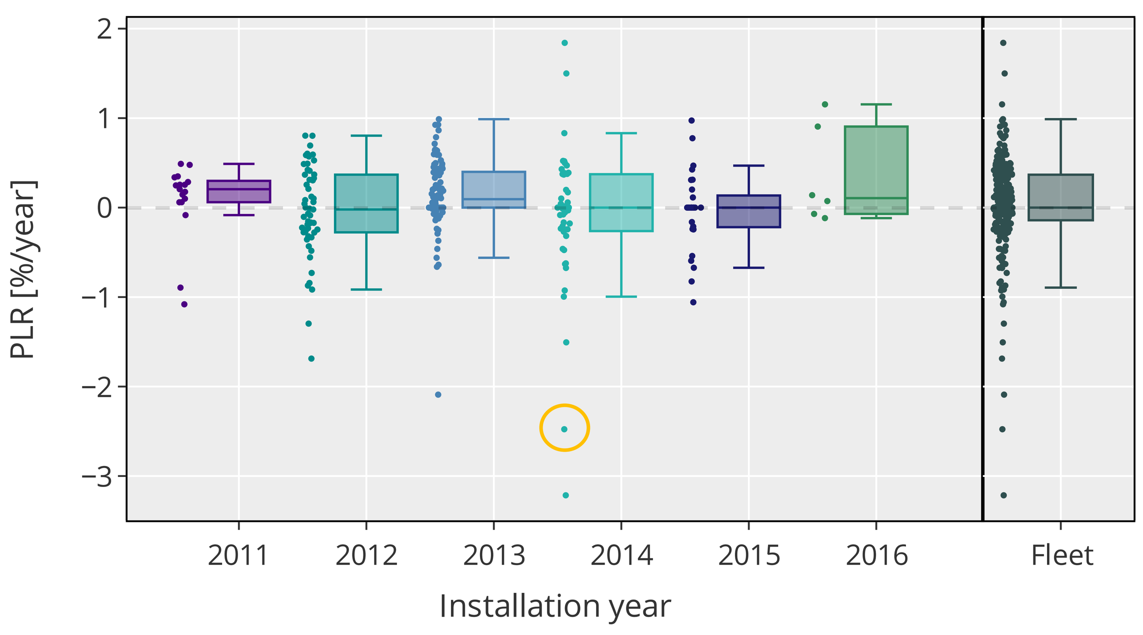

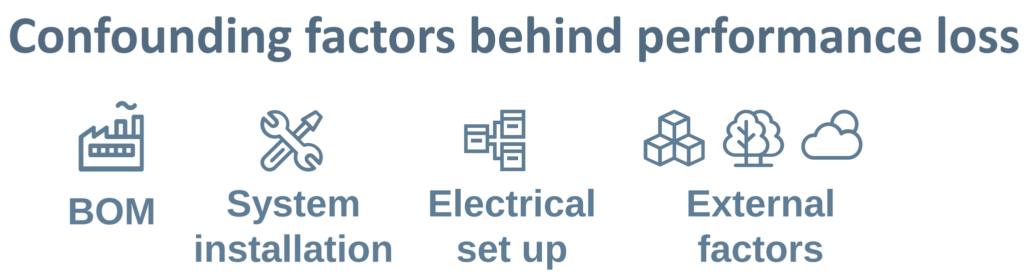

Fig. 1: PLRs [% year^{-1}] for 52 BIPV systems (242 module strings) by installation year showing median, confidence intervals (CI, 25–75% and 5–95%), and outliers. Outlier used for the case study is circled.

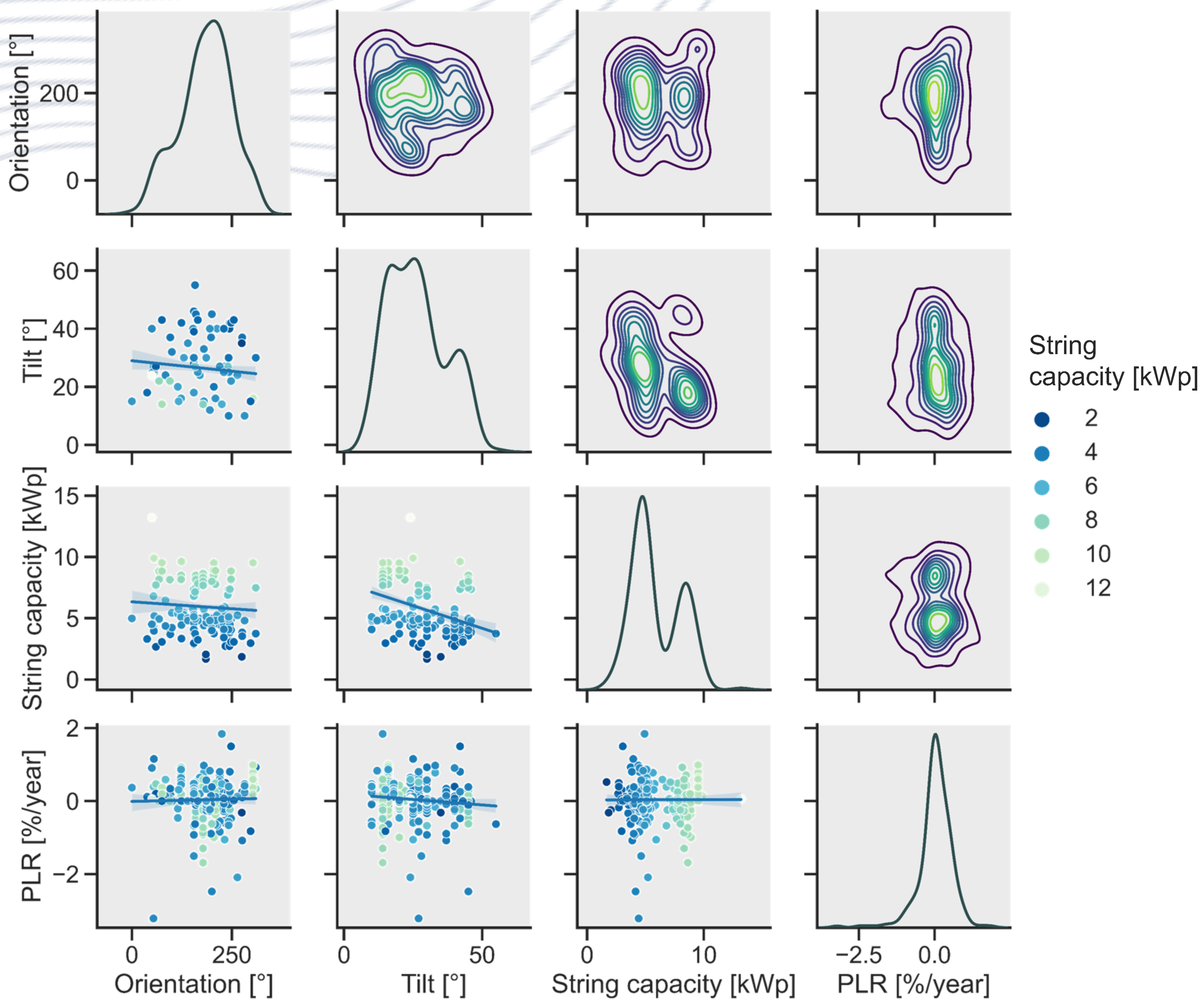

Fig. 2: Pair grid matrix overview of the BIPV fleet characteristics. Diagonal: probability distributions, Upper: kernel density estimate (KDE) distributions, Lower: scatter plots with linear trends and string capacity colour map.

4 Case study – shaded system

- A fault detection and diagnosis algorithm (FDDA) was developed to automatically identify shading faults.
- An outlier system with high PLR was identified for a case study analysis:

Fig. 3 shows the fault-type heat map of the outlier string, where recurring shading is observed, linked to the chimney and surrounding trees.

Fig. 4 shows the PLR year-on-year analysis and performance ratio (PR) trends, comparing the shaded string with the neighbouring string. Severe performance loss is observed for string 1, whilst string 2 is stable.

Given that the two strings are from the same rooftop BIPV system, the remaining distinguishing confounding factor behind PLR is shading, and a clear link between shading and higher PLR is observed.

In a previous large-scale analysis [1], the shading factor was found to delineate an upper limit on the PLR. Moreover, average shading factors were found to increase in newer systems and decrease in larger capacity systems.

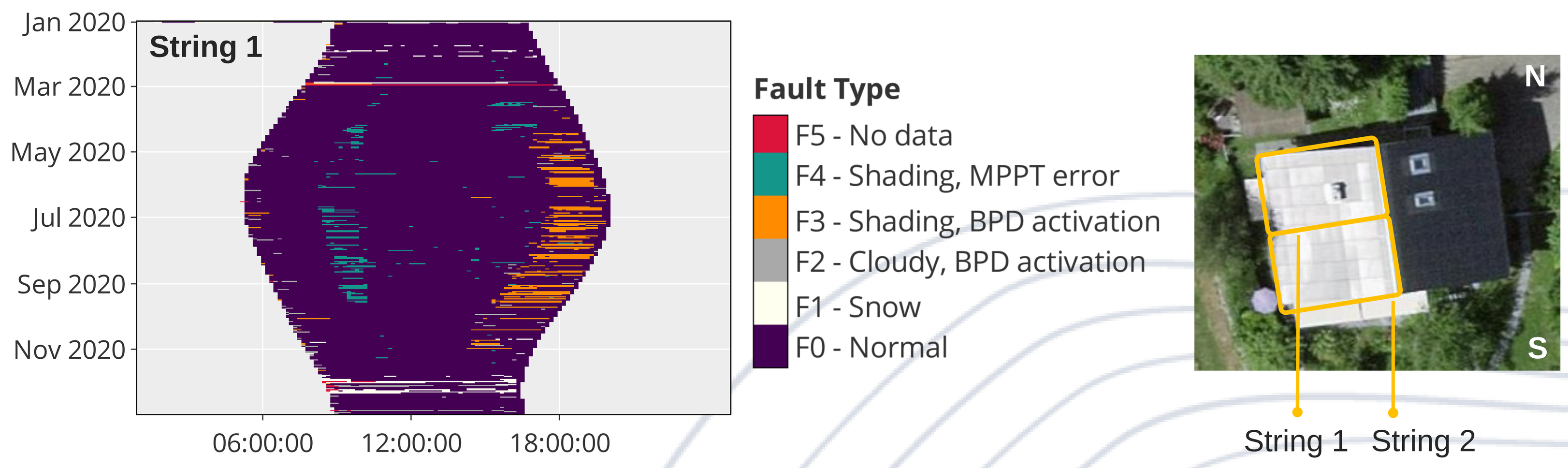

Fig. 3: Fault-type heat map of the top string of the analysed West-facing BIPV system, in 2020. Recurring shading events are observed in the morning and evening hours.

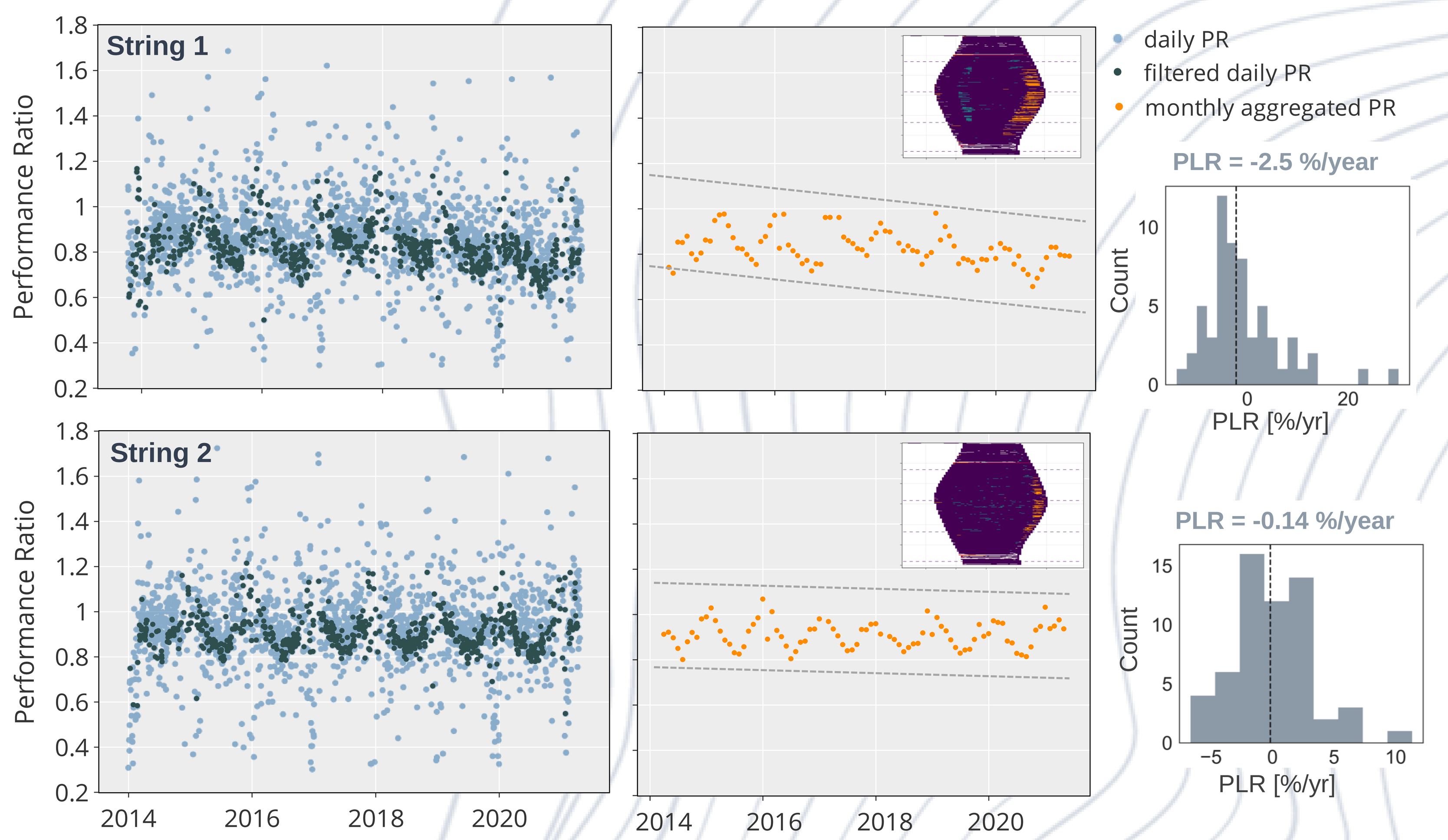

Fig. 4: Daily performance ratio (PR) trends for the two system strings (before and after filtering and monthly aggregation) and PLR distribution plots with indicated median value. A clear performance loss trend is observed for the heavily shaded string 1.

5 Conclusion

Overall, the BIPV fleet average PLR is found to be essentially zero (median of 0.1 %/year), but a large spread of rates is observed.

Low performing systems show recurrent shading through a fault detection and diagnosis algorithm, but other confounding factors should be further analysed.

Highlights the importance of alleviating shading stresses through innovative BIPV system design, which has particular relevance to the Swiss PV market.

Acknowledgements

3S Solar Plus supervision: Pascal Müller, Philipp Wälchli
EPFL thesis supervisor: Prof. Christophe Ballif,
EPFL co-supervision: Dr. Alessandro Virtuani, Dr. Andrew Fairbrother
The authors thank Baur AG for providing access to the system data, and Solcast for providing satellite-derived meteorological data.

References

[1] Fairbrother et al. (2021), doi: 10.1002/solr.202100583
[2] Lindig et al. (2021), doi: 10.1002/pip.3397
[3] Jordan et al. (2018), doi: 10.1109/JPHOTOV.2017.2779779
[4] Kraus et al. (2019), doi: 10.1063/1.5128171
[5] Livera et al. (2019), doi: 10.1016/j.renene.2018.09.101

University of Applied Sciences and Arts
of Southern Switzerland

SUPSI

ÉCOLE POLYTECHNIQUE FÉDÉRALE DE LAUSANNE

Institute for Applied Sustainability to the Built Environment

20. Nationale Photovoltaik-Tagung 2022

Schweizerische Eidgenossenschaft
Confédération suisse
Confederazione Svizzera
Confederaziun svizra

Swiss Federal Office of Energy SFOE

Quantifying Performance Loss Rates of Photovoltaic Modules Using Ground-based vs Satellite-based Meteorological Data

E. Özkalay[1,2], A. Virtuani[2], A. Fairbrother[2] , A. Skoczek[3], G. Friesen[1], M. Caccivio[1], C. Ballif[2,4]

[1] Insitute of Applied Sustainability to the Built Environment, SUPSI, Via Flora Ruchat-Roncati 15, 6850 Mendrisio, Switzerland

[2] École Polytechnique Fédérale de Lausanne (EPFL), Institute of Microengineering (IMT), Photovoltaics and Thin Film Electronics Laboratory (PVLAB), Rue de la Maladière 71b, 2000 Neuchâtel, Switzerland

[3] Solargis s.r.o., Mytna 48, 811 07 Bratislava, Slovakia

[4] CSEM PV-Center, Rue de Jaquet-Droz, 2002 Neuchâtel, Switzerland

ABSTRACT

Accurate assessment of the long-term performance of photovoltaic (PV) systems is critical for manufacturers, investors, plant owners and O&M companies. Many PV systems, especially residential and some commercial/industrial systems, are not equipped with meteorological monitoring systems such as irradiance and temperature sensors. Whereas to calculate the performance ratio (PR), a common performance measure, the plane of array irradiance (G_{POA}) is an input parameter. The irradiance data is the largest contribution to uncertainty in PR. Therefore, in this study, we first evaluate satellite-based irradiance and compare to ground-based irradiance data. Next, we investigate the accuracy of using the satellite-based meteorological data in long-term performance analysis of three test modules in the absence of ground-based data. We use (1) ground-based and (2) satellite-based data separately as input irradiance. We calculate 60 PR time series and performance loss rates (PLR) for each irradiance data using different filtering methods and performance metrics. As a representative PLR value, we used the mean value (excluding outliers) of the various PLR values obtained as suggested by IEA PVPS Task 13. For the first module, this method gave almost identical PLR values (-0.5% error) when ground- and satellite-based data are used. For the other two modules, the values are not identical, but standard deviations largely overlap. We show that when the mean of PLR values is used, it is possible to accurately evaluate the long-term performance using satellite-based meteorological data.

Method

- Table I provides a definition of the ground-based and satellite-based meteorological monitoring systems that have been used in this work. **Ground G_{POA}** (20˚tilt and -4˚ azimuth from South) and **module temperatures** were monitored every minute between December 2015 and May 2019 by well-calibrated (and maintained) **thermopile pyranometer** and **Pt100** sensors, respectively, on the outdoor test site of SUPSI, in Canobbio (Switzerland, 46.02°N and 8.91°E).
- The **PLR of three crystalline silicon (c-Si) PV modules** were calculated. The DC yields were monitored for almost four years between December 2015 and May 2019 at SUPSI, in Canobbio, Switzerland. The electrical performance parameters of the modules were acquired using maximum power point (MPP) trackers at 1-minute intervals.
- Not a single PLR analysis method was applied, but various PLR analysis methods applied to each long-term performance of PV modules as suggested by IEA PVPS Task 13. Each PLR analysis method is a combination of **data filtering method**, **performance metric** and **statistical analysis tool**. We created **60 PLR analysis methods** using **30 different data filtering methods, 2 different performance metrics** and **1 statistical tool (Figure 1)**. The 30 data filtering methods were created using different combinations of **irradiance**, **power**, **instantaneous PR**, **power-irradiance relation** and **clear-sky** filters **(Table II)**.

Table I. Definition of ground-based and satellite-based input meteorological data.

	Ground-based Monitoring System	Satellite-based Monitoring System
G_{POA}	On-site pyranometer (properly maintained and calibrated)	Satellite-derived
Module Temperature	Temperature sensor - Pt100 (back of module) (properly maintained and calibrated)	Calculated from satellite-derived ambient temperature using Ross' approximation

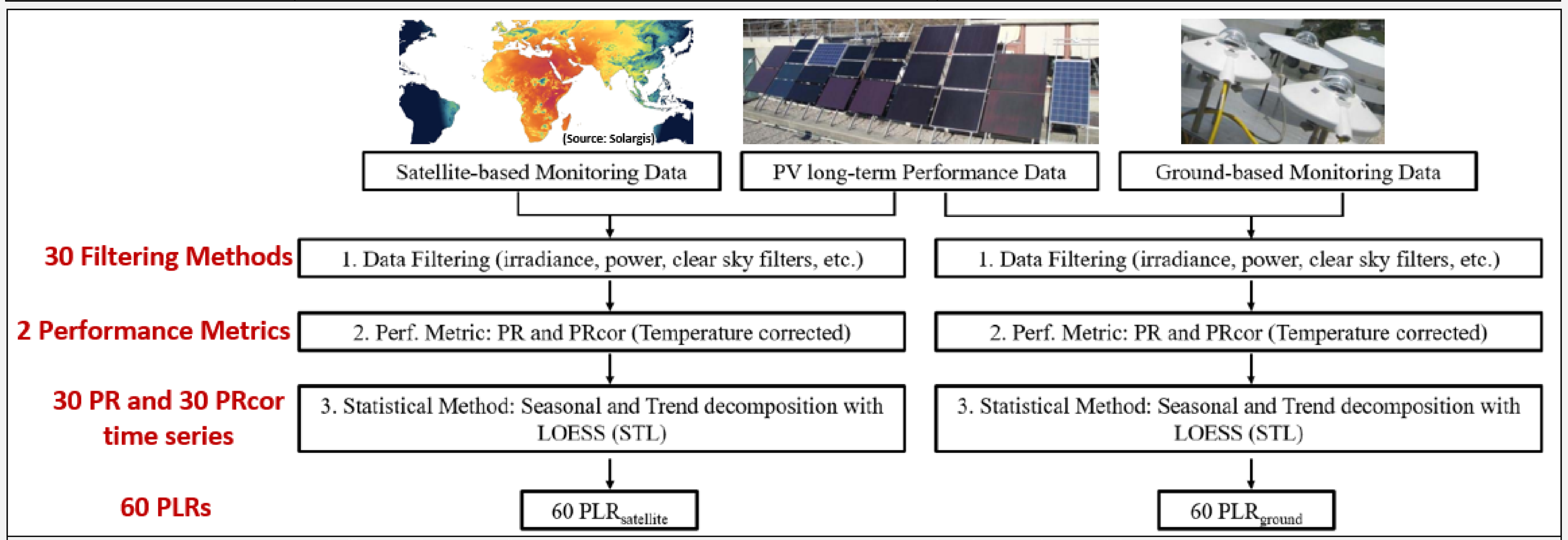

Figure 1. Conceptual flowchart of our PLR analysis approach including data filtering, performance metric computation and statistical method steps.

Results

- Figure 2a shows monthly **normalized bias series of satellite-derived G_{POA} ($G_{POA,satellite}$)**. The monthly $G_{POA,satellite}$ is **overestimated in summers** and **underestimated in winters.** As expected, this bias has an effect on **monthly $PR_{satellite}$(Figure 2b)**.

Figure 2a. Time-series of normalized bias for monthly satellite-derived G_{POA} with respect to ground-measured insolation **b.** Time-series of monthly PR computed using ground- and satellite-based insolation.

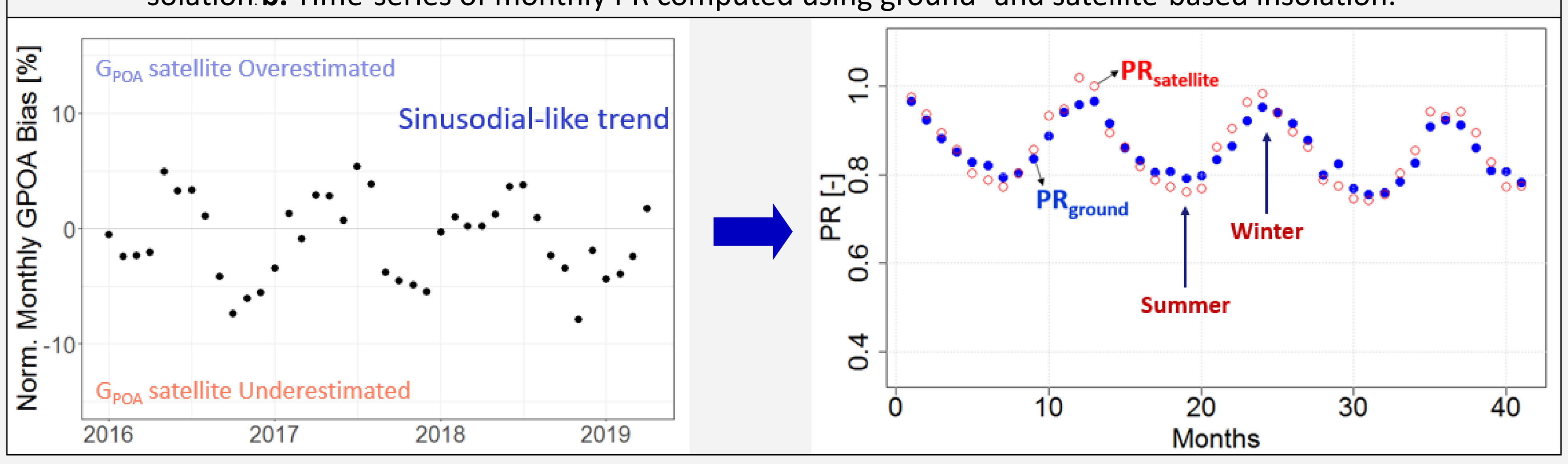

Table II. Summary of the data filtering techniques used. The parameters changed are written in bold.

Filter-1: Irradiance Threshold	Filter-2: Clear Sky
50 W/m^2 < G_{POA} < 1250 W/m^2 **100** W/m^2 < G_{POA} < 1250 W/m^2 **200** W/m^2 < G_{POA} < 1250 W/m^2 **500** W/m^2 < G_{POA} < 1250 W/m^2	RdTools' CSI (Clear sky index)
Filter-3: Power Threshold	**Filter-4: Power - Irradiance**
0.01 x P_{nom} < P_{meas} < **1.2** x P_{nom} 0.01 x P_{nom} < P_{meas} < **1.02** x P_{nom}	LQ: **20th**, UQ: **80th** LQ: **10th**, UQ: **90th** LQ: **5th**, UQ: **95th**
Filter-5: Instantaneous PR (5-minute)	
±1σ ±2σ **0.3** < PR_{ins} < **1.2**	

G_{POA}: Plane of array irradiance, **P_{nom}:** Nominal power, **P_{meas}:** measured power, **PR_{ins}:** instantaneous PR, **LQ:** Lower quantile, and **UQ:** Upper quantile.

- **Figure 3a and 3b** show the **60 PLR_{ground}** and **60 $PLR_{satellite}$** values, respectively, with the $PLR_{ref,ground}$ for the same module. $PLR_{ref,ground}$ is the refenrence value which is the mean of the different PLR_{ground} values as suggested by IEA PVPS Task 13. The $PLR_{satellite}$ values are more scattered than the PLR_{ground} values, which may be due to uncertainty of satellite data and temperature modelling.

Figure 3a. PLR_{ground} values with $PLR_{ref,ground}$ (red dashed line), the mean of the remaining (without outliers) PLR_{ground} values (dark) for module-3. Gray PLR_{ground} values are outliers. **b.** 60 $PLR_{satellite}$ values with $PLR_{ref,ground}$ for module-3.

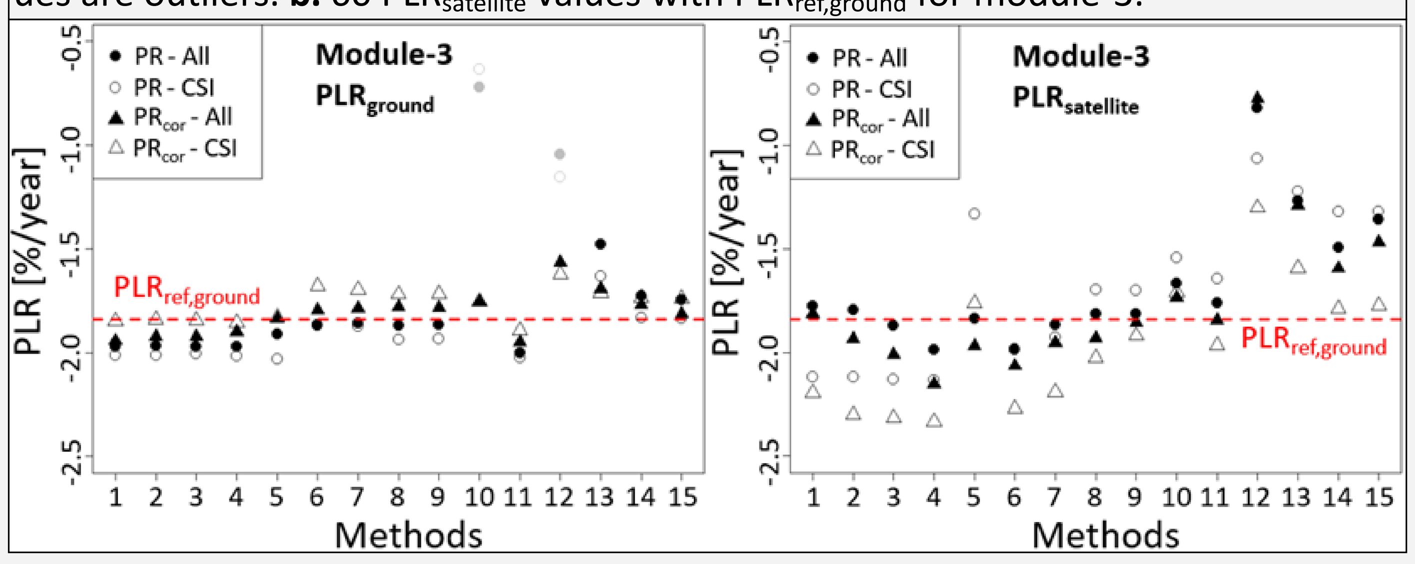

- **Figure 4** shows the $PLR_{ref,ground}$ and $PLR_{ref,satellite}$ (mean of $PLR_{satellite}$ values) each module. For **module-3**, the $PLR_{ref,ground}$ and $PLR_{ref,satellite}$ are almost identical whereas for **module-1** and **module-2**, $PLR_{ref,satellite}$ values fall slightly outside of the 1σ band surrounding $PLR_{ref,ground}$. However, there are overlaps between the standard deviations computed for $PLR_{ref,ground}$ and $PLR_{ref,satellite}$ for the both modules. Considering the relatively large uncertainty associated to outdoor measurements, satellite-derived insolation data and long-term performance analysis, we do not spot major differences between the $PLR_{ref,ground}$ and $PLR_{ref,satellite}$ calculated for each module.
- This work demonstrates that an accurate long-term performance assessment using satellite-based monitored data instead of ground-based monitored data is in principle possible by computing the mean of various PLR values obtained from different data filtering methods and performance metrics.

Figure 4. Reference performance loss rates using ground- and satellite-based monitoring, $PLR_{ref,ground}$ and $PLR_{ref,satellite}$, of the three modules with their standard deviation.

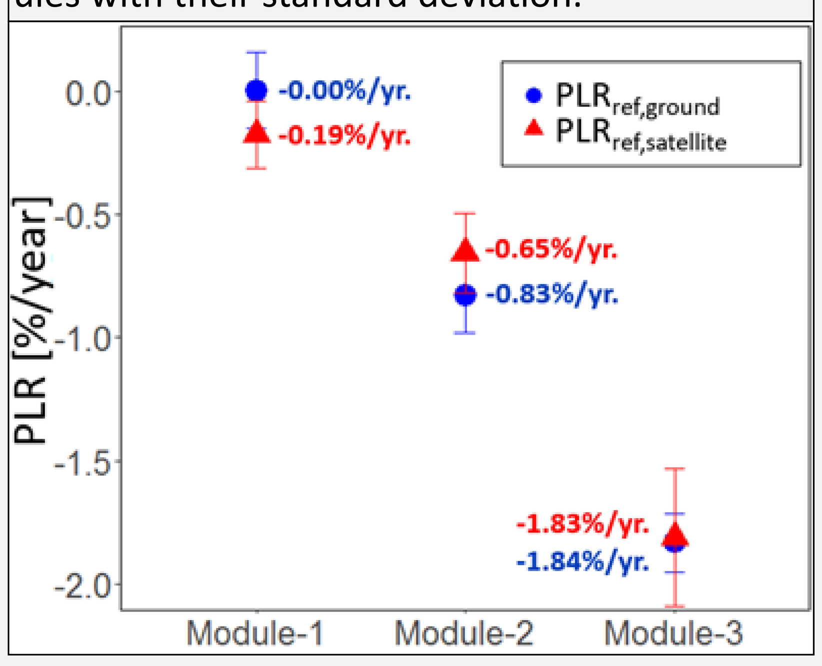

SNSF

This work is supported by the Swiss National Science Foundation under COST IZCOZ0_182967.

University of Applied Sciences and Arts
of Southern Switzerland

SUPSI

Institute for Applied Sustainability to the Built Environment

20. Nationale
Photovoltaik-Tagung 2022

Schweizerische Eidgenossenschaft
Confédération suisse
Confederazione Svizzera
Confederaziun svizra

Swiss Federal Office of Energy SFOE

VSE AES

SWISSOLAR

40 years of the TISO PV plant: update on the oldest PV system connected in Europe

M. Caccivio, D. Chianese, E. Özkalay, G. Friesen, F. Valoti, G. Bellenda

SUPSI PVLab, Institute for Applied Sustainability to the Built Environment (ISAAC),
Via Flora Ruchat-Roncati 15, 6850 Mendrisio

* mauro.caccivio@supsi.ch, +41 (0)79 521 80 09 , pvlab.solar

ABSTRACT

The 13th May 1982, the energy produced by the TISO 10 photovoltaic plant was fed into the electric grid in Lugano for the first time. A part of the 288 modules is still delivering energy today, 40 years after the installation, far beyond the most optimistic expectations. The project, started to study the possible technical and safety problems posed by the connection of a PV plant to the electrical grid, has become a living example of the long-term reliability of photovoltaics. The regular quality checks, performed indoor on 18 reference modules and outdoor with visual and infrared inspections, among the other things, are the key to understand the correlation between power degradation and defects. In this poster, we will present the last measurements on 12 modules from the 48 still installed and we will analyse the evolution of power performances and failures. The 12 modules removed and analysed in laboratory represent one complete substring over four, the one mounting the less performing modules of the new set.

Results after 35 years

- The degradation rate of the electrical performances of the modules, precisely measured with indoor measurements throughout the whole life of the system are far to be uniform: 2 different groups could be identified; one with a negligible degradation rate of -0.2%/year, the other with a degradation rate of -0.69%/year, much higher but still compatible with a 25 years' warranty at 80% of the original power.
- The two distinct behaviours were most probably related to the use of different suppliers for PVB encapsulants.
- The different evolution of the yellowing of the encapsulant (browned PVB, yellowing of the central cells' row, transparent PVB) led to the classification of modules in 3 classes (Class "A" white module, class "B" mild yellow module, class "C" browned module), which matches the information of three different PVB suppliers.
- Class 'A' modules were all included in the best perfomers' distribution.
- After 35 years there were multiple mechanisms, working together towards a faster, not linear degradation.

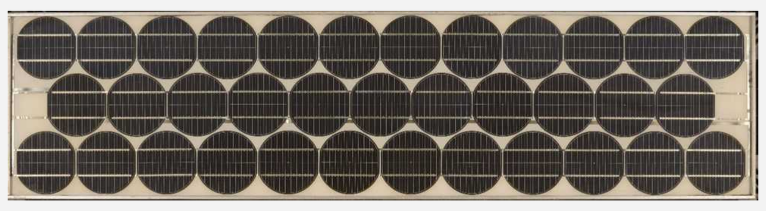

Class "A" module: no yellowing

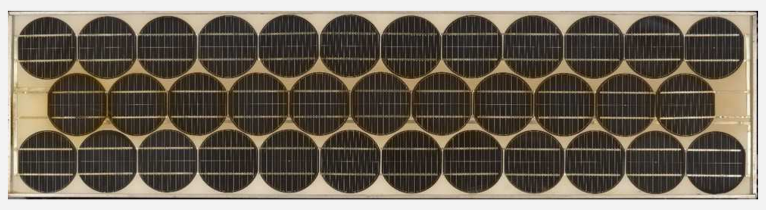

Class "B" module: mild yellowing in the middle

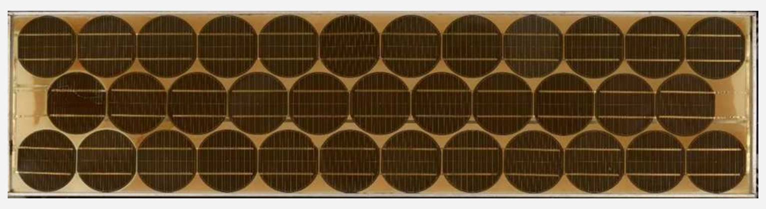

Class "C" module: browning

Verification after 40 years

- 48 modules of the 288 original plant were re-installed, all with successful insulation test results, without critical hot spots and with the highest performances of the lot, measured indoor in the SUPSI PVLab.
- The modules of the new TISO PV plant have been organised in 4 substrings of 12, connected to one SMA 1200 inverter and monitored at single string level.
- The system is back operative since October 2019. Data acquisition, for problems related to the LAN connection, absent after the moving of the SUPSI DACD campus in Mendrisio, has started again in May 2020.
- In March 2022, 3 modules were changed because of problems on 2 out of the 4 strings. Two modules were changed in the first string, the one mounting lower performances modules.
- The 10 modules installed originally in String 1 have been analysed in laboratory, comparing the original results with the ones obtained five years before. Further to electrical performance test and electroluminescence test, high resolution pictures of all the modules were shot, to quantitatively detect changes in the visual inspection.

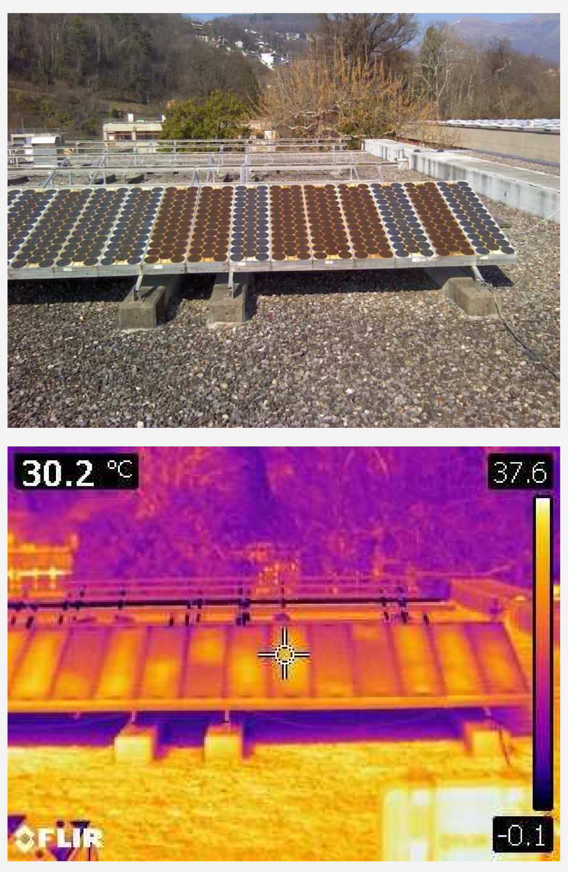

String 1 modules (Visual and IR)

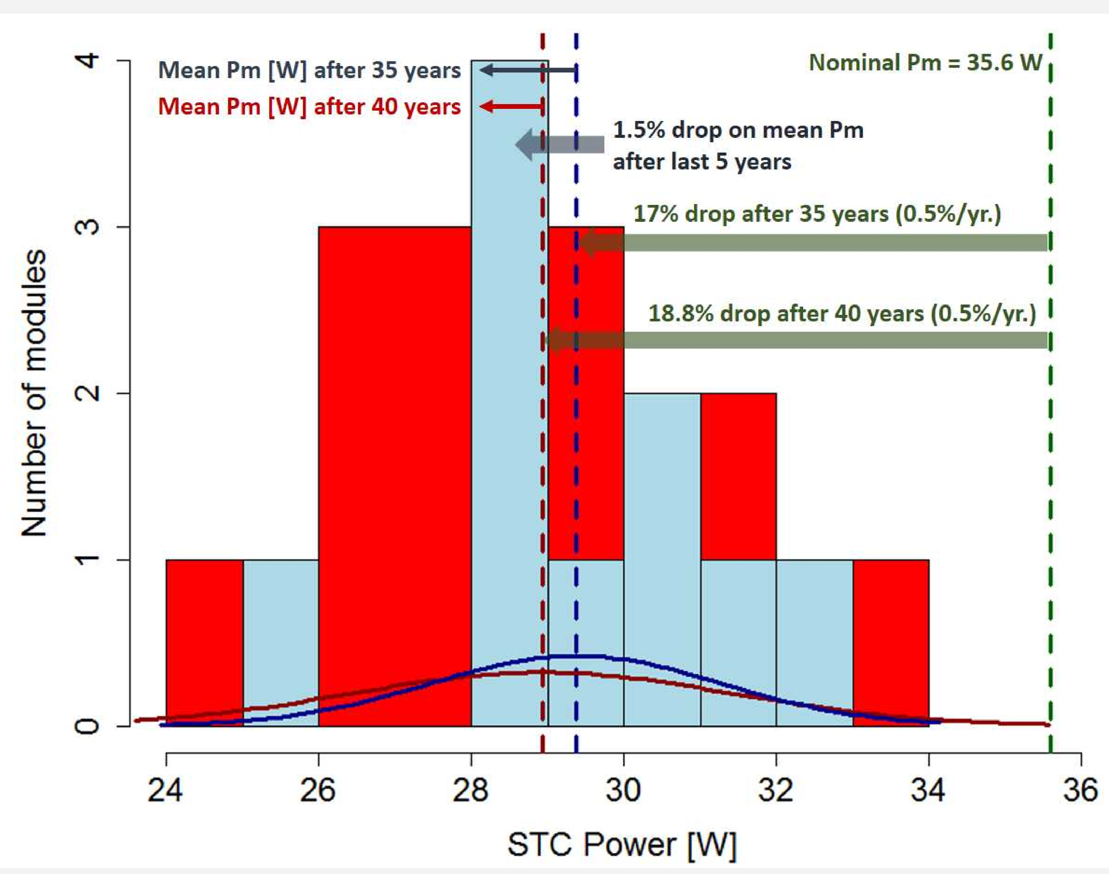

Distribution of power classes of String 1 after 35 (blue)and 40 years(red)

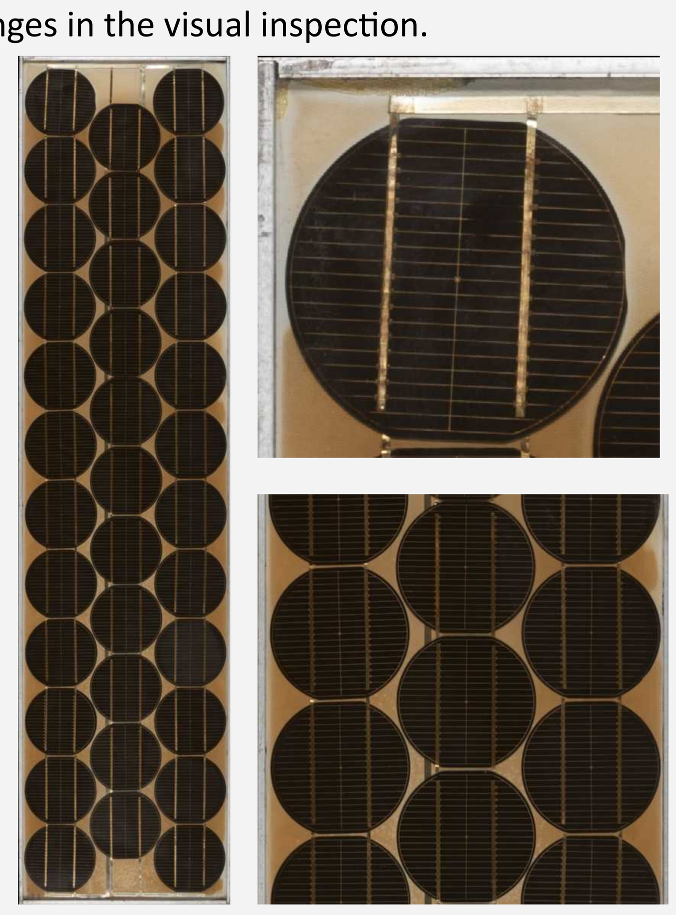

Visual inspection after 35 years

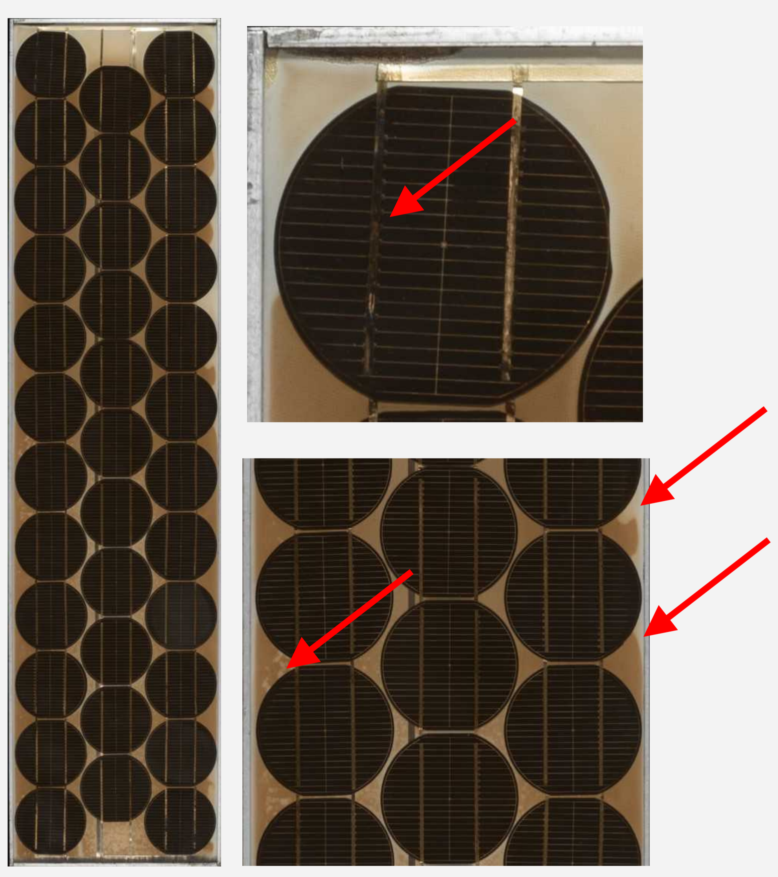

Visual inspection after 40 years

Results after 40 years

- The mean power of 10 modules out of 48 of the new TISO PV plant has lost 1.5% after 5 years. The loss over 40 years is –0.47%/year, still in line with the standard 80% warranty of modern panels. Considering that in 1982 the warranty of ARCO solar was 5 years [M.Green, PIP 2005], the result is excellent.
- The visual inspection on the worst module, (6.9% power loss in five years) performed through high resolution digital images, highlights an important degradation of cell contacts, with increase in series resistance, increase in yellowing , confirmed by 2.1% Isc loss and oxygen bleaching due to increasing losses of the encapsulant: despite the increasing degradation patterns the module is still retaining 77% of the average nominal power for the TISO modules, as measured in laboratory (35.6W).
- On two out of three of the replaced modules the problem is at wiring level, with one connector blown for an electric arc.
- The monitoring of the strings 2,3 and 4 exhibits still values of 70% in terms of DC performance ratio, in line with the indoor results.
- TISO is the living demonstration that a lifetime of more than 40 years for a PV plant is possible.

Incidence Angle Modifier von blendarmen PV-Modulen

Posterbeitrag zur 20. Nationalen PV-Tagung 2022 von Matthias Burri, Peter Wüthrich, Sina Spring und Prof. Dr. Christof Bucher, PV-Labor der Berner Fachhochschule

Der Incidence Angle Modifier (IAM) zeigt auf, wie stark sich die Transmission eines PV-Modulglases bei flachem Sonneneinfallswinkel verkleinert. Damit lassen sich einerseits Simulationsalgorithmen zur Berechnung des Energieertrags kalibrieren, andererseits kann direkt abgeschätzt werden, wie sich der Energieertrag einer PV-Anlage im Winter oder zu den Randstunden des Tages verändert. In diesem Poster werden die IAM von drei blendarmen PV-Modulen miteinander verglichen und Schlussfolgerungen für den Energieertrag gezogen.

Methode

Um den IAM zu bestimmen, wurde die Einstrahlung und der Kurzschlussstrom kontinuierlich gemessen, während der Einstrahlungswinkel variiert wurde. Dafür wurde eigens ein Gestell angefertigt, mit welchem das PV-Modul gekippt werden kann, um den Winkel zu variieren. Die Messungen fanden bei strahlend schönem Wetter statt, um möglichst konstante Verhältnisse zu haben.

Damit der Einfluss der Diffusstrahlung herausgerechnet werden kann, wurde diese aufgenommen, indem die Direktstrahlung der Sonne auf den Sensor abgeschattet wurde. Damit kann für jeden Winkel der Anteil der Direktstahlung auf das Modul bestimmt werden. Der Kurzschlusstrom ist näherungsweise proportional zur Einstrahlung, somit kann der gemessene Kurzschlussstrom rechnerisch korrigiert werden, um nur noch den durch die Direktstrahlung verursachten Strom zu erhalten.

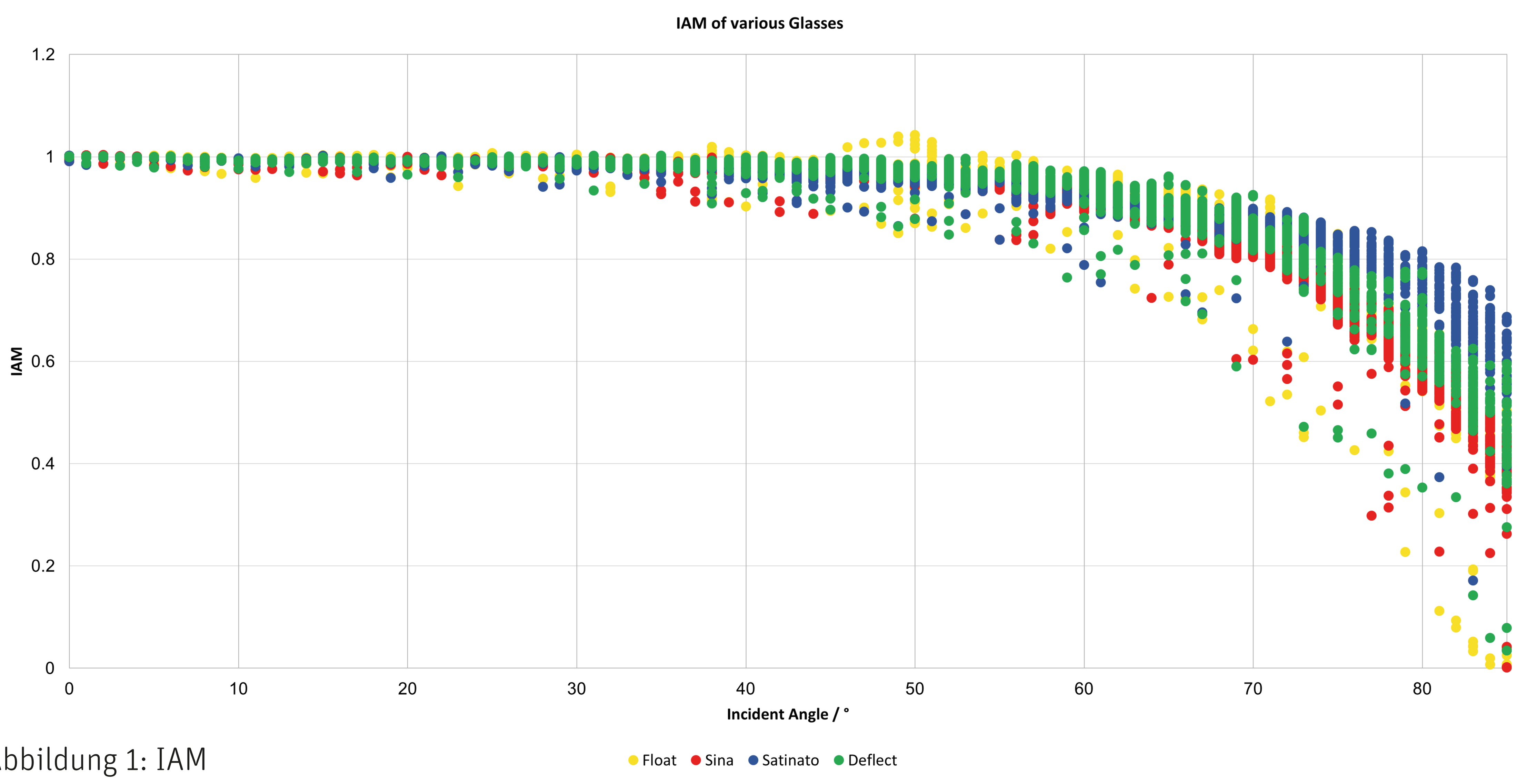

Abbildung 1: IAM

Resultate

Folgende Module wurden ausgemessen:

Modul	Glastyp
3S Megaslate II	Float
3S Megaslate II	Sina (Standard-Glas)
3S Megaslate II	Satinato
Kioto KPV ME NEC	Deflect

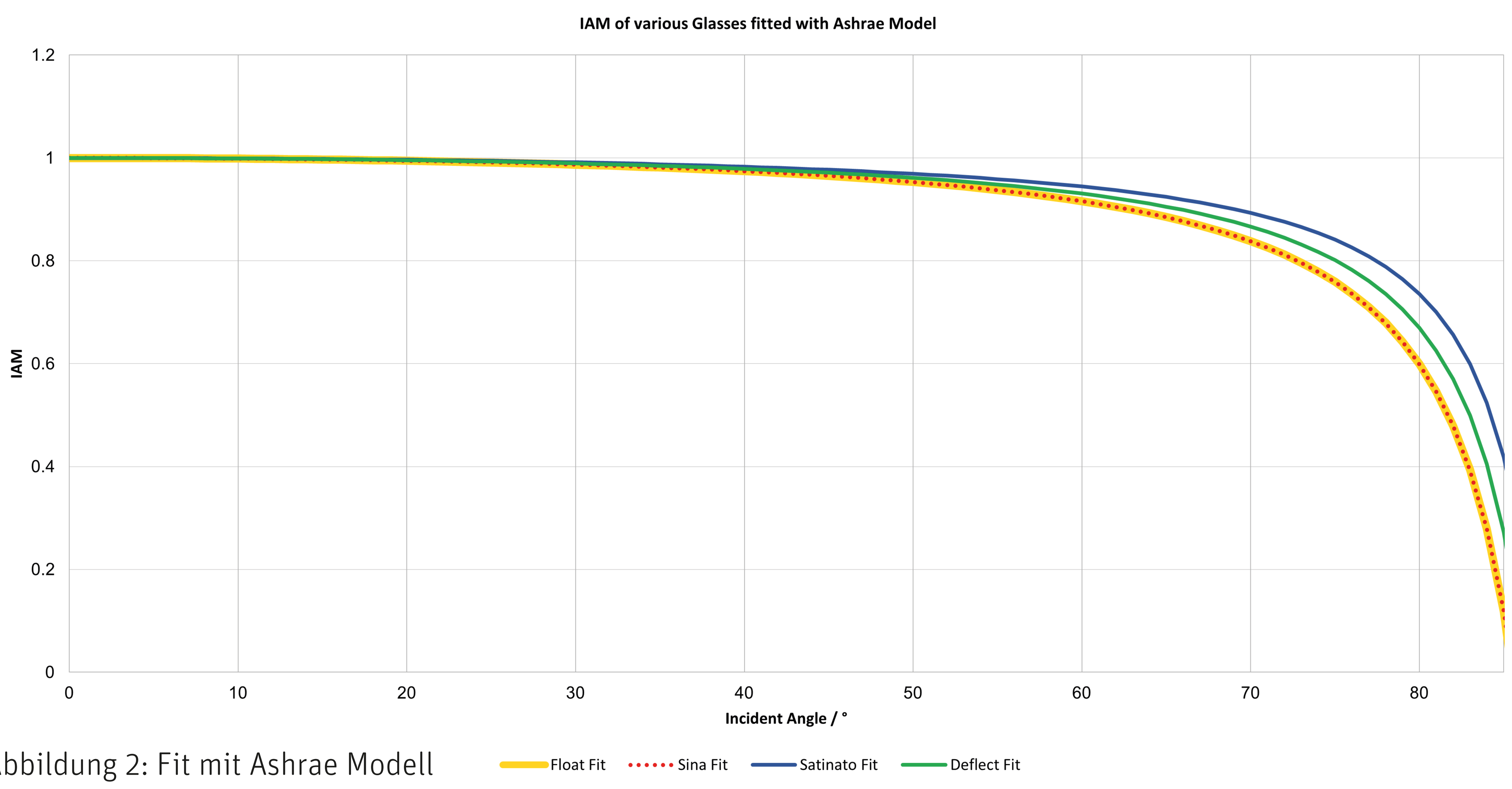

Abbildung 2: Fit mit Ashrae Modell

Die Messungen haben gezeigt, dass blendarme Gläser wie erwartet ein besseres Verhalten zeigen bei flachen Einstrahlungswinkeln. Am besten schneidet hierbei das "Satinato"-Glas ab.

Die Resultate zeigen, dass blendarme Gläser nicht nur ihren namensgebenden Vorteil der geringeren Blendwirkung aufweisen, sondern auch einen erhöhten Energieertrag haben können. Insbesondere in Situationen mit hohem Anteil an Diffusstrahlung, wie zum Beispiel im Winter, kommt diese Eigenschaft zum Tragen.

Berner Fachhochschule

https://www.bfh.ch/pvlab

▶ Technik und Informatik

Labor für Photovoltaiksysteme | Jlcoweg 1 | 3400 Burgdorf | Schweiz
bfh.ch | wip3@bfh.ch

IV-Curve Tracer

Posterbeitrag zur 20. Nationalen PV-Tagung 2022 von Mischa Müller, Luciano Borgna, Sina Spring und Prof. Dr. Christof Bucher, PV-Labor der Berner Fachhochschule

In diesem Poster wird ein neu entwickelter IV-Curve Tracer (IVCT) vorgestellt, der parallel zu einem handelsüblichen Modulwechselrichter (WR) betrieben wird. Die PV-Modulkennlinie wird in weniger als200 ms gemessen, so dass der WR keinen Betriebsunterbruch feststellen kann. Der IVCT wurde im Rahmen einer Bachelorarbeit am PV-Labor der BFH entwickelt und zeigt in der ersten Testphase eine hohe Genauigkeit von 0.5%.

Die Einzelüberwachung von Photovoltaikmodulen (PV-Modulen) ermöglicht es, ihr Betriebs- und Alterungsverhalten im Detail zu untersuchen. Mit dem regelmässigen Messen der Kennlinie können diverse Alterungseffekte wie Zellbruch oder inhomogene Verschmutzung detektiert werden. Mit dem hier vorgestellten IVCT soll das Langzeitverhalten von PV-Modulen im Rahmen von Forschungsarbeiten untersucht werden.

Konzept

Hardware: Mittels Leistungs-MOSFET wird das am WR betriebene PV-Modul auf einen variablen Widerstand umgeschaltet. Der Widerstand wird von einem Microcontroller angesteuert und fährt in programmierbarer Geschwindigkeit die Kennlinie des PV-Moduls ab. Der Microcontroller wird von einem Raspberry PI angesteuert, welches mithilfe der DAQ-Karte MCC128 auch Strom, Spannung, Temperatur und Einstrahlung misst. Strom und Spannung werden mit einer Frequenz von 100 kHz gemessen und nach Bedarf gemittelt.

Software und Kommunikation: Das Hauptprogramm ist in Python 3 geschrieben und läuft auf dem Raspberry PI. Dieses kommuniziert über den I2C-Bus und einem digitalen Trigger-Signal mit dem Mikrokontroller. Die Steuerung erfolgt per Fernzugriff über ein Webinterface.

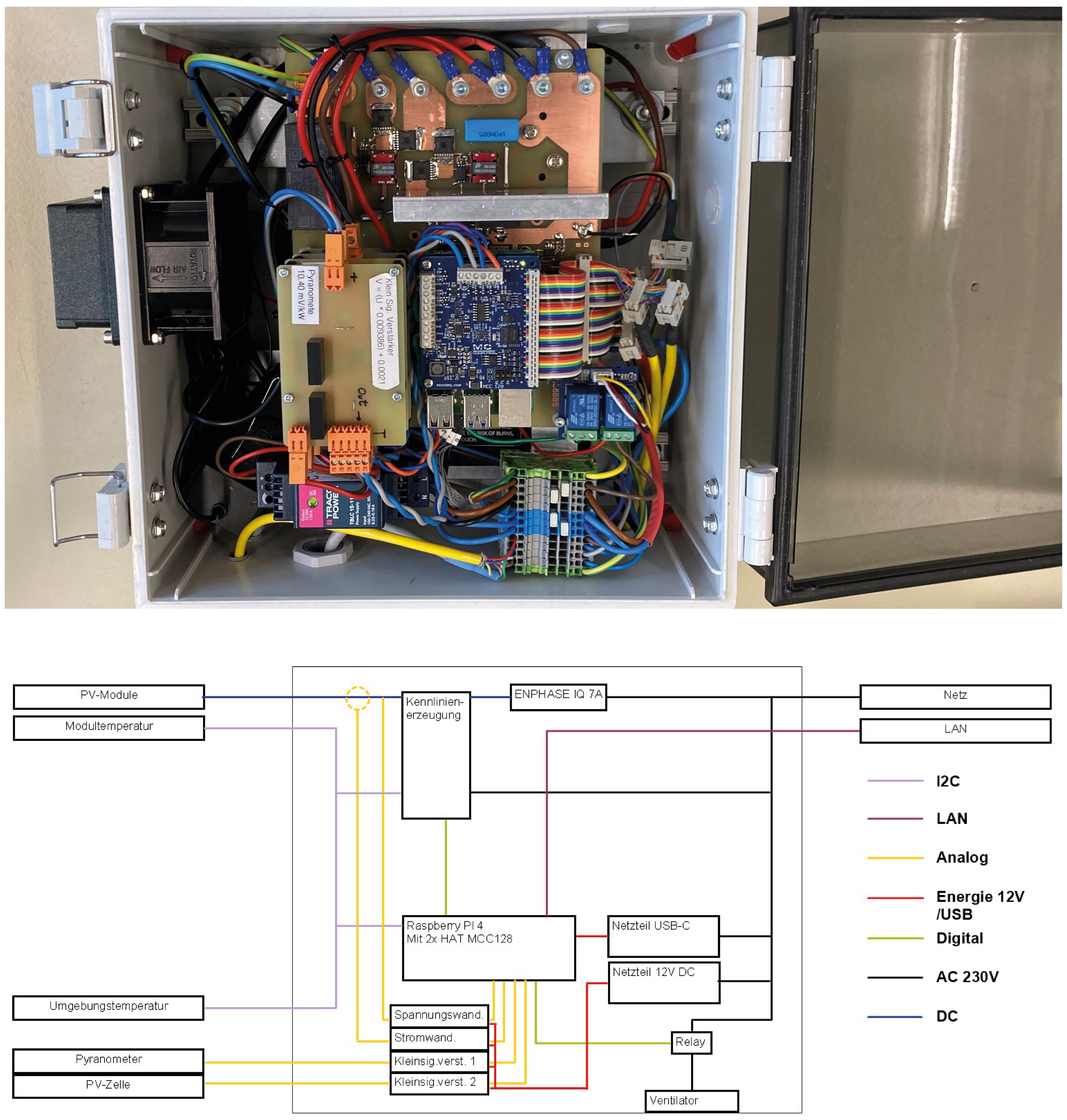

Abbildung 1: Prototyp und Prinzipschema IVCT

Ausblick

- Weiterentwicklung zur Überwachung von mehreren PV-Modulen an einem IVCT.
- Datenspeicherung auf zentralem Server oder externem Speicher
- Kompaktere Bauweise

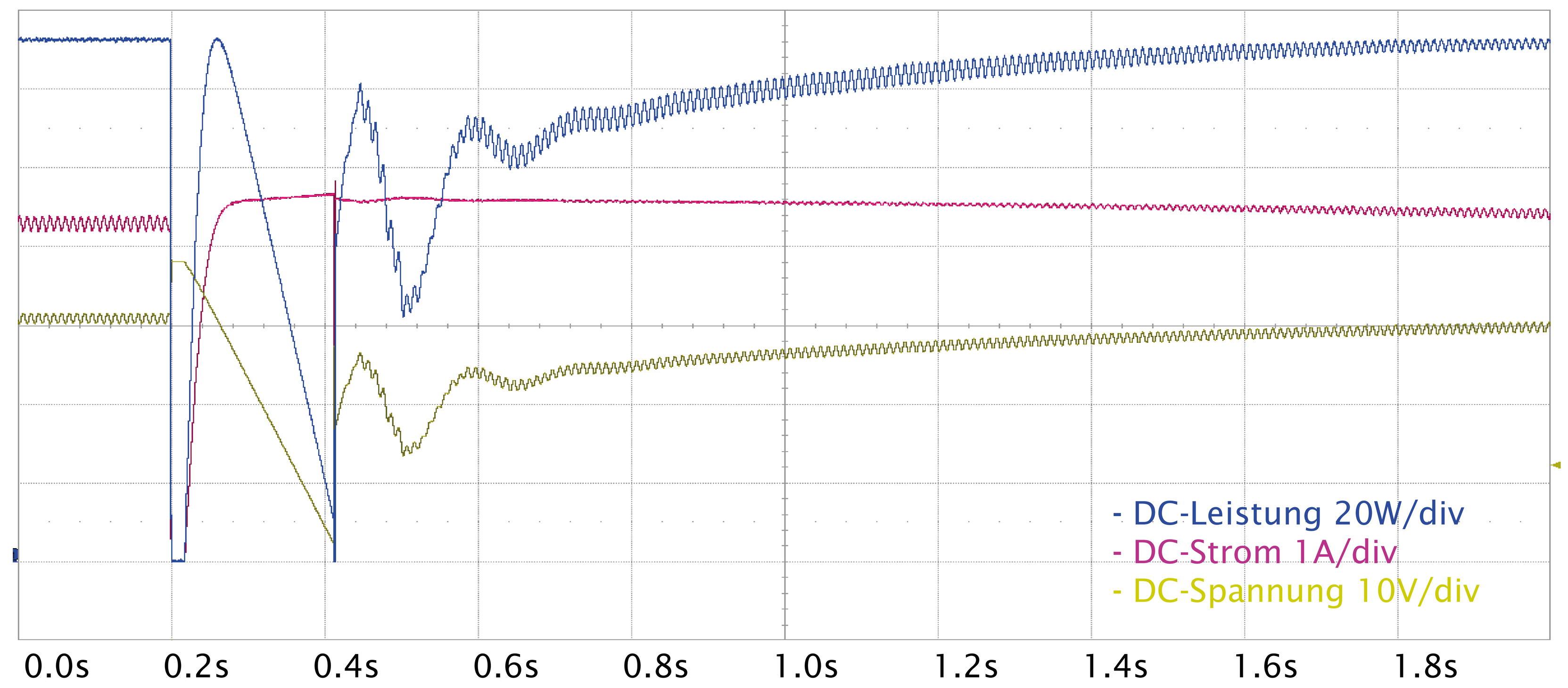

Abbildung 2: Kennlinienmessung mit Wiederaufnahme Einspeisebetrieb WR

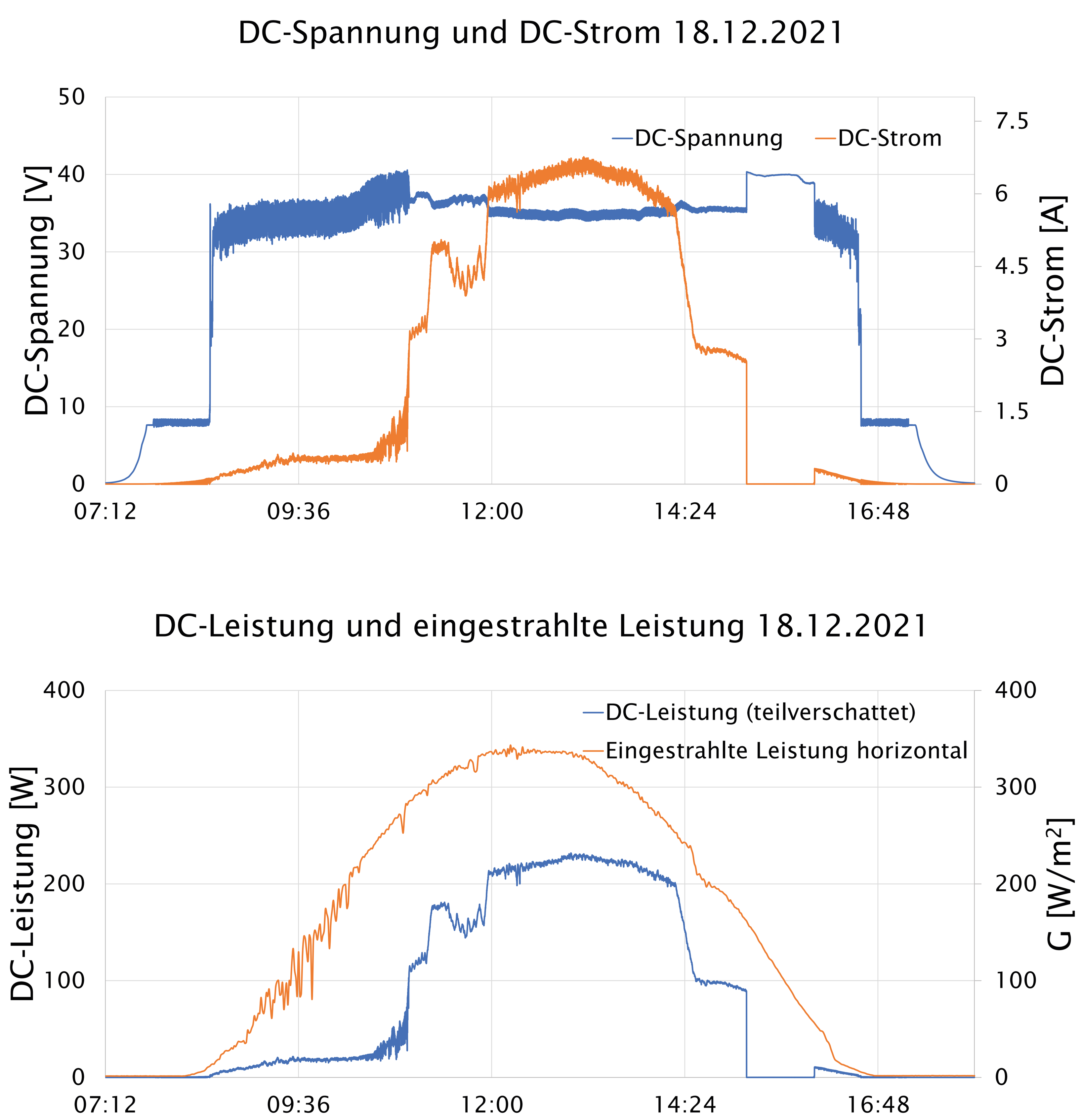

Abbildung 3: Messungen vom 18.12.2021

Berner Fachhochschule

▶Technik und Informatik

Labor für Photovoltaiksysteme | Jlcoweg 1 | 3400 Burgdorf | Schweiz
bfh.ch | mlm14@bfh.ch

Visual Inspection of PV Modules

20th National Photovoltaics Conference, March 2022, Bern
Matthias Burri, Sina Spring and Prof. Dr. Christof Bucher, Bern University of Applied Sciences, PV Lab

The state of health of a PV module can be assessed using various methods. Electroluminescence (EL), indoor and outdoor infrared (IR), UV luminescence, current-voltage-curve measurement (IV) and visual inspection are some of them. This poster compares these methods and shows the advantages and disadvantages of each.

New module | Shaded module | Module with cell cracks

Visual

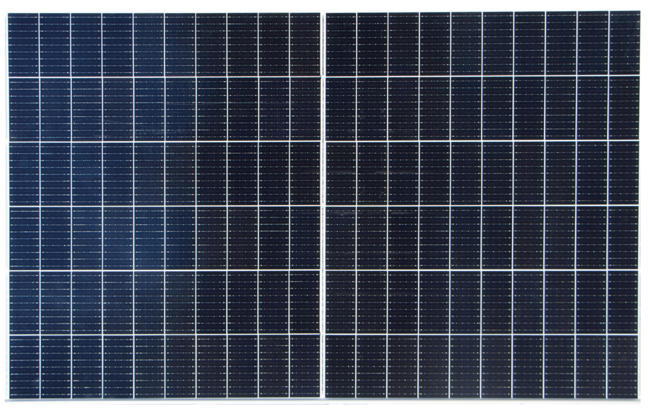
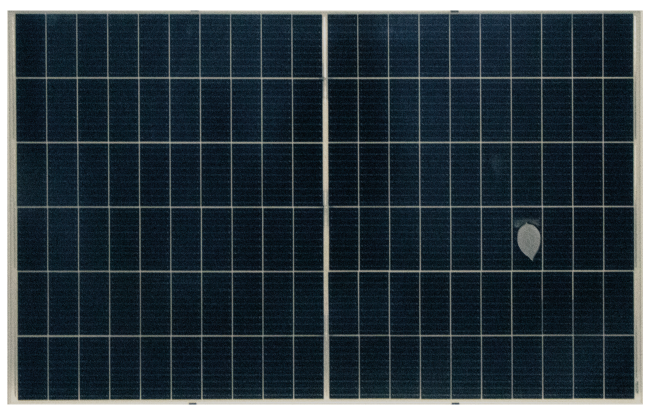
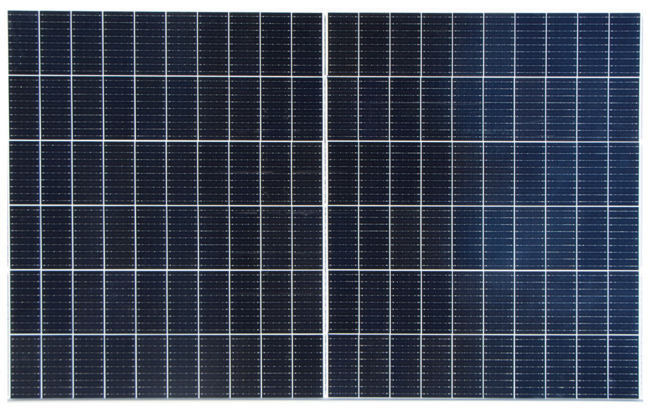

Visual inspection of a PV module.

Advantages:
- No specialized equipment needed
- Mechanical defects with no electrical implication visible

Disadvantages:
- Most electrical defects not visible
- Not quantifiable

Outdoor IR

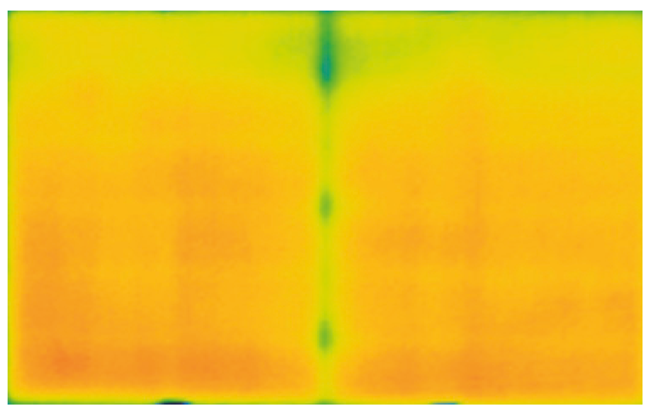
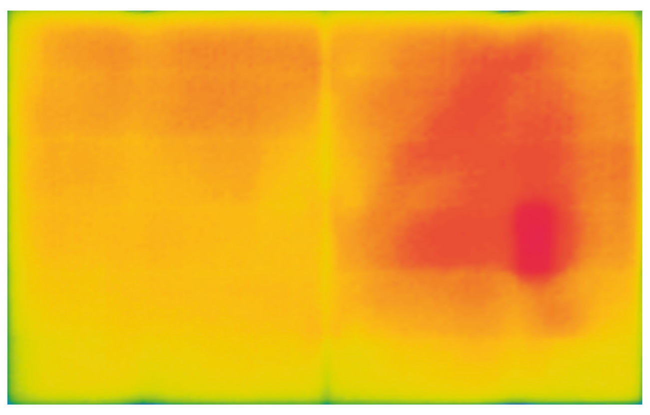
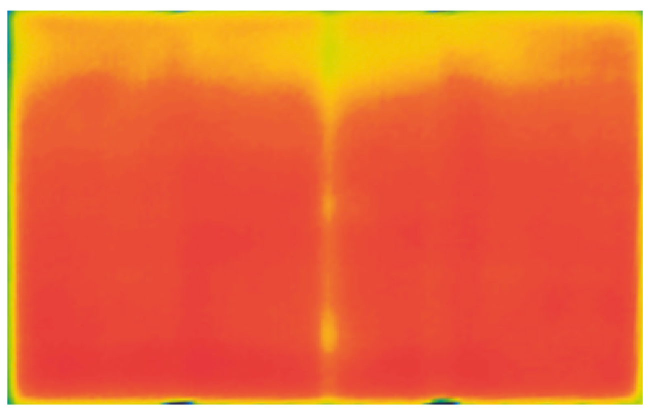

Thermographic imaging of a module in maximum power point (MPP) operation.

Advantages:
- No system manipulation required
- Identifies energy relevant failures
- Measurement can be done for a full system
- The modules do not have to be dismantled.

Disadvantages:
- Weather influence
- Poor accessibility to panels
- High temperature ≠ defect
- Cell cracks not necessarily visible

Indoor IR

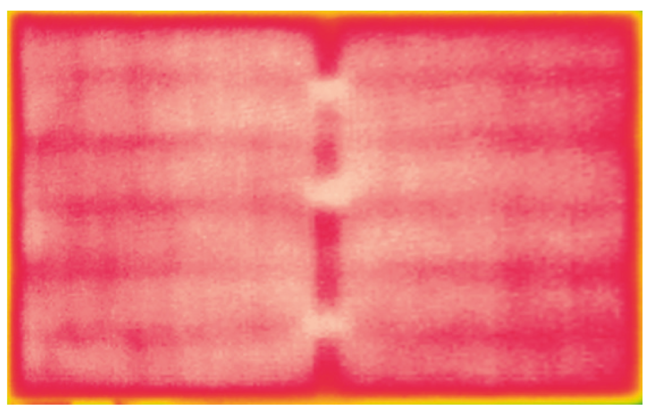

←Test module, intact cells
Test module, cell cracks→

Indoor IR imaging won‘t show shading, since the heat registered isn‘t produced by incident light but instead by the current running through the module.

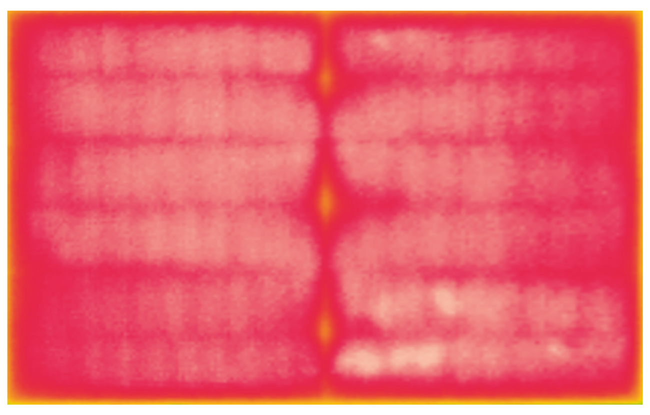

Thermographic imaging of a module in laboratory conditions under rated current.

Advantages:
- Identifies shunts, hot spots, moisture, installation failures
- More reproducible than outdoor

Disadvantages:
- Not representative for MPP operation
- High temperature ≠ defect
- External power suppy necessary
- Low shunt and high series resistance not easy to distinguish

Indoor EL

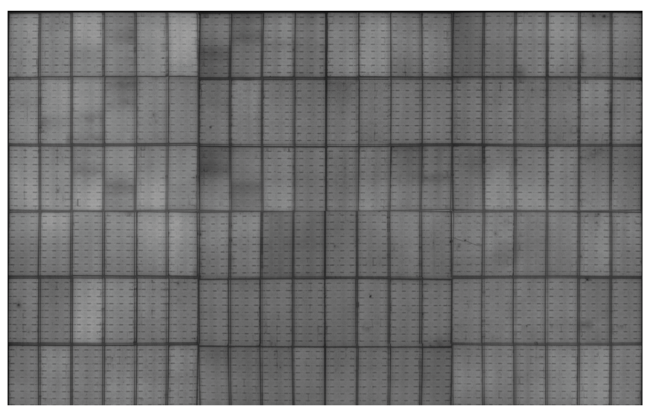
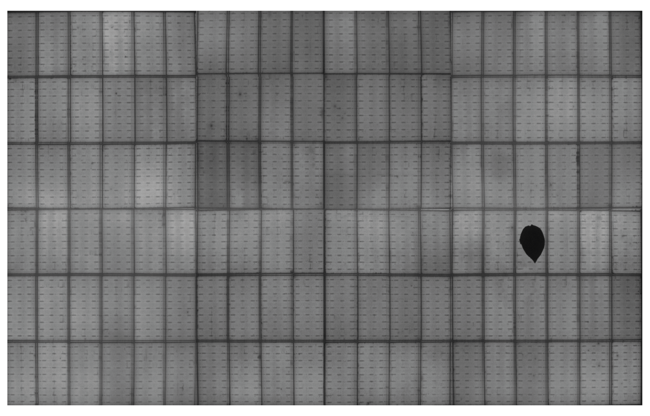
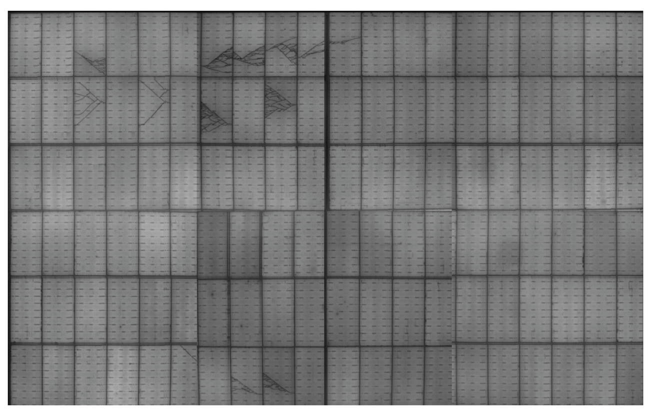

Electroluminescence imaging of a module in laboratory conditions under DC current.

Advantages:
- High-Resolution
- Identifies cell cracks, microcracks, shunts, layer defects, diode failure, disconnected cell regions, soldering defects

Disadvantages:
- Defect origin not identifiable
- Defect influence on performance not identifiable
- xpensive laboratory equipment needed
- Modules must be dismantled

Indoor UV

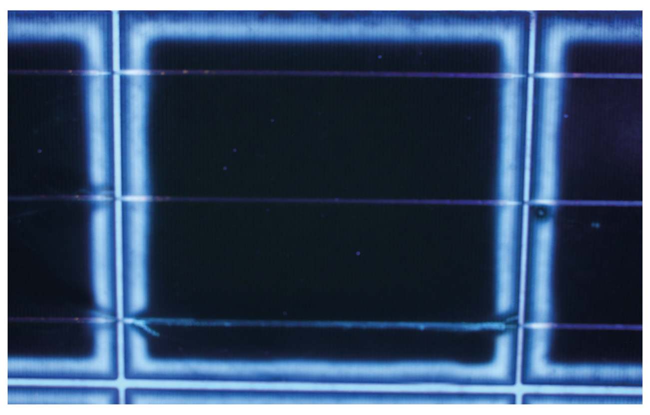

←Monocrystalline module, intact cell
Monocrystalline module, cell cracks→

UV fluorescence doesn‘t show recent cell cracks. These images show old PV modules.

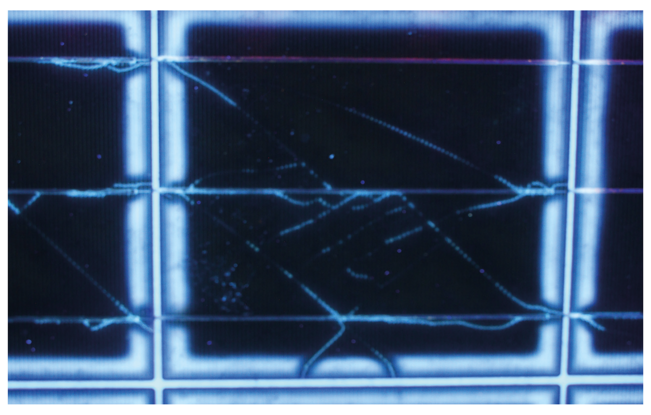

Photographic imaging of UV fluorescence of a module under ultraviolet light.

Advantages:
- Shows chronology of cell cracks (photo-bleaching)
- High-Resolution
- No power supply necessary
- Modules do not have to be dismantled
- indicates thermal history of cells

Disadvantages:
- Doesn‘t work well on newer modules and new defects
- Defect influence on performance not necessarily identifiable
- Complete darkness needed

Indoor IV curve

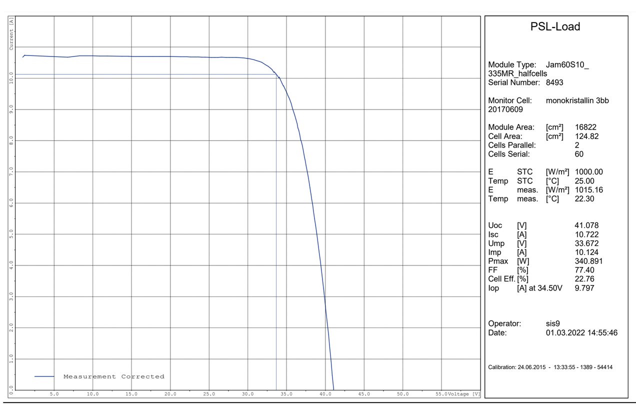

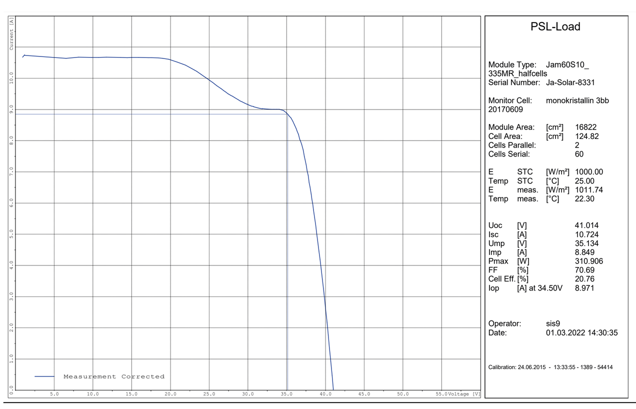

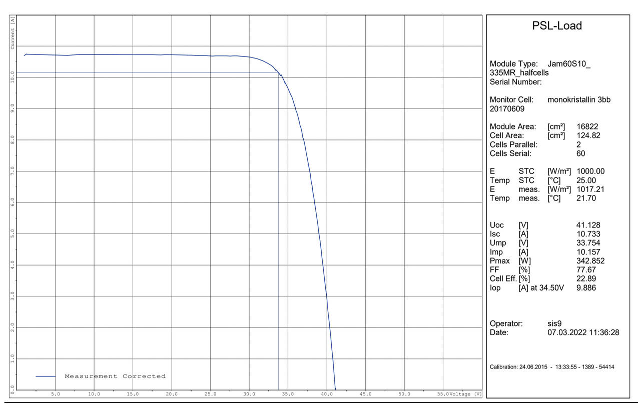

IV curve tracing under laboratory conditions.

Advantages:
- Shows (partial) shading, soiling, degradation
- Shows series resistance, shunts
- Short test time
- Reproducible results

Disadvantages:
- Expensive laboratory equipment needed
- Modules must be dismantled
- On-site effects (i.e. partial shading) not visible

Outdoor IV curve

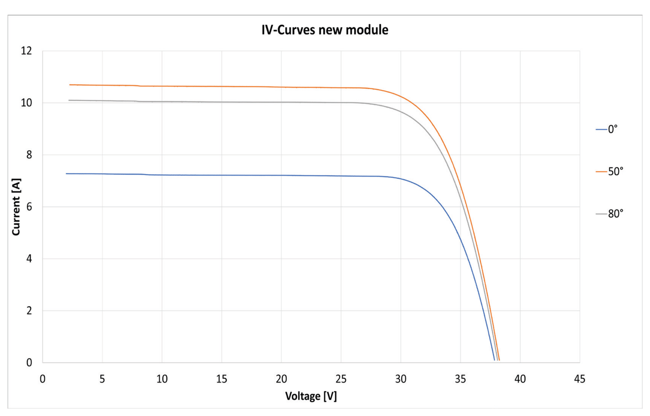

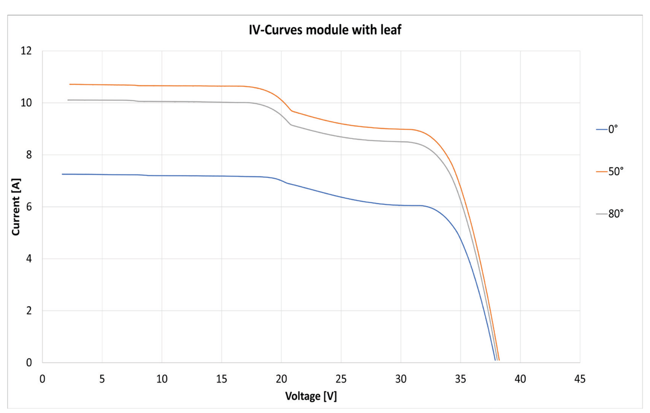

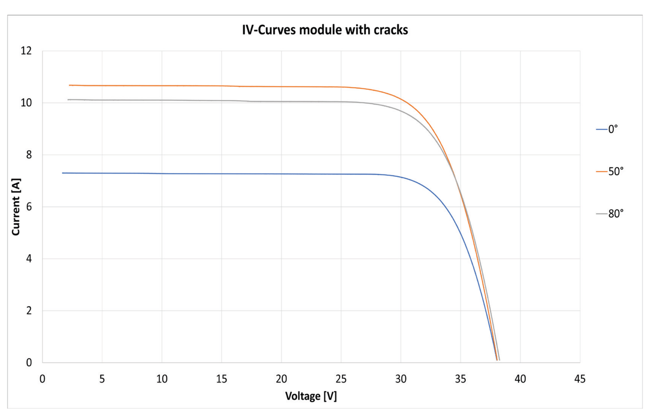

Mapping relationship between current and voltage from open circuit to short circuit electrical load in actual use.

Advantages:
- Real usage (e.g. shading) shown
- Modules do not have to be dismantled.
- Measurement can be done on module level or for a full system

Disadvantages:
- Results not fully reproducible
- Temperature correction needed
- Correction with irradiance data needed

Berner Fachhochschule

▶Technik und Informatik

Labor für Photovoltaiksysteme | Jlcoweg 1 | 3400 Burgdorf | Schweiz
bfh.ch | christof.bucher@bfh.ch

University of Applied Sciences and Arts
of Southern Switzerland

SUPSI

Institute for Applied Sustainability to the Built Environment

20. Nationale
Photovoltaik-Tagung 2022

Schweizerische Eidgenossenschaft
Confédération suisse
Confederazione Svizzera
Confederaziun svizra

Swiss Federal Office of Energy SFOE

VSE AES

SWISSOLAR

Improvement of hail test setup for larger hailstones

M. Caccivio*, M. Ronchi, M. Ceretti, F. Valoti, G. Bellenda

SUPSI PVLab, Institute for Applied Sustainability to the Built Environment (ISAAC),
Via Flora Ruchat-Roncati 15, 6850 Mendrisio

* mauro.caccivio@supsi.ch, +41 (0)79 521 80 09 , pvlab.solar

ABSTRACT

Climate change is playing a major role in the increasing of severe weather phenomena, even more when we consider alpine environment, where hailstorms are more frequent and intense: in 2021 the damages due to storms and hailstorms amounted to 1,9 billion Euro only in Switzerland. This trend is subject of detailed scientific studies, aiming at the definition and validation of risk maps to forecast the frequency of events, with extended ranges up to 50 years, in order to choose the appropriate, robust products to reduce the insurance costs in higher risk areas. The hail damage is of particular relevance for photovoltaics, for this reason, a dedicated IEC working group for the definition of a new technical specification (IEC TS 63397) has been set up. The traditional hail test, foreseen at IEC level to qualify a PV module (IEC 61215-2, MQT17), is set to 25mm of diameter and 80 km/h (22 m/s) of speed. In Switzerland, due to the particular conditions of the environment, the applied standard, issued by VKF (Vereinigung Kantonaler Feuerversicherungen) is more demanding, setting minimum requirement at 30 mm but in practical terms, raising it to 40 mm and more. In this framework, SUPSI PVLab, the only ISO 17025 accredited test laboratory for PV modules in Switzerland, is working on improvements of the hail test stand, to reach up to 100mm of diameter and 166 km/h of speed, in order to grant sufficient test margins for the module manufacturers to evaluate the robustness of their products.

Normatives

GENERAL REQUIREMENTS

The VKF (APIB) test specifications are used for the determination of the hail impact resistance of building components on the basis of consistent, product-neutral testing and classification methods. They include the generally valid guidelines for the execution of a hail impact resistance test (APIB Test Specification No. 00a - GENERAL SECTION A, Part A), binding instructions on the documentation of the test set-up and the results achieved (APIB Test Specification No. 00b - GENERAL SECTION B, Part B), as well as supplementary specifications relevant to specific building components.

The standard SIA 261/1 (2003), Art. 6.2.4 refers to the Swiss Hail Impact Protection Register of the CFIA. Published in the Hail Impact Protection Register for the building components entered are the hail impact resistance classes achieved in the hail impact resistance test for all the component functions required in the component-specific test specifications. The Swiss Hail Impact Protection Register of the CFIA should make it easier for users to select a product that has been tested and classified. It has a similar structure to the Swiss Fire Protection Register of the CFIA.

Classification VKF and IEC

The VKF definition of a hail impact resistance class (HW n) is based on the diameter of a hailstone:

- Hail resistance class 1 (**HW 1**) is defined by the kinetic energy at impact of a hailstone with a diameter of **10 mm**
- Hail resistance class 2 (**HW 2**) is defined by the kinetic energy at impact of a hailstone with a diameter of **20 mm**
- Hail resistance class 3 (**HW 3**) is defined by the kinetic energy at impact of a hailstone with a diameter of **30 mm**
- Hail resistance class 4 (**HW 4**) is defined by the kinetic energy at impact of a hailstone with a diameter of **40 mm**
- Hail resistance class 5 (**HW 5**) is defined by the kinetic energy at impact of a hailstone with a diameter of **50 mm**

For the hailstones of 10 to 50 mm diameter the following Class boundaries, in terms of impact kinetic **energy**, mass and velocity are defined, including the intermediate values for the projectile diameters 25 mm, 35 mm, 45 mm, 55 mm, 65 mm and 75 mm (from Appendix B -Table 4 of the VKF reference standard), and the values for the larger projectile sizes (60 mm, 70 mm and 80 mm - from Appendix B -Table 3 of the VKF reference standard). The impact energies as defined in in the international IEC and European standardization are shown as well:

Hail resistance **CLASS**	Hailstone **diameter**	G_{min} - **min. mass**	G_{MAX} - **MAX mass**	v_R - **Velocity** on impact	**Impact energy** - min. limit **E_{min}**	**Impact energy** - MAX limit - **E_{MAX}**
	[mm]	≥ [g]	≤ [g]	[m/s]	≥ [J]	≤ [J]
HW1	**10**	0.43	0.51	13.77	0.04	0.09
	15	1.46	1.71	16.87	0.22	0.37
HW2	**20**	3.46	4.04	19.48	0.69	1.0
	25	6.76	7.90	21.77	1.69	2.3
HW3	**30**	11.68	13.65	23.85	3.50	4.4
	35	18.55	21.67	25.76	6.5	7.9
HW4	**40**	27.70	32.35	27.54	11.1	13.2
	45	39.43	46.06	29.21	17.7	20.9
HW5	**50**	54.09	63.18	30.79	27.0	31.5
	55	72.00	84.10	32.30	39.5	45.9
	60	93.47	109.18	33.73	56.0	64.7
	65	118.85	138.81	35.11	77.1	89.0
	70	148.43	173.38	36.44	104	120
	75	182.57	213.25	37.72	137	157
	80	221.57	258.80	38.95	177	204

VKF definition of a hail impact resistance class

min	**DIAM.**	max	min	**MASS**	max	min	**VEL.**	Max	min	**ENERGY**	Max
	[mm]			[g]			[m/s]			[J]	
23.75	**25**	26.25	7.15	**7.53**	7.91	22.31	**23.0**	24.15	1.78	**2.0**	2.31
33.25	**35**	36.75	19.67	**20.7**	21.74	25.84	**27.2**	28.56	6.57	**7.7**	8.86
42.75	**45**	47.25	41.71	**43.9**	46.10	29.17	**30.7**	32.24	17.74	**20.7**	23.95
52.25	**55**	57.75	76.19	**80.2**	84.21	32.21	**33.9**	35.60	39.51	**46.1**	53.35
61.75	**65**	68.25	125	**132.0**	139	34.87	**36.7**	38.54	76.22	**88.9**	102.91
71.25	**75**	78.75	193	**203.0**	213	37.53	**39.5**	41.48	136	**158**	183

EN-IEC 61215-2:2021 hail test parameters

Basic principles of VKF hail resistance test

Natural hailstones can assume different shapes. In principle, however, spherical projectiles made of transparent, optically clear ice (produced by different methods) are used for testing. The ice quality is periodically checked by the testing house, by means of inter-laboratory tests.

The test parameters are deliberately selected so that, in comparison with natural hailstones, the projectiles travel at a higher speed. By doing this, it could be ensured that the hailstones that occur in nature would, most probably, have a lower impact kinetic energy than those used for testing. For the determination of the physical data in the nature and in the testing laboratory, the following equations are used:

Calculation of kinetic **energy**:

$$E_H = \frac{m_H \cdot v_A^2}{2}$$

E_H : impact energy of hailstone [J]
m_H : mass of hailstone [kg]
v_A : speed on impact ("velocity") [m/s]

Calculation of the **mass** of the hailstone:

$$m_H = V_H \cdot \rho_{Eis} = \frac{4 \cdot \pi \cdot \left(\frac{d_H}{2}\right)^3}{3} \cdot \rho_{Eis}$$

m_H : mass of hailstone [kg]
V_H : volume of hailstone [m³]
ρ_{Eis} : ice density [kg/m³]
d_H : diameter of hailstone [m]

Calculation of the **velocity** on impact:

The speed on impact according to SIA 261/1 (referred also as "velocity of fall" in SIA 261/1) is calculated from the diameter of the hailstone, density of the ice and density of the air, gravitational acceleration and air drag coefficient:

$$v_{max} = \sqrt{\frac{4 \cdot \rho_{Eis} \cdot d_H \cdot g}{3 \cdot \rho_{Luft} \cdot c_w}}$$

v_{max} : maximum speed on impact ("velocity") [m/s]
ρ_{Eis} : ice density [kg/m³]
ρ_{Luft} : air density [kg/m³]
d_H : diameter of hailstone [m]
g : gravitational acceleration = 9.81 [m/s²]
c_w : air drag coefficient of a sphere with a slightly rough surface [-]

Values assumed for the evaluation of impact kinetic energy:
ρ_{Eis} = 870 [kg/m³] - density of projectile
ρ_{Luft} = 1.2 [kg/m³] – air density at ambient temperature =20°C, 1 atm.
c_w = 0.5 [-] air drag coefficient of a sphere with a slightly rough surface

Methods, results and improvements achieved

- Study about the possibility to increase the capability of hail test setup to shoot at 70, 80, 90 and 100mm, in order to give margin to the manufacturers to understand effective behaviour under extreme events.
- Need to increase the air speed out of the compressive air cannon in order to control the speed of 110-450g of ice: VKF standard is more stringent than IEC standard for what concern limits on impact energy.
- Use of schematic for "ultra sonic ping pong ball" with 3D printed "De Laval" nozzle and Venturi valve to create vacuum: ⇨ Not OK. Insufficient pressure and heavy weight of the projectile are limits.
- Increase of valves' diameter to have larger flow on the new, larger cannons of 70, 80, 90 and 100mm, simplification of setup: ⇨ OK. Speed limit of 64.8 m/s with 70mm hail, well above the needs.
- Ice ball silicon moulds not OK for the production of repeatable ice balls, the use of larger aluminium moulds is under investigation.

- Successful test for use of accredited hail test up to 70 mm, above the previous limit of 60mm. Margins to be further explored.

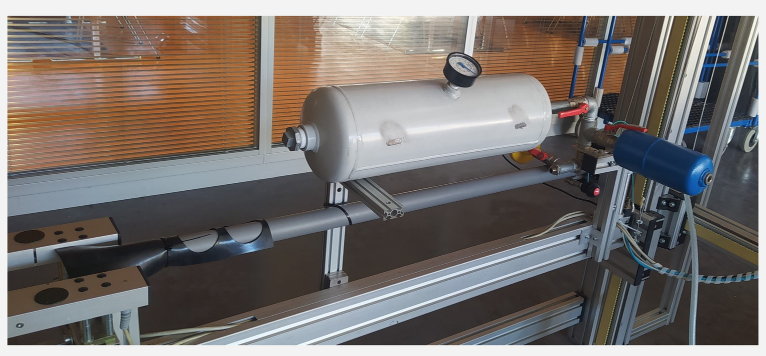

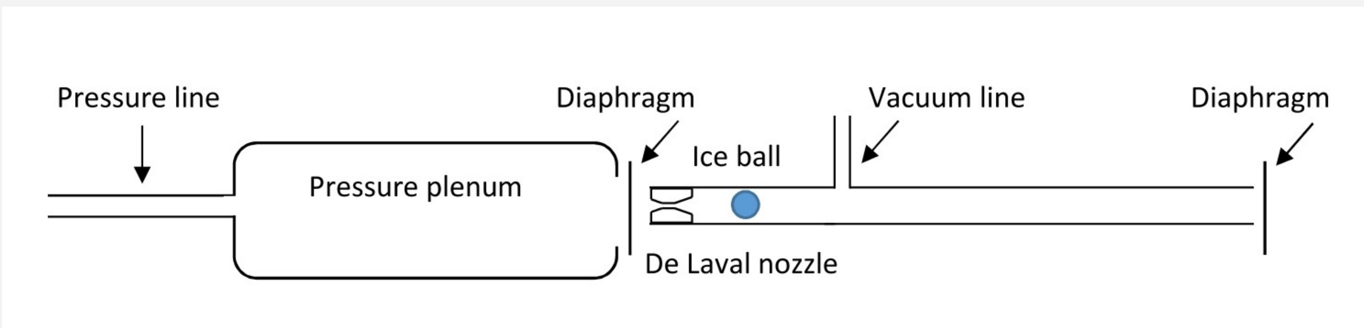

Experiment with 3d printed parts, experimental setup and schematic of ultra sonic system.

NOT OK

OK

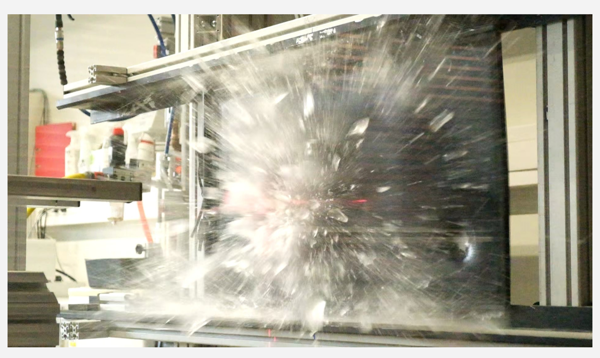

New test setup,cannon for larger diameters, silicone moulds for larger ice-balls, comparison with real hailstone in July 2021, Canton Luzern, impact of 100mm on module

Laborautomatisierung mit MUSCLE

Posterbeitrag zur 20. Nationalen PV-Tagung 2022 von David Joss, Mischa Müller, Peter Wüthrich, Sina Spring, Marco Zaugg, Matthias Burri und Prof. Dr. Christof Bucher, PV-Labor der Berner Fachhochschule

Ein Prüflabor an einer Fachhochschule soll einerseits korrekte und wiederholbare Prüfergebnisse erzielen, andererseits Studierenden Kenntnisse im Bereich der Prüfung und Laborautomation vermitteln können. An der Berner Fachhochschule wurde dafür das MUSCLE-Konzept entwickelt: In einer Embedded Linux Umgebung wird die Kommunikation zwischen Benutzer:in, den zu steuernden Simulatoren und den Messgeräten sichergestellt. Die browserbasierte Bedienoberfläche ermöglicht es, typische Prüfungen am PV-Labor wie die Kennlinienmessung an PV-Modulen oder automatisierte Wechselrichtertests durchzuführen.

Wirkungsfeld PV-Labor

Das PV-Labor der Berner Fachhochschule ist in der Photovoltaik-System tätig und führt regelmässig Messungen an PV-Modulen und Wechselrichtern durch.

Das Rückgrat der modernen Messeinrichtungen bildet MUSCLE. MUSCLE ist ein Open Source Projekt zur Laborautomatisierung, welches an der Berner Fachhochschule entwickelt wurde. Es ermöglicht eine gut strukturierte Ansteuerung der unterschiedlichsten Geräte im Prüflabor.

Konzept von MUSCLE

Das Konzept von MUSCLE basiert auf drei Hauptelementen.

Frontend - Mittels einer Single Page Webapplikation, welche über Smartphone, Tablet oder Computer aufgerufen wird, werden verschiedene Laborinstrumente/ systeme gesteuert und ausgelesen.

Device - Zur direkten Verbindung mit dem Laborinstrument oder Laborsystem wird ein Embedded Linux Gerät eingesetzt, welches anhand eines unterstützten Protokolls (gängig sind TCP/MODBUS/GPIB/CAN) mit dem Instrument/System kommuniziert.

Backend - Im Hintergrund verwaltet ein Backend-Server sämtliche Benutzer und Geräte.

Die Daten oder Befehle werden über AJAX-HTTP- und JSON RPC Protokolle zwischen dem Device und dem Frontend ausgetauscht. Die Implementation der Peripheriegeräte am PV-Labor ist in Python umgesetzt und für die APIs kommt Flask zum Einsatz.

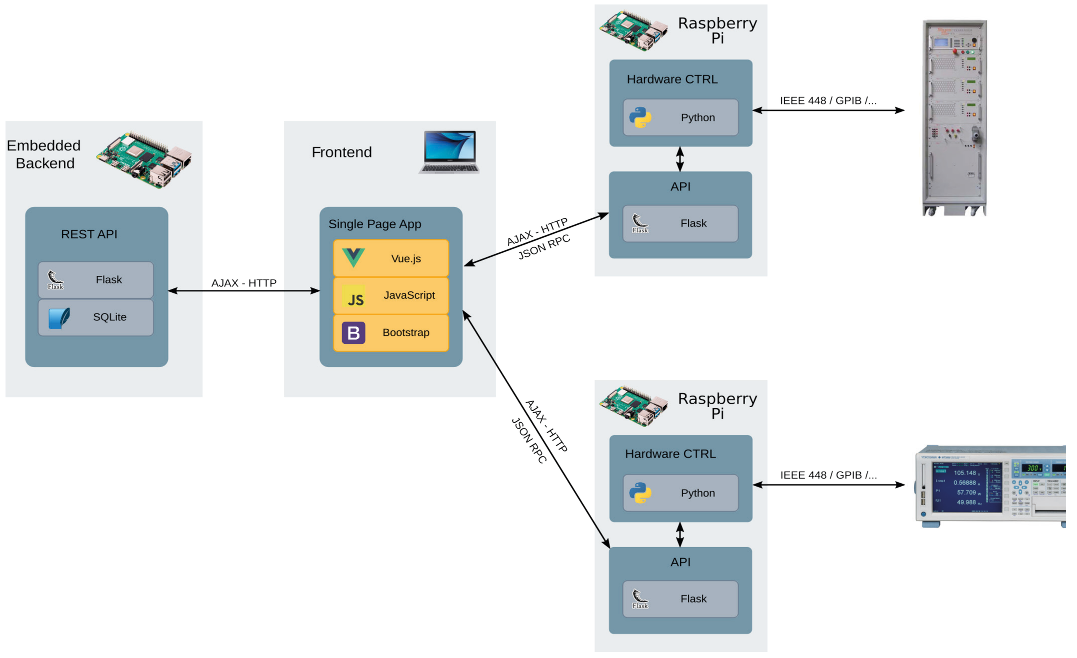

Abbildung 1: Konzept von MUSCLE

Wechselrichter-Teststand

Im Wechselrichter-Teststand wird das Regelverhalten von Wechselrichtern in realen Stromnetzen genauer analysiert. Hier liegt der Fokus auf der Wirk- und Blindleistungsanpassung in Abhängigkeit der Netzspannung oder -frequenz.

Im Teststand werden 2 Geräte angesteuert, um ein Verteilnetz zu emulieren und um die Veränderung darin zu registrieren. Für die Emulation des Netzes wird die lineare Dreiphasen-Netznachbildung PAS15000/ SyCore von Spitzenberger+Spies verwendet. Die Messungen über das Regelverhalten der zu testenden Wechselrichter werden mittels YOKOGAWA WT3000 Power Analyzer durchgeführt. Beide Geräte werden über die GPIB Schnittstelle vom dem jeweiligen Device (hier ein Raspberry Pi) angesteuert und ausgelesen.

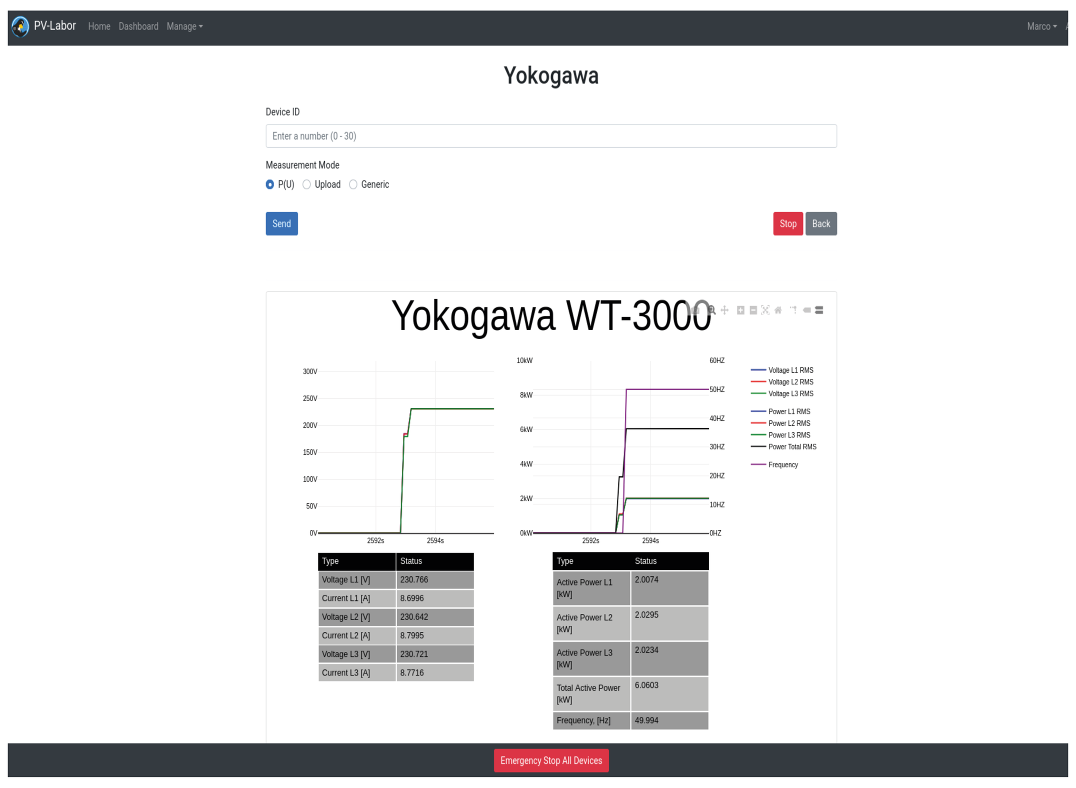

Abbildung 2: Bildschirmaufnahme Bedienoberfläche Wechselrichter-Teststand

Die Konfiguration, Datenübergabe und grafische Darstellung der Instrumentenmesswerte wird durch MUSCLE koordiniert. Mittels Frontend können nun die Geräte einfach z.B. über ein Tablet bedient werden. Die Daten werden repräsentativ auf dem Dashboard des Frontends des Devices veranschaulicht und können zu Dokumentationszwecken in hoher Auflösung heruntergeladen werden.

Zurzeit werden auf dem Wechselrichter-Teststand im Zuge des Pilot+Demonstrations-Projektes „GODA - Netzoptimierung mit dezentralen Aktoren" die optimalen Regelparameter zur Wirkleistungsreduktion bei zu hoher Netzspannung ermittelt.

MLPE-Teststand

MLPE steht für Module-Level-Power-Electronics, also für Leistungsoptimierer und Modul-Wechselrichter. Mit dem wachsenden Marktanteil dieser Gerätegruppe steigt auch der Bedarf zur Erforschung dieser Systeme. Im MLPE-Teststand können bis zu 15 Modulwechselrichter oder Leistungsoptimierer individuell betrieben und deren Wirkungsweise im Gesamtsystem erforscht werden.

Abbildung 3: Nahaufnahme MLPE-Teststand

Mit MUSCLE werden über ein Raspberry PI als Device sämtliche parametrierbaren DC-Quellen angesteuert, um beliebige Modulkennlinien statisch oder dynamisch zu simulieren. Jede einzelne Quelle als auch das Gesamtsystem wird über MUSCLE überwacht und es können Arbeitspunkts-, Regel- und Trackingsverhalten erforscht werden.

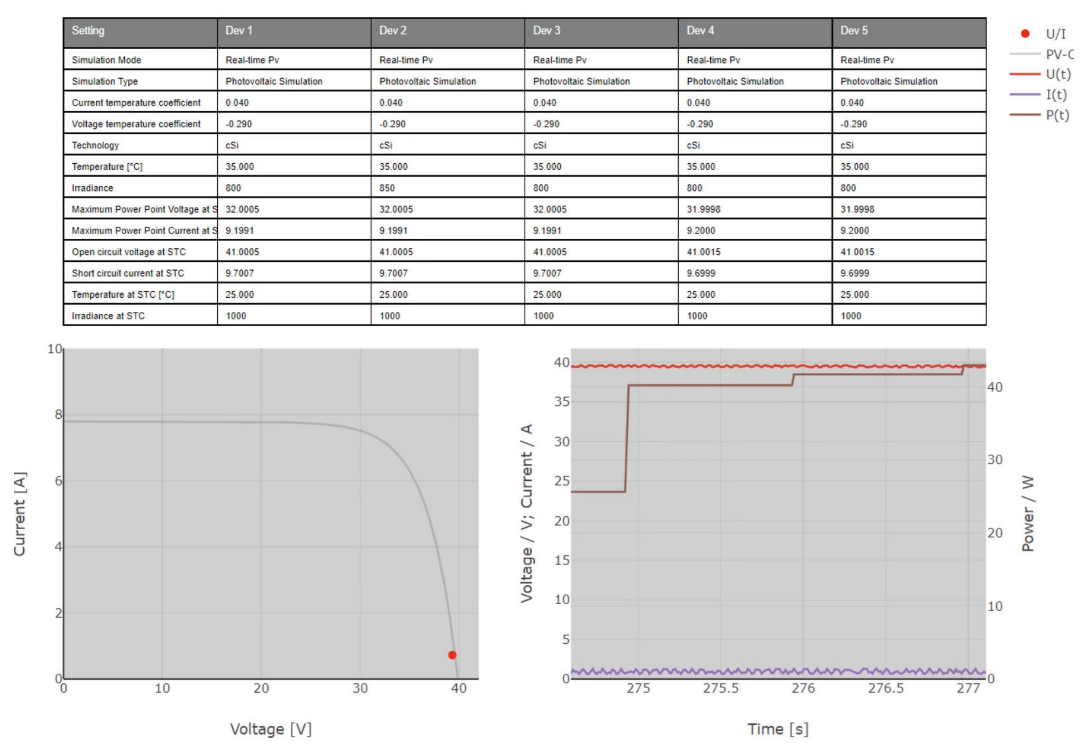

Abbildung 4: Bildschirmaufnahme Überwachungsoberfläche MLPE-Teststand

Ausblick

MUSCLE wird künftig bei allen Testständen zum Einsatz kommen und auch bereits bestehende Infrastruktur ansteuern können. Neue Simulatoren und Messgeräte werden eingebunden und normative Prüfabläufe implementiert.

Berner Fachhochschule

Finden Sie mehr zur stetig weiterentwickelnden Open-Source Laborautomatisierung mit MUSCLE und über die Kompetenzen des PV-Lab heraus.

https://muscle.ti.bfh.ch/projects/pvlab.html

https://www.bfh.ch/pvlab

▶Technik und Informatik

Labor für Photovoltaiksysteme | Jlcoweg 1
3400 Burgdorf | Schweiz
bfh.ch/pvlab | david.joss@bfh.ch

Photovoltaik Potenzial auf Dachflächen in der Schweiz

Synthese aus Sonnendach.ch und einer repräsentativen Stichprobe an Dachbelegungen

Dionis Anderegg, Sven Strebel, Jürg Rohrer
Zürcher Hochschule für Angewandte Wissenschaften
Institut für Umwelt und Natürliche Ressourcen, Forschungsgruppe Erneuerbare Energien

Zürcher Hochschule für Angewandte Wissenschaften
zhaw
Life Sciences und Facility Management
IUNR Institut für Umwelt und Natürliche Ressourcen

Einleitung

Verschiedene Studien beziffern das Potenzial für Photovoltaik auf Dachflächen in der Schweiz mit 16 und 53 TWh pro Jahr (Abbildung 1) [1-5].

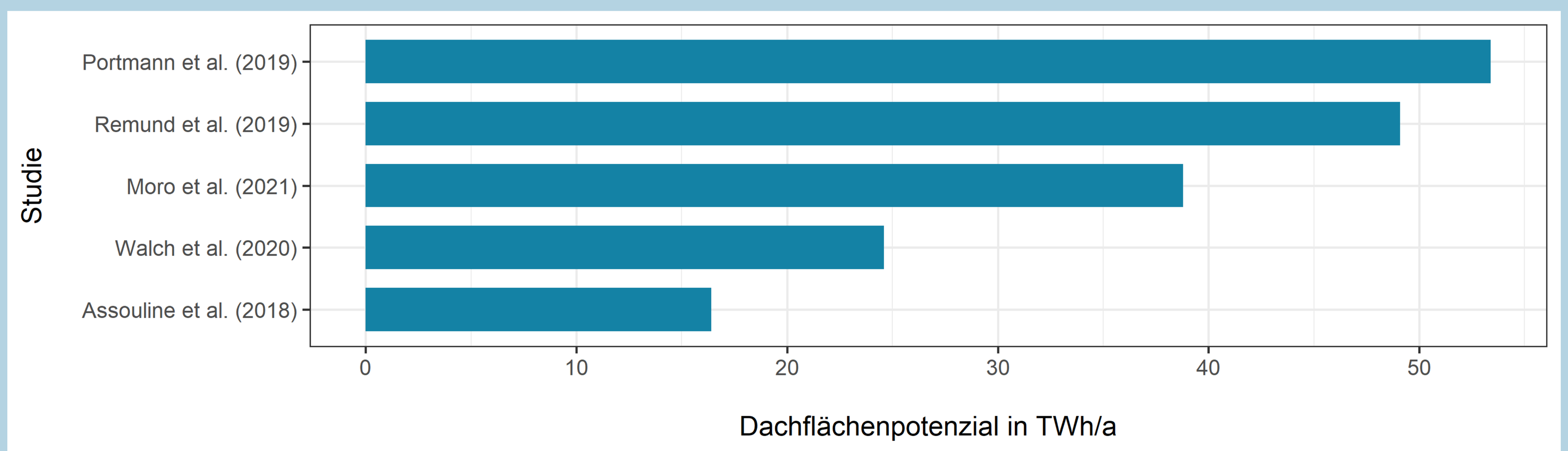

Abbildung 1: Schätzung des Dachflächenpotenzials verschiedener bisheriger Studien [1-5].

Diese grosse Spannweite kann auf unterschiedliche Datengrundlagen und Annahmen in Bezug auf den nutzbaren Flächenanteil von Dachflächen zurückgeführt werden [1]. Das Ziel dieser Studie ist die Ermittlung des für PV nutzbaren Dachflächenanteils mit einer Genauigkeit von ± 2.5 %. Dazu wurde eine repräsentative Stichprobe von 658 Dachflächen mit Standard-Photovoltaikmodulen belegt. Das Ertragspotenzial von Dachflächen wurde mithilfe der für PV nutzbaren Flächenanteile neu bestimmt.

Methode

Dachflächen: Für die Analyse werden gemäss Klassifizierung von Sonnendach.ch nur Dachflächen mit Eignungskategorien «gut» bis «hervorragend» berücksichtigt (≥1000 kWh/m²/a) und kleine Dachflächen ausgeschlossen (Abbildung 2, oben).
Stichprobe: Aus den Dachflächen wird pro Kategorie (gemäss Kategorisierung in Abbildungen 4 und 6) eine zufällige Stichprobe gezogen.
Dachbelegung: Die Belegungen werden anhand Satellitenbildern vorgenommen. Dabei werden Hindernisse (z.B. Kamine und Dachfenster), Abstände zu Dachrändern und minimale Ansprüche an die Ästhetik berücksichtigt (Abbildung 2, unten).

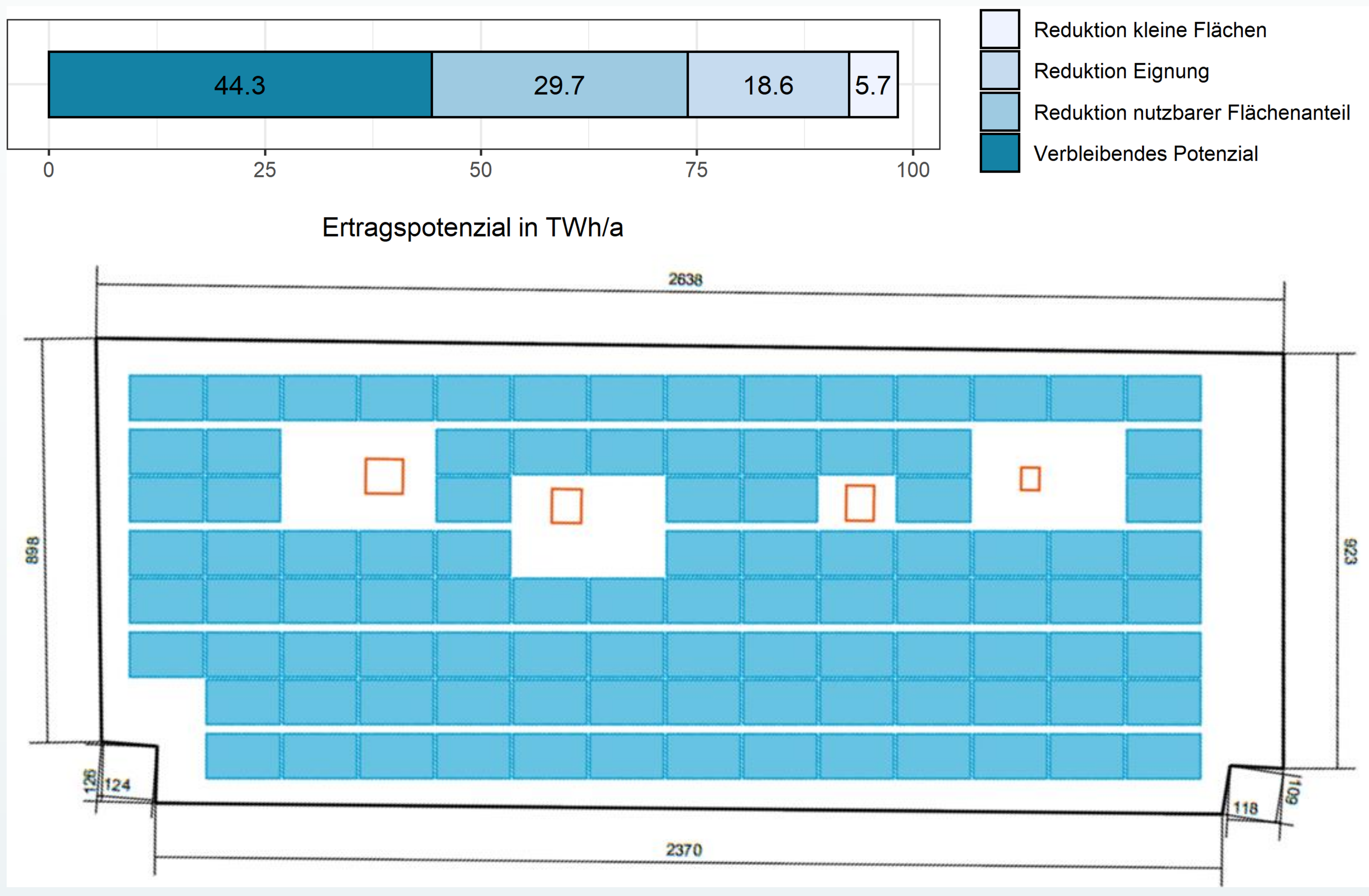

Abbildung 2: Methode der Berechnung (oben). Von der Summe aller Dachflächen gemäss Sonnendach.ch werden kleine Flächen und Flächen mit einer Einstrahlung < 1000 kWh/m²/a ausgeschlossen. Für die verbleibenden Flächen wird der nutzbare Dachflächenanteil mittels einer Stichprobe bestimmt (Belegung von Dachflächen, siehe Beispiel unten): Orange sind Hindernisse eingezeichnet. Dachfläche gemäss Sonnendach = 262 m², Modulfläche bei Belegung = 165 m². Ergibt einen nutzbaren Dachflächenanteil von 63 % .

Bestimmung nutzbarer Dachflächenanteile: Pro Kategorie wird der für PV nutzbare Flächenanteil gemittelt, indem die Gesamtfläche der Kategorie durch die Modulfläche der Kategorie dividiert wird.
Potenzialschätzung: Basierend auf dem nutzbaren Flächenanteil pro Kategorie wird das jährliche Ertragspotenzial bestimmt. Jedem Dach wird jeweils der für PV nutzbare Flächenanteil zugeordnet. Der Ertrag basiert auf einem Modulwirkungsgrad von 17 % und einer Performance Ratio (PR) von 80 %.

Resultate

Die nutzbaren Dachflächenanteile für PV Anlagen unterscheiden sich innerhalb der Stichprobe stark (Abbildung 3). Ausserdem wurde bei vielen, insbesondere kleinen Dachflächen bis 200 m², ein nutzbarer Flächenanteil von 0 % ermittelt. Dies ist beispielsweise bei Dachterrassen der Fall. In der Tendenz zeigen sich für Steildächer höhere nutzbare Flächenanteile als bei Flachdächern. Besonders bei den Steildächern steigt der nutzbare Flächenanteil mit der Dachgrösse an. Abbildung 4 stellt den mittleren nutzbaren Anteil von Dachflächen in Abhängigkeit von der Grösse der Dachfläche sowie den Fehlerbereich dar.

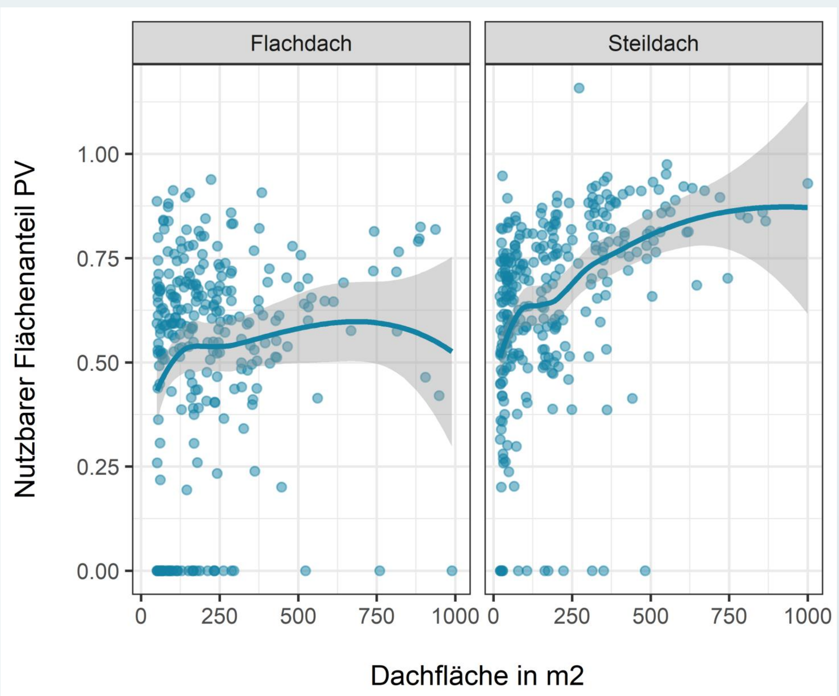

Abbildung 3: Nutzbarer Dachflächenanteil von PV Anlagen nach Dachfläche. Jeder Punkt entspricht einer Dachfläche. Nutzbare Flächenanteile von 0 % ergeben sich z.B. bei Dachterrassen.

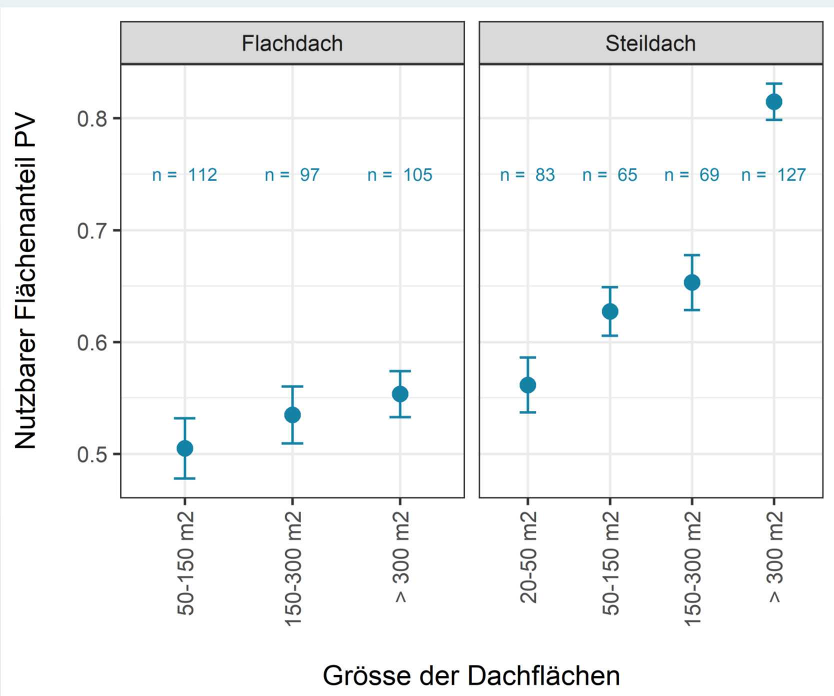

Abbildung 4: Mittlerer nutzbarer Dachflächenanteil pro Kategorie mit Fehlerbereich und Stichprobenumfang (n) pro Kategorie.

Werden die nutzbaren Flächenanteile in die Potenzialberechnung einbezogen, ergibt sich für Dachflächen ein Gesamtpotenzial von 44.3 TWh/a (± 1.6 TWh/a).
Über alle Dachflächen beträgt der mittlere nutzbare Anteil 60 % (± 2%).
Das Potenzial teilt sich gemäss Abbildung 5 zu 12.6 TWh/a (± 0.5 TWh/a) auf Flachdächer und 31.7 TWh/a (± 1.0 TWh/a) auf Steildächer auf.
Die Potenziale pro Kategorie sind in Abbildung 6 gezeigt.

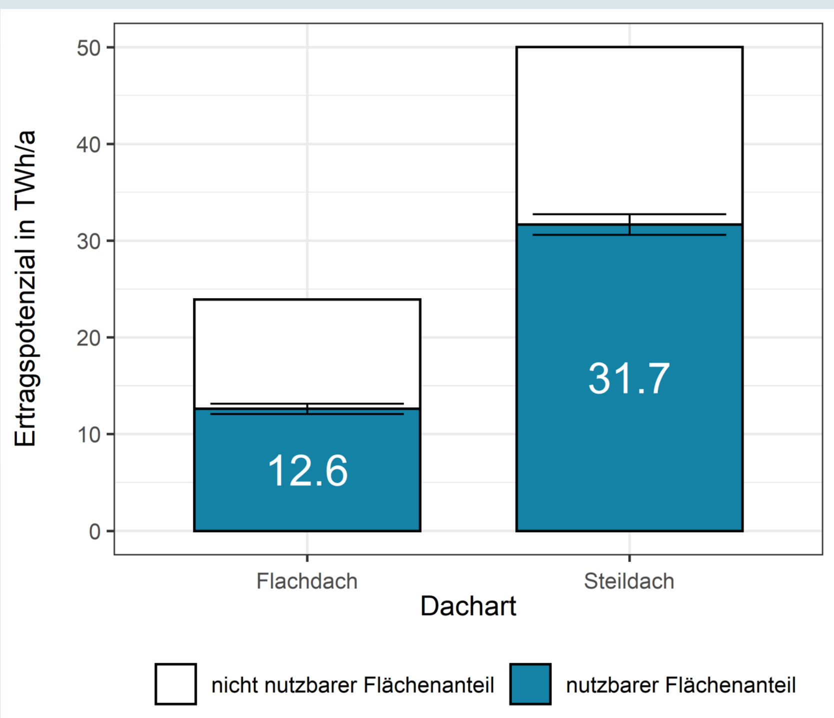

Abbildung 5: Ertragspotenzial für Flach- und Steildächer (blau) unter Berücksichtigung der nutzbaren Dachflächen-anteile. Der Fehlerbalken zeigt Fehlerbereiche von rund 2 %. (Modulwirkungsgrad 17 % und PR 80 %)

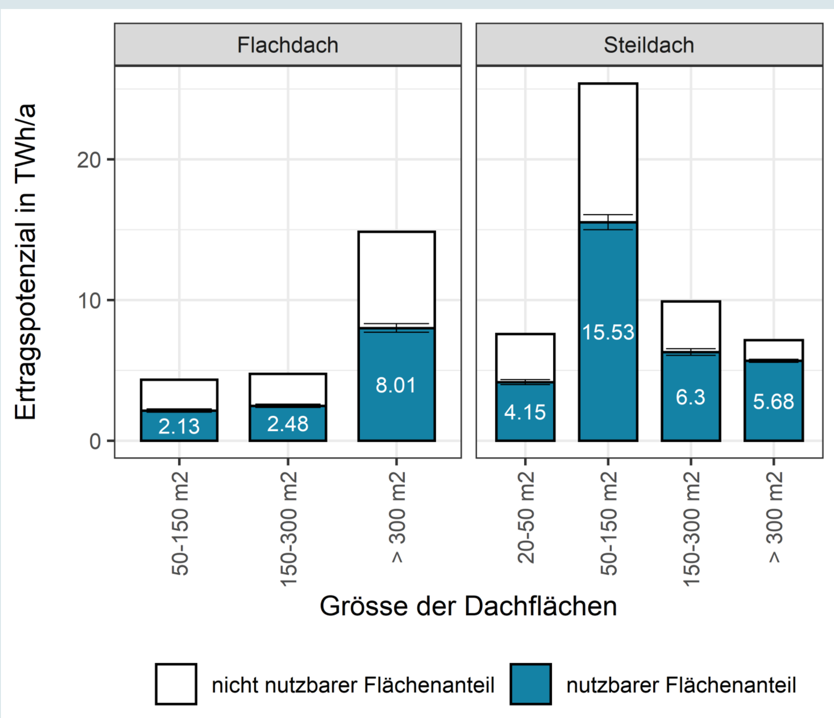

Abbildung 6: Ertragspotenzial pro Kategorie (blau) unter Berücksichtigung der nutzbaren Dachflächenanteile. Die Fehlerbalken zeigen den Unsicherheitsbereich. (Modulwirkungsgrad 17 % und PR 80%)

Schlussfolgerung

Dachflächenpotenzial der Schweiz: Im Vergleich zu vorherigen Potenzialstudien werden bisher auf Annahmen basierende nutzbare Dachflächenanteile für Photovoltaik rechnerisch ermittelt. Dies lässt eine höhere Genauigkeit erwarten. Ausserdem kann zwischen verschiedenen Dachtypen (Steil- und Flachdach) sowie Dachgrössen unterschieden werden.
Unter Berücksichtigung der nutzbaren Dachflächenanteile, einer Moduleffizienz von 17 % und einer PR von 80 % besteht in der Schweiz ein jährliches Potenzial von 44.3 TWh (± 1.6 TWh).
Für neu gebaute Anlagen sind Modulwirkungsgrade von 20 % realistisch. Daraus folgt eine lineare Erhöhung des Potenzials auf 52.1 TWh/a (± 2.0 TWh/a).
Ausschöpfung des Potenzials: Die hier ermittelten nutzbaren Flächenanteile sind als Maximalwerte bei Vollbelegung von Dächern zu verstehen. Die tatsächliche Ausschöpfung des Potenzials konnte in dieser Studie nicht näher untersucht werden und ist Gegenstand einer weiteren Untersuchung.
Übertragbarkeit: Die nutzbaren Flächenanteile pro Kategorie können für kleinräumige Potenzialberechnungen (z.B. auf Gemeinde- Bezirks- oder Kantonsebene) eingesetzt werden. Damit kann neben den regionalen Einstrahlungs- und Gebäudedaten nun auch ein dem Gebäudepark entsprechender nutzbarer Dachflächenanteil eingesetzt werden.

Dank

Die Autoren der Studie danken dem Bundesamt für Energie (BFE) für die Finanzierung, den Studierenden Sarah Herger, Raphael Jakobi und Janik Küffer für die Durchführung der Dachbelegungen und Ivo Kälin für die Beratung im Bereich der Datenauswertung und Statistik.

Der abschliessende Bericht wird unter folgender DOI erscheinen: https://doi.org/10.21256/zhaw-2425

Literatur:

[1] D. Assouline, M. Nahid, und J.-L. Scartezzini, «Large-scale rooftop solar photovoltaic technical potential estimation using Random Forests», *Appl. Energy*, Nr. 217, S. 189–211, Mai 2018, doi: 10.1016/j.apenergy.2018.02.118.
[2] N. Moro, D. Sauter, S. Strebel, und J. Rohrer, «Das Schweizer Solarstrompotenzial auf Dächern. Eine Analyse anhand von Sonnendach.ch», Januar 2021, doi: 10.21256/zhaw-2652
[3] M. Portmann, D. Galvagno-Erny, P. Lorenz, D. Schacher, und Markus Portmann, David Galvagno-Erny, Priska Lorenz, David Schacher, Rolf Heinrich, «Sonnendach.ch und Sonnenfassade.ch: Berechnung von Potenzialen in Gemeinden», Bundesamt für Energie (BFE), Bern, März 2019.
[4] J. Remund, S. Albrecht, und D. Stickelberger, «Das Schweizer PV-Potential basierend auf jedem Gebäude», Meteotest & Swissolar, Bern, 2019
[5] A. Walch, R. Castelloa, N. Mohajerib, und J.-L. Scartezzini, «Big data mining for the estimation of hourly rooftop photovoltaic potential and its uncertainty», *Appl. Energy*, Bd. 262, Nr. 114404, 2020, doi: https://doi.org/10.1016/j.apenergy.2019.114404.

Mit Unterstützung von
energieschweiz

Micro Stockage Intelligent Distribué (MSID)

Prof. D. Wannier[1], J.Vianin[1], J.-M. Alder[1], H. Pereira[1], J. Ferreira Da Silva[1], L. Perrier[2], P.-A. Clivaz[2]

[1] University of Applied Sciences Western Switzerland (HES-SO), Switzerland, [2] SEIC-Teledis Groupe, Switzerland

Summary

The Swiss Federal Office of Energy (SFOE) MSID is a three-year project that brings together the interests of 4 distribution service operators (DSO). Their objectives include remote network stabilization (use cases 1 and 2), optimization of self-consumption and co-creation of new business models to make photovoltaic storage profitable (use cases 3 and 4). This project aims to aggregate micro-storage systems (electric vehicles, batteries, heat-pumps, hotwater), test and demonstrate flexibility services. The SEIC-Teledis use case is highlighted in this poster. The objective is to optimise the self-consumption of production PV and manage remotely aggregated batteries.

Introduction

A three-phase inverter and an Apollion Cube 6kWh battery (6kW of power) from Leclanché were installed at two private customers of our partner SEIC-Teledis (Figure 1). A microcomputer was also installed at each site and connected to the inverter's Modbus with an RS 485 cable. An information system controls the inverter but also to retrieve data from smart meter and local meteo station to predict PV.

Figure 1 : Installation of SEIC Teledis in the context of the MSID project with the meteo station concept

Project methodology

A Two Tracks Unified Process (2TUP) methodology with technical and functional branch helped us to define the business needs and explore IT technologies. To implement the platform, we opted for a scrum agile methodology with short iterations called “Sprints” to develop and deploy product increment regularly. The artefacts that were created allowed us to setup essential elements for the the Release Roadmap (Figure 2) where we see COVID impact.

The Proof-of-Concept created in the technical branch of 2TUP works well in the laboratory. During the Scrum implementation in the pilot sites over more than a year, we have detected problems with data collection (Figure 3). On this example, we can see that the data collected for the grid current L1 has a lot of noise and is unusable for the Machine Learning Prediction Algorithm without cleaning. Several iterations were needed to clean up the collected data and try to optimise the data collection with the help of an automatised python cleaning Algorithms and a second time series instance to keep original data and be able to visualise cleaned data.

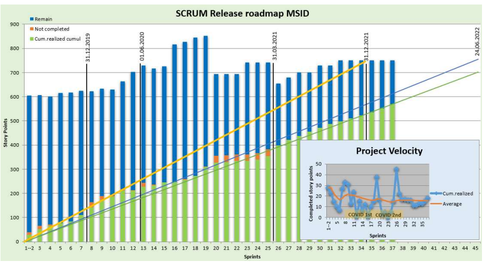

Figure 2 : Release Roadmap of the MSID project

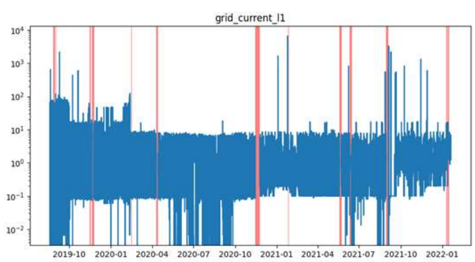

Figure 3 : RAW data collected for the grid current L1

Partners

SEIC-TELEDIS GROUPE, STUDER, icare, ELECTRINFO

Results

The DSO can visualise a virtual power plant (VPP) with the batteries of his customers and control them individually or aggregated in order to optimise the power he offers to the end customers.

Figure 4 : Visualisation on the DSO side

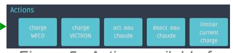

Figure 5 : Action available for the automated algorithm

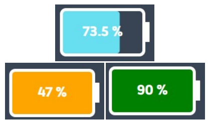

Figure 6 : Possible status of a battery

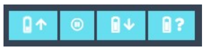

Figure 7 : Battery control and diagnostic button

Figure 8 : Hot water relay management

The DSO has three control buttons and one diagnostic button. He can manage different strategies and parametrize the logic to optimize micro-storage services (Figure 5), he can choose individually for each battery to charge, discharge or pause (Figure 7) it’s also possible to choose the number of hot water relay active (Figure 8) and define new devices. The end customer can visualise his personal battery as well as collected data (production power and energy, consumption power and energy, SOC of the battery) (Figure 9) on an online platform.

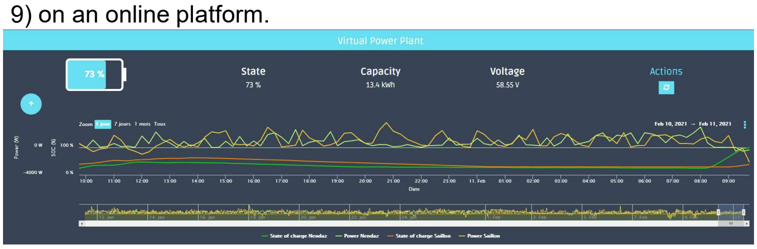

Figure 9 : Visualisation platform, end-customer side

The end user can also observe the status of the battery (Figure 6). When the battery is orange, it means that it is being discharged. If it is blue, it is neither discharging nor being discharged and finally if it is green, it is charging. A prediction algorithm based on machine learning is in development and will be deploy soon. With this prediction, we will be able to predict future production according to the weather and thus optimize the decision making of our management algorithm.

Conclusions

We aggregated micro-storage to build a virtual power plant for our partner (SEIC-Teledis). The final objective is the control of several inverters in order to promote self-consumption and to allow the DSO to optimize the supply of power to prosumers regarding's their predictions.

Contact and more information: david.wannier@hevs.ch, https://www.hevs.ch/en/minisites/projects-products/easilab/

info@csem.ch www.csem.ch

SHAMAN: Shadow mask localization of thin films for back-contacted crystalline silicon solar cells & energy harvesters

G. Nogay, J. Zhao, J. Geissbühler, N. Badel, G. Christmann, L.-L. Senaud, P. Wyss, C. Allebé, B. Paviet-Salomon, & C. Ballif

PV-Center, Centre Suisse d'Électronique et de Microtechnique (CSEM), Rue Jaquet-Droz 1, CH-2002 Neuchâtel, Switzerland

Interdigitated Back-Contacted c-Si Solar Cell Concept with High Temperature Stable Passivating Contacts

Motivation:

High efficiency potential of IBC cells with passivating contact has been demonstrated with efficiencies up to 26.1% using complex processing

→ Up to today there is no established simple way for fabrication of such solar cells

Target back contacted solar cell design and process flow:

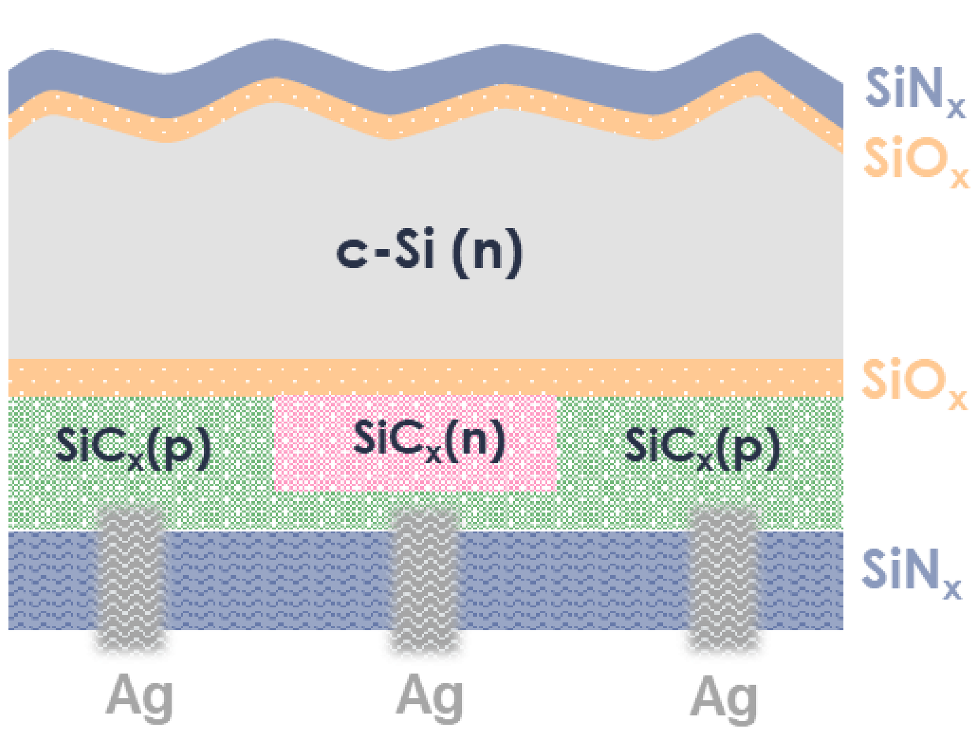

- $SiC_x(n)$ depo through mask
- $SiC_x(p)$ depo full-area
- Firing for contact formation
- Front & rear SiN_x deposition
- Screen printing metal finger
- Firing for hydrogenation & sintering

Advantages:

- Flexibility in material choice: Possibility to use low-cost base material thanks to high temperature treatment
  - Impurity gathering
  - Thermal donor killing
- Possibility to avoid TCO and compatibility with industrial firing-through direct metallization processes
- Potentially better compatibility for tandem application with perovskite top cell for 2TT applications

Front side optimization

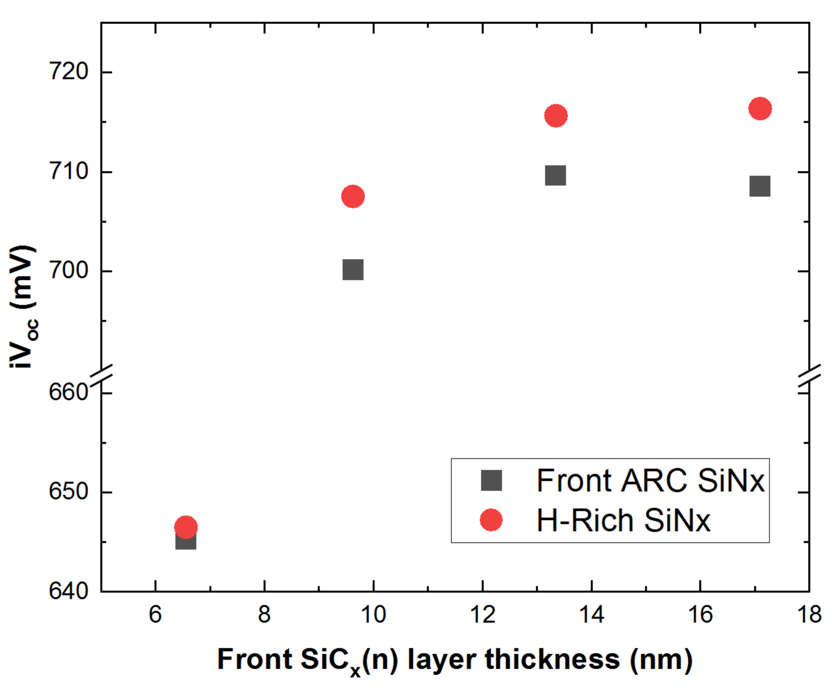

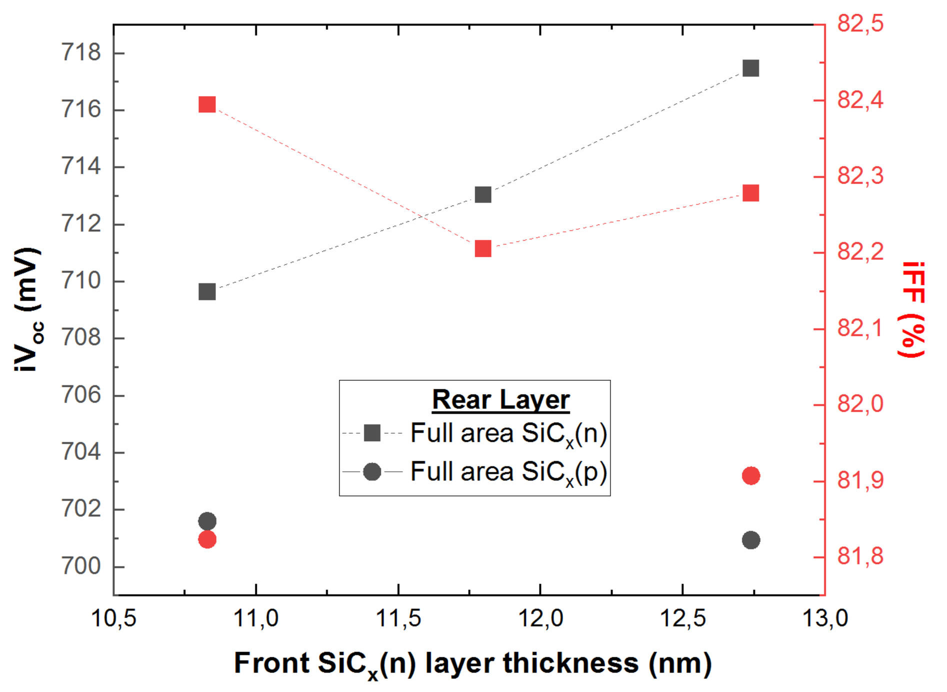

- Minimum and optimum thickness range for the front side is defined as 10 – 13 nm
- ARC - SiN_x optimized for front gives 6 to 8 mV lower iV_{oc} compared SiN_x optimized for hydrogenation
- Linear passivation dependence is observed as a function of front $SiC_x(n)$ layer (4mV/nm). This dependence is visible when the rear side has $SiC_x(n)$. When rear is covered with full $SiC_x(p)$ no clear dependence as the passivation is limited by the $SiC_x(p)$

Rear electron contact optimization

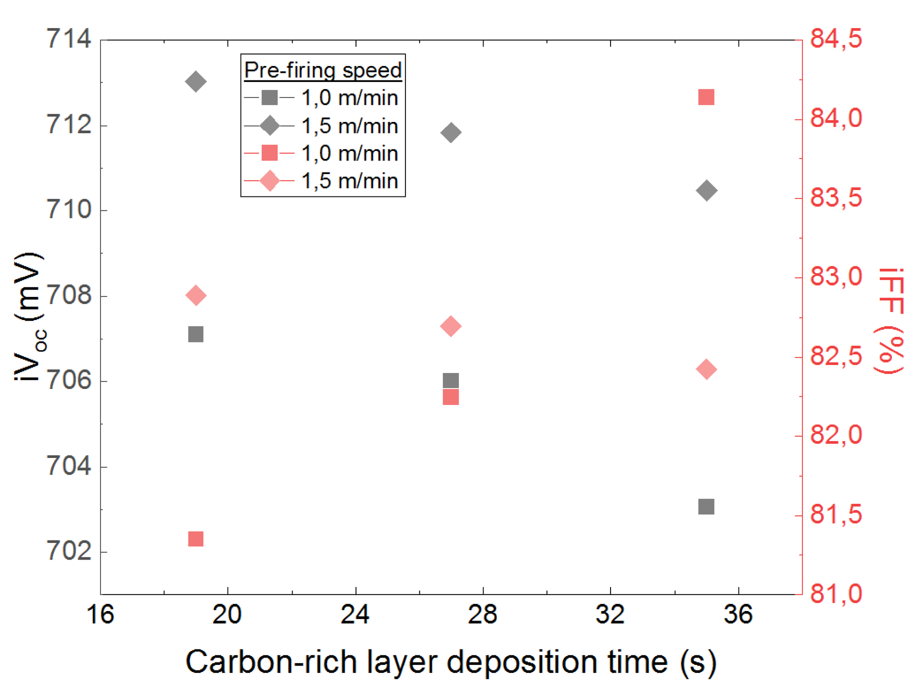

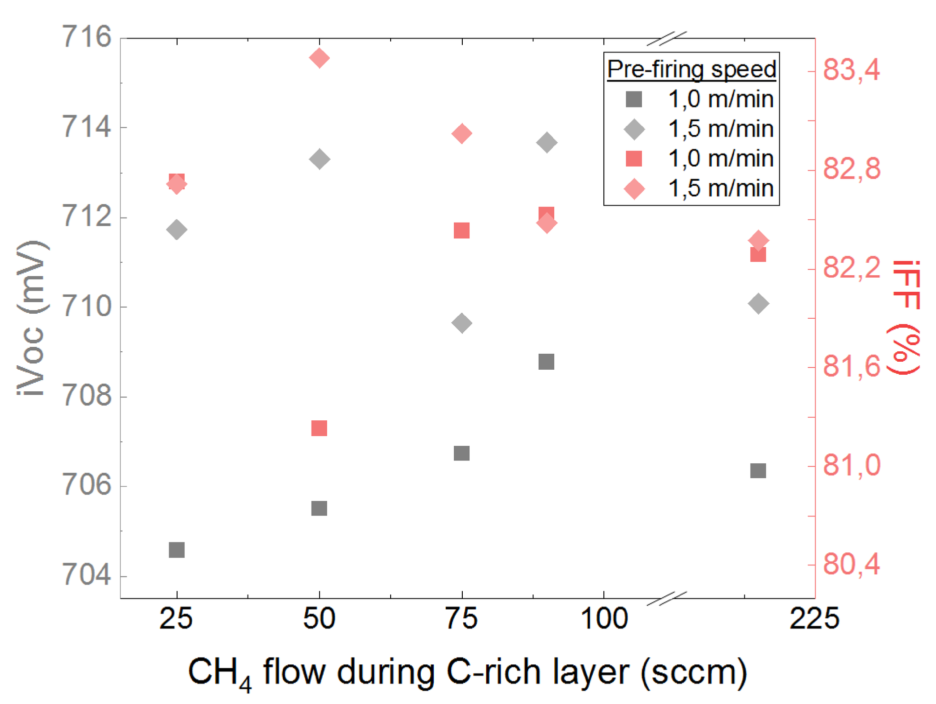

- Thinner the C-rich defective layer better the iV_{oc}

→ More efficient hydrogenation as less hydrogen can trap at the C-rich layer

- With increasing C-concentration, surface passivation improves but there is an optimum

→ Higher the C-concentration, higher the bandgap of the layer that can lead to favorable band bending

Conclusions & Outlook

- Front side $SiC_x(n)$ layer thickness optimization and rear electron contact optimization is realized leading to the cell precursors with iV_{oc} values up to 718 mV
- Proof of concept cell with efficiency up to 19.2% has been demonstrated with single shadow masking and firing process for contact formation of both polarities
- Next steps are (i) high temperature metallization development, (ii) further interface & layer optimization to improve V_{oc} and FF, testing different designs with various pitches

This work receives funding from the Swiss National Science Foundation under grant agreement 200021_192310/1 "SHAMAN"